Double-Pulse and Calibration-Free Laser-Induced Breakdown Spectroscopy (LIBS) on quantitative analysis

Victor Ulises Lev Contreras Loera

A thesis submitted in partial fulfillment of the requirements for the degree of Doctor of Philosophy

Principal supervisor: Oracio C. Barbosa García

Co-Supervisor: Marco A. Meneses Nava

Centro de Investigaciones en Óptica A.C.

January 2013

Declaration

I, hereby declare that investigations presented in this thesis have been carried out by me. The work is original and has not been submitted totally or partially in a thesis or dissertation to get a degree or diploma at CIO or any other University or Institution.

Victor Ulises Lev Contreras Loera

To my parents,
my brothers,
and all my friends.

Acknowledgments

First I would like to thank to my supervisor Barbosa for giving me the opportunity to work in his group, Grupo de Propiedades Ópticas de la Materia (GPOM) at Centro de Investigaciones en Óptica A. C. I would like to express my sincere gratitude to Dr. Meneses, co-advisor and teacher, for his patient and helpful guidance during last four years. Also I would like to thank to all researchers and members of GPOM, especially to Dr. Ramos and Dr. Maldonado for supporting me, inside and outside the classroom; thank them for sharing me their personal and professional experiences.

Thanks to the evaluation committee, Dr. Ramon Carriles, Dr. Roberto Machorro and Dr. Gabriel Ramos, for their critical comments and suggestions that improved the present dissertation. I'd like to express my gratitude to Conacyt because of its support through Dirección Adjunta de Posgrado y Becas by the scholarship 33141. Also I would like to express my gratitude to Dirección de Formación Académica (DFA) and all CIO personnel for their great support during my PhD studies.

Last but not least, my sincere and special acknowledgements to Dr. Iván Moreno who brings me into the amazing world of Optics and has motivated my critical judgment in under-graduate school and over my graduate studies.

Abstract

Laser-induced breakdown spectroscopy (LIBS) represents a powerful tool for qualitative analysis and can achieve quantitative results with acceptable accuracy and precision. Nevertheless, due to the high laser pulse energies used in LIBS, sample damage represents a drawback for some applications. In recent years, novel techniques, such as Double Pulse LIBS (DP-LIBS), have been developed to overcome main LIBS drawbacks. In order to diminish sample damage, this dissertation studies the use of signals from orthogonal DP-LIBS obtained at low ablative energies for quantitative analysis by a self-calibrated method called Calibration Free (CF)-LIBS. Before testing DP-LIBS with CF-LIBS, this dissertation presents the implementation of conventional single pulse LIBS (LIBS or SP-LIBS) as well as orthogonal DP-LIBS approaches. For optimal implementation of quantitative analysis, two problems are solved by different techniques (calibration curves and CF-LIBS). In the first case, a series of experiments, based on calibration curves technique, were conducted to quantify the Active Pharmaceutical Ingredient (API) in commercial pellets by estimating their Cl content. Results from LIBS were compared and validated with those obtained by High Performance Liquid Chromatography (HPLC). In the second problem, CF-LIBS is presented as a technique capable of determining the chemical composition of multi-elemental samples. Fe, Cr, Mn, and V elements from a steel sample were successfully quantified. Results obtained by CF-LIBS satisfactorily agree with microprobe technique results and certified elemental values in the sample. After successful DP-LIBS and CF-LIBS implementation we demonstrated, for the first time to the best of our knowledge, that CF-LIBS can be successfully applied to spectral lines obtained from orthogonal DP-LIBS configuration. The great improvement in atomic emission, signal-to-noise ratio (SNR), signal-to-background ratio (SBR) and reproducibility offered by DP-LIBS has been tested in CF-LIBS in order to reduce the use of high energies. As a consequence, when DP-LIBS is applied to CF-LIBS instead of conventional SP-LIBS, the mass removed by laser ablation is reduced by a factor of 13 without losing signal intensity. This is a remarkable finding

that can be exploited in critical applications where sample damage represents a drawback.

Motivation

Conventional approaches for elemental analysis offer excellent detection limits – nowadays detection of parts per trillion (ppt) for trace components are not unusual– however, they are destructive techniques and require sample preparation and analytical time-consuming steps making those techniques unpractical for many real-life problems. Moreover, conventional methods rely on the use of dangerous solvents producing chemical reactions polluting the environment.

Consider the hypothetical case where the only way to determine the provenance of an archeological and historical important gemstone is by the determination of its elemental chemical composition. The use of conventional techniques, e.g. inductively coupled plasma mass spectrometry (ICP-MS) would give excellent analytical results. However, ICP-MS would destroy a portion of the gemstone because it requires sample digestion and laborious sample pretreatment; so, the need of an alternative technique with features as minimal sample preparation and destructiveness, real time and in-situ analysis becomes evident. For this one and other specific cases, conventional approaches are not an option. In contrast to conventional techniques, all-optical techniques represent a more effective and feasible option.

The invention of the laser with its special properties has opened up new possibilities in analytical spectroscopy allowing the development of laser based techniques such as

LIBS. The development of LIBS has progressed to the point that the technique represents a powerful tool for qualitative analysis and can achieve quantitative results with acceptable precision and accuracy in many situations. Current precision and accuracy of the LIBS technique is good enough for monitoring and controlling production processes and for the use in on-site environmental and industrial applications. However, LIBS still presents some drawbacks in order to be accepted as a universal analytical technique in elemental analysis and quality control processes. The limit of detection for solid samples is already acceptable particularly in alloys and metallic samples. However, for general applications, best results depend on calibration curves and other auxiliary conventional techniques. Furthermore, sample damage represents a drawback in some circumstances but it can still be diminished without losing sensitivity.

Objective

In recent years CF-LIBS has become increasingly popular for quantitative analysis. Compared with traditional quantitative methods, CF-LIBS represents a faster and more practical way to determine the chemical composition of an unknown sample. As a drawback, the approach is not mature yet and its applications are restricted to some specific fields, besides, its use depends strongly on good signal emission yielding to high sample damage because of the use of high laser pulse energies.

On the other hand, different LIBS-based approaches have been developed in order to decrease sample damage. It would be interesting if quantitative analysis can be done by minimizing sample damage without losing sensitivity. Keeping this idea in mind, the main objective of this dissertation is to analyze the effects of orthogonal double pulse (DP) LIBS approach on the Calibration Free (CF) LIBS technique looking for quantitative analysis with minimal sample destruction by means of low ablative energies.

Before achieving the main objective, specific tasks had to be completed. The first task was the implementation of the LIBS technique. Experimental details about the technique implementation are discussed in chapter 3. Besides the experimental set up, we developed software capable of analyzing experimental signals, processing data and

performing quantitative analysis. Details of the software called AtomicSpectra are presented in Appendix A. After the experimental set up and software implementation, the LIBS approach was tested by solving two specific problems dealing with quantitative techniques. Those problems are described in chapter 4. Chapter 5 presents details of the quantitative analysis by CF-LIBS and DP-LIBS using minimal energy in order to produce minimal sample damage.

TABLE OF CONTENTS

List of Figures

Figure 3.1. Schematic representation of a custom-made sample holder. Lens to sample distance (LTSD) may be constant for samples with different thicknesses.

Figure 3.2. Temporal emission evolution of plasma is in the microsecond scale. Delay time and gated time for data acquisition depend on energy, sample properties and other parameters. Typical delay time values in our experiments are about 200 ns. Gate time values for signal acquisition could be 1 – 10 μs.

Figure 4.1. (a) Metformin and (b) Glyburide molecular structures. Halogen atoms, like Cl, are present in Active Pharmaceutical Ingredients (APIs).

Figure 4.2. Typical excipients used in anti-diabetic tablets show spectral differences between each other over the visible-NIR region. As an example, it is shown two spectral windows at (a) 732-769nm and (b) 833-867nm. Spectral differences can be used as particular excipient optical “fingerprints”.

Figure 4.3. Raman spectra (200-1200cm-1) from two references of lactose and four commercial samples containing Gly as API and lactose as excipient.

Figure 4.4. Emitted spectra from (a) metformin and (b) glyburide commercial samples mixed with an internal standard (KBr). The Cl and Br lines used for the analysis are arrow pointed on both graphs. In the case of glyburide spectra, an amplified zone illustrates the Cl emission at 837.24nm.

Figure 4.5. (a) Metformin-containing commercial samples (1-4) are well predicted according to calibration curve analysis. Seven synthetic samples at different Cl

concentrations were fitted achieving linearity higher than 99%. (b)According to statistical analysis two pharmaceutical brands (2 and 3) presents wider spread distributions. The outlier (in brand 1) is present in the analysis.

Figure 4.6 (a) Glyburide-containing commercial samples (1–4) are well predicted according to their respective calibration curve analysis. For the sake of clarity, only a fraction of the curve containing commercial samples is shown (0.1–0.7%). Achieved linearity is higher than 99%. (b) According to statistical analysis the two pharmaceutical brands (1 and 2) present wider spread distributions.

Figure 4.7. Spectral "fingerprint" of a steel sample taken by LIBS technique. Spectral emission of Fe, Cr, Mn and V elements are present in the range 400 – 440 nm.

Figure 4.8. FWHM of 426.04nm Fe spectral emission used to calculate the electron density ne from steel sample plasma. Experimental data (black line) fits fairly well with a Lorentzian curve supporting the hypothesis of broadening by Stark effect.

Figure 4.9. A family of lines in Boltzmann plot for Fe (21 spectral lines), Cr (8), Mn (4), and V (9) species from a steel sample. The slope is the same for all Boltzmann family lines and was calculated by fitting Fe data points. This calculated slope from Fe line was fixed for other element lines.

Figure 4.10. Elemental concentration of Fe, Cr, V, and Mn in a steel sample calculated with CF-LIBS (black bars) and Microprobe (red bars) method. Bars are plotted in a logarithmic scale.

List of Tables

1. Introduction

Laser-Induced Breakdown Spectroscopy (LIBS) has been proven to be a versatile and practical technique for elemental analysis in a wide number of applications and materials. Many advantages such as simple or non-sample preparation, simultaneous multi-element analysis, rapid, non-contact, and *in situ* analysis position LIBS as a highly competitive technique compared with conventional techniques. Unfortunately, LIBS also presents some limitations. For example, Single Pulse LIBS (LIBS or SP-LIBS), the most commonly configuration used for LIBS, involves a plasma ignition process which is inherently a violent and destructive event. As a consequence, good precision is compromised and, in cases where sample damage is important, LIBS is considered a destructive technique. Moreover, LIBS sensitivity is compromised because analyte signal is masked by an intense background signal produced from both, bremsstrahlung and electron–ion recombination processes. Increasing the laser pulse energy in this approach would increase the sensitivity up to certain limit, but unfortunately also it would increase the ablated material. In recent years, novel techniques improving LIBS features have emerged. This chapter reviews two of the most appealing techniques with great potential to improve LIBS features, the so-called double pulse (DP)-LIBS and Calibration Free (CF)-LIBS approaches. The focus of this review will be on the development of both techniques and their applications highlighting the use of relatively high pulse energy used in the reported experiments.

1.1. Review of DP-LIBS literature

One of the most appealing approaches to improve LIBS sensitivity is the DP-LIBS configuration. With DP-LIBS it is possible to increase the signal intensity without increasing the ablated material and keeping LIBS features. DP-LIBS relies on the addition of a second laser pulse to the traditional SP-LIBS enhancing atomic emissions. Though the full comprehension of the enhancement is not well understood, intensive work has been carried out using collinear and orthogonal configurations trying to understand physical effects related with the enhancement such as inter pulse delay times, pulse energies, wavelength dependence, sample properties, and so on. Since Cremers reported the use of two consecutive laser pulses (in the same direction) to improve the limits of detection in aqueous solutions over 30 years ago [1], researchers keep interest mainly in DP-LIBS collinear configuration and most papers report the use of this geometry [2-9]. Nevertheless, because we are looking for minimal sample damage, this section will emphasize a configuration where only the first laser pulse hits the sample, while the second pulse is used as a probe pulse, that is, orthogonal reheating configuration. Review in pre-ablative and collinear configurations also will be mentioned. Figure 1.1 shows a schematic representation of the three main DP-LIBS configurations; i.e. collinear, orthogonal pre-ablative and orthogonal reheating configurations.

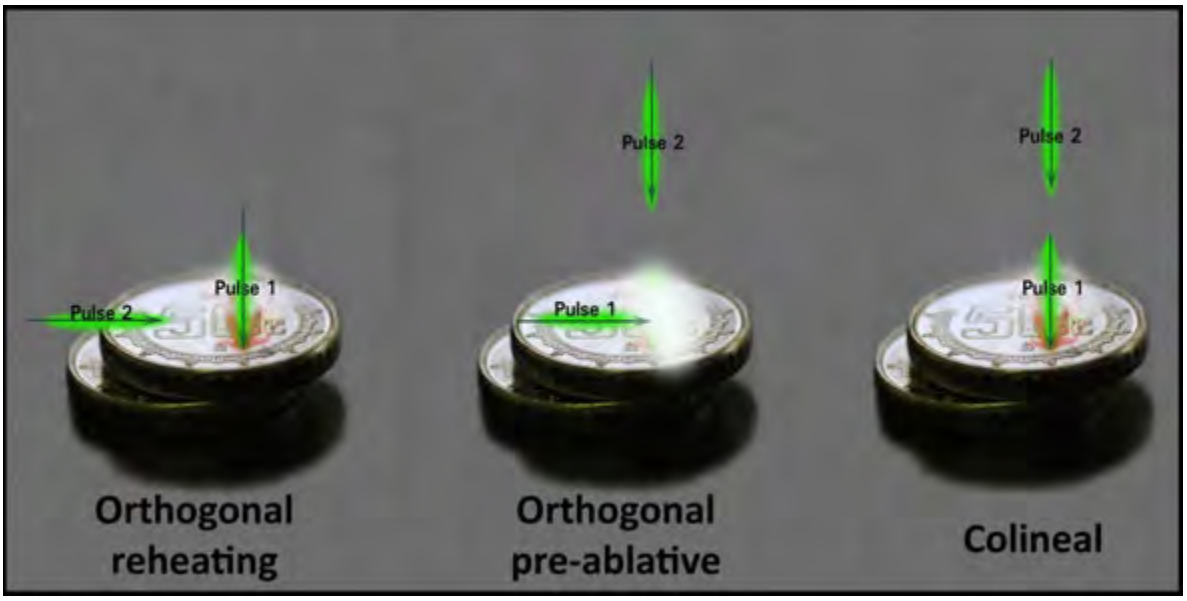

Figure 1.1. Main Double Pulse LIBS configurations, orthogonal reheating, orthogonal pre-ablative and collinear configurations. In all configurations, second pulse is temporally delayed with respect to the first pulse a certain time (inter-pulse delay time).

In 1991, Uebbing published an interesting effect of reheating laser-produced plasmas by adding a second pulse [10]. In the reported experiment by Uebbing, a 13 mJ at 1064nm laser pulse was used as ablative pulse directed perpendicularly to the sample. The second laser pulse (115 mJ at 1064 nm) was directed parallel to the sample surface and hit the plasma produced by the first pulse 1.5mm above the sample surface. The impact of the second pulse on the plasma raises its temperature from 6000K to 10000K approximately. With the reported experimental conditions (Ar atmosphere at reduced pressure), the increase in temperature increases more than ten times the signal intensity of Zn and Cu from a brass sample without increasing the amount of ablated material by adding the second pulse. Stratis et al. developed the so called pre-ablative DP-LIBS scheme in 2000

[11]. In this configuration the first pulse is focused above the sample surface and the second pulse hit the sample in order to produce the plasma (Figure 1.1). Besides Uebbing and Stratis publications there was no active interest in the orthogonal geometries until very recently. In particular for the reheating scheme, Gautier et al. published in 2004 a comparison between LIBS and DP-LIBS features by analyzing aluminum samples at atmospheric pressure [12]. Gautier et al. analyzed the influence of the delay time between two laser pulses. Laser pulses at 532 nm (110 mJ) were used to ablate the samples and 1064 nm (110 mJ) laser pulses were used to reheat the plasma. This work concluded that more ionic emission lines are present in DP-LIBS than in LIBS set up when the same total energy is used. Moreover, they established a correlation between the increase in line intensities and their excitation energy levels. In the following year, Gautier et al. published another work reporting intensity enhancement comparison between both, reheating and pre-ablation configurations [13]. Comparison was performed under same total energies (110 mJ + 110 mJ) but longer optimum inter-pulse delays were determined for pre-ablative (15 μs) than in reheating scheme (200 ns) due to the different physical mechanisms involved in each case. In this work, Gautier et al. confirmed the correlation between the increase in line intensity and its excitation energy level in both schemes. They concluded that the reheating scheme improves LIBS sensitivity more than pre-ablative scheme under the same energy and wavelength parameters. The same group tested collinear DP-LIBS approach in different materials (synthetic glasses, rocks, steels) [6]. On that work, authors used 55 mJ per pulse from two synchronized Nd:YAG lasers (at

532 nm). Authors proved that the enhancement factor is related with energy levels in collinear geometry.

On the other hand, pre-ablative scheme has been more extensively analyzed by several groups than reheating scheme. Most of the publications tend to explain the mechanisms involved in the signal enhancement [11, 14-17]. Suliyanti et al. reported the use of low ablative energies [17]. They performed the experiments in He ambient gas using an ablative energy of 2.5mJ. With those experimental conditions they produced crater diameters on the order of 10 µm. This remarkable finding suggests that LIBS can be used for practically non-destructive quantitative analysis. Using calibration curves technique, authors estimated a Cl limit of detection (LOD) of 80 ppm in alumina samples. Nevertheless, pre-ablative scheme requires the use of two different lasers due to the large inter-pulse delay (usually in the µs scale) and vacuum chamber to control atmospheric pressure and He flux. Those requirements increase set up costs and limit LIBS applications in atmospheric conditions.

When collinear geometry is applied in quantitative analysis, the use of relatively high energies is also reported. Burakov et al. analyzed the presence of heavy toxic metals (Pb) in environmental samples and the content of S in coal samples [7]. Authors reported energies on the range 50 – 120 mJ per pulse. Quantitative analysis was performed with auxiliary calibration curves technique. Kwak and co-workers quantified As traces in mine tailing soils from Korea using pulse energies of 90 mJ [8]. Using DP-LIBS, authors show an improvement in signal-to-noise ratio and in standard deviation parameters with respect to SP-LIBS. They used internal standardization and calibration curves for quantitative

analysis. Brai et al. reported the use of DP-LIBS in the field of cultural heritages [9]. In this work, reported energies were in the range of 50 – 120 mJ per pulse. Standard materials were analyzed by X-ray fluorescence as a reference in quantitative analysis. Double and multiple laser pulses in collinear geometry have been already applied to online monitoring in industrial processes, especially in steel industry [18-20]. Sturm et al. used three laser pulses using a Q-switch system. The burst energy amounts to 300 mJ on the reported experimental set up [18]. Blazer et al. measured online the thickness and depth profiling of Zn [19] and Al [20] coatings in galvanized steel sheets. In this case, the total energy employed ranged between 0.2 and 3 mJ in order to achieve controlled ablation depths in the coating. Estimated thickness resolution with DP-LIBS is comparable with standard XRF gauges.

As can be read in this section, DP-LIBS has a great potential in the near future for online, in-situ and real time applications. Most of the reported studies have been devoted to analyze DP-LIBS effects at relatively high energies trying to achieve better sensitivities and better enhancement factors. For the reported studies the micro-sized sample damage has not been an important issue. Nevertheless, the use of low ablative energies still remains for an extensive analysis and its use becomes increasingly important when critical applications, such as the analysis of art works, archeological artifacts, jewelry, etc., are considered.

1.2. Review of CF-LIBS literature

The use of DP-LIBS in quantitative analysis has been increasing in recent years [6-9, 21-22]. In general, for quantitative analysis DP-LIBS requires calibration reference standards, internal standards, calibration curves, etc. In many situations (on-line in-situ measurements, process monitoring, hostile environments, etc.), time and preparation steps required in calibration techniques limit quickness and versatility of LIBS. Paradoxically, for the use of calibration reference standards, sample composition need to be known a priori, but in some applications the information is not available. In other cases, e.g. archeological applications, reference standards simply do not exist. An alternative approach for quantitative analysis is the called Calibration Free LIBS (CF-LIBS) proposed by Palleschi´s group at the end of the 90´s [23]. In a brief graphical representation, each spectral line is represented by a point in the Boltzmann plane where the X coordinate represents the energy of the upper level of the radiative transition and the Y coordinate is related to the line intensity. Lines for a single element, i.e. Fe I lines, can be fitted by a linear regression in the Boltzmann plot, where the slope of the line is related with the plasma temperature and the intercept value from the linear regression can be related to the concentration of each element. Figure 1.2 shows a Boltzmann plot example where Fe and Cr information is plotted as numbers (black and blue numbers respectively).

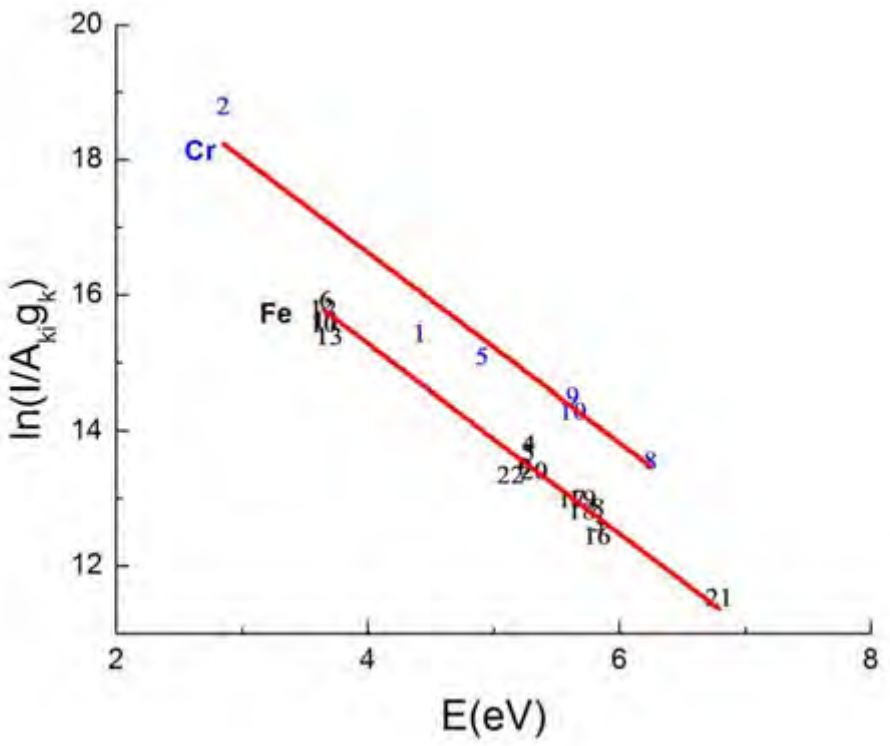

Figure 1.2. Calibration Free LIBS is based on Boltzmann plot analysis. In Boltzmann plot analysis each spectral line is represented by a point where the X coordinate represents the energy of the upper level of the radiative transition and the Y coordinate is related to the line intensity. In this example, Fe I and Cr I lines are fitted by a linear regression and the slope of the (red) lines are related with the plasma temperature and the intercept value from the linear regression can be related to the concentration of each element.

When CF-LIBS is applied, typically it is assumed that plasma is in ideal conditions, that is, spatially homogeneous plasma in Local Thermodynamic Equilibrium (LTE) and emission lines involved in the analysis are optically thin (not involving self-absorption effects), nevertheless, care should be taken when dealing with those assumptions.

The Boltzmann plot method has been used commonly to determine the temperature in plasmas [24-26]. Yalcin et al. proposed the so-called Saha-Boltzmann plots [27]. In this method, Saha–Boltzmann plot is obtained using spectral lines from neutral and ionized stages, and, similarly as Boltzmann plots, temperature is calculated using the slope of a linear fit. Aguilera and Aragón used Saha-Boltzmann plot method to spatially characterize laser induced plasmas in nickel-iron alloys [28]. They showed that Saha-Boltzmann plots constructed from local emissivity lines predict local temperatures compatible with LTE conditions. On the other hand, when Saha-Boltzmann plots are constructed from spatially-integrated line intensities, two apparent temperatures are obtained (one from neutral and other from ionized species). However, the difference was not considerably high. The same Group of Aguilera, proposed a multi-element Saha-Boltzmann equation applicable to emissivities from neutral and ionized lines [29]. Plots obtained from 58 lines (from neutral and ionized Fe, Ni and Mn) showed linear shape supporting LTE conditions. They used laser pulses from an Nd:YAG system (100 mJ pulse energy at 1064 nm and pulse width of 4.5 ns). In the case of optically thin plasmas, typically lines involving self-absorption effects are avoided; however, some papers deal with self-absorption correction in order to use those lines [30-32]. Sun and Yu proposed a recursive algorithm for correcting the self-absorption effect in order to use strong lines from major elements in CF-LIBS analysis [32]. Other groups deal with improvements and correctness of CF-LIBS. Tognoni et al. analyzed effects of experimental irregularities, inaccuracy on theoretical parameters and plasma non-ideality conditions on the accuracy and reproducibility of quantitative results [33]. Authors remark that the problem regarding the calculation of partition functions for all

elements is still open. Moreover, discrepancies in the listed partition function values in the literature and uncertainties in electron density calculations are not as significant as initially believed; nevertheless their effect is more evident in trace element quantification and cool plasmas.

Other groups have been focused in CF-LIBS applications. Since the first CF-LIBS publication in 1999, the approach has been applied satisfactorily to solid materials such as aluminum, cooper, and steel alloys, jewelry, archeological artifacts, glasses, etc. Tognoni et al. summarize CF-LIBS applications after its first decade in a review [34]. In this review, most of the summarized analyses were carried out in ambient conditions and a few number of papers reported on CF-LIBS simulating other atmospheres such as those found in Mars. Tognoni reported a wide range of values for experimental settings (wavelength, pulse energy, covered spectral range, timing, etc.). Typically, fundamental and harmonic-generated wavelengths from Nd:YAG lasers are employed for CF-LIBS applications. In the first ten years since the introduction of CF-LIBS, ns-laser pulse regime and pulse energies varying from 10 mJ to more than 100 mJ are common parameters. The following discussion will be mainly focused on CF-LIBS applications emphasizing on the energy used in the reported experiments.

Shah et al. published recently the quantitative analysis of a steel sample using CF-LIBS [35]. Authors reported the use of 70 mJ of energy in pulses from the second harmonic of an Nd:YAG laser (7 ns FWHM pulse duration) and determined Fe, Cr, Ni, Mn, and Si with relative uncertainties lower than 5% according to the concentration certified values in the steel. Pandhija et al. combined CF-LIBS and calibration curves (based on LIBS signals) to

quantify toxic heavy metals in environmental samples [36]. This work reported that line emission and background signals are linearly dependent with the pulse energy. Authors used 532 nm laser pulses at 34 mJ for optimum signal-to-background ratio. De Giacomo et al. classify meteorites by CF-LIBS using 7 ns laser pulses at 532 nm with energies up to 400 mJ and removing about 50-100 ng of mass [37]. Even for the high energies employed authors called a non-destructive analysis of meteorites compared with 1 g used in the referenced method. Besides fast meteor classification, authors proposed selection criteria to select spectral lines that can be used for optical emission diagnostics of meteors crossing the atmosphere. Palleschi group reported CF-LIBS for the determination of chemical composition of precious alloys using the third harmonic emission of an Nd:YAG delivering pulses of 150 mJ and 7 ns [38]. Compared with traditional cupellation method in the jewelry industry, CF-LIBS analysis is considered non-destructive by the authors. In all mentioned CF-LIBS applications, relative high pulse energies are reported by authors. However, in most cases the analysis is considered as non-destructive if compared with reference methods. The use of high energies is required for a better signal-to-noise ratio (SNR) and higher line intensities. Mainly for those reasons, the use of low energies in CF-LIBS analysis has not been a subject of interest. Table 1.1 summarizes applications discussed above where sample damage can be considered important and the use of relative high energy is employed.

Table 1.1. Examples of quantitative analysis based on CF-LIBS. The use of relatively high energy is employed in SP-LIBS configuration for all cases.

Target	Energy	Number of shots	LIBS configuration	Year of publication	Reference
Steel	70 mJ	120	SP-LIBS	2012	[35]
Environmental	34 mJ	N. R.	SP-LIBS	2010	[36]
Meteorites	+ 400mJ		SP-LIBS	2007	[37]
Metallic alloys	150 mJ	60	SP-LIBS	2001	[38]
Coral skeletons	45 mJ	50	SP-LIBS	2009	[39]
Pigments	N. R.	20	SP-LIBS	2000	[40]

N. R. – Not reported

Nevertheless, to the best of our knowledge, the use of DP-LIBS together with CF-LIBS has not been reported yet. The great improvement in atomic emission, SNR, signal-to-background ratio (SBR) and reproducibility offered by DP-LIBS could be tested in CF-LIBS instead of high energies. Moreover, DP-LIBS could be tested on CF-LIBS in terms of improving accuracy levels and sensitivity, especially in the case of trace detection. Further use of low ablative energies could expand CF-LIBS applicability on critical cases where sample damage is considered an important issue. Our interest is focused on the use of DP-LIBS for quantitative analysis by the self-calibrated CF-LIBS approach. In the last chapter of the thesis, the effects of the ablative pulse energy on the signal enhancement using the orthogonal reheating configuration are discussed. Additionally, we compared the effects of DP-LIBS and SP-LIBS on CF-LIBS technique when the signal intensity of the spectral lines is comparable. This thesis stands on the analytical context and emphasizes on the use of DP-LIBS at low ablative energies for quantitative analysis reducing sample damage.

1.3. References

[1] D. A. Cremers, L. J. Radziemski, T. R. Loree, “Spectrochemical analysis of liquids using the laser spark”, Applied Spectroscopy, 38, 721-729 (1984).

[2] R. Ahmed, M. Aslam, “A comparative study of single and double pulse laser induced breakdown spectroscopy”, Journal of Applied Physics, 106, 33307.1-7 (2009).

[3] F. Colao, V. Lazic, R. Fantoni, S. Pershin, “A comparison of single and double pulse laser-induced breakdown spectroscopy of aluminum samples”, Spectrochimica Acta B, 57, 1167-1179 (2002).

[4] R. Viskup, B. Praher, T. Linsmeyer, H. Scherndl, J. D. Pedaring, J. Heitz, “Influence of pulse-to-pulse delay for 532 nm double-pulse laser-induced breakdown spectroscopy of technical polymers”, Spectrochimica Acta B, 65, 935-942 (2010).

[5] C. Gautier, P. Fichet, D. Menut, Jean-Luc Lacour, D. L´Hermite, J. Dubessy, “Main parameters influencing the double-pulse laser-induced breakdown spectroscopy in the collinear geometry”, Spectrochimica Acta B, 60, 792-804 (2005).

[6] C. Gautier, P. Fichet, D. Menut, J. Dubessy, “Applications of the double-pulse laser-induced breakdown spectroscopy (LIBS) in the collinear beam geometry to the elemental analysis of different materials”, Spectrochimica Acta B, 61, 210-219 (2006).

[7] V.S. Burakov, N.V. Tarasenko, M.I. Nedelko, V.A. Kononov, N.N. Vasilev, S.N. Isakov, “Analysis of lead and sulfur in environmental samples by double pulse laser induced breakdown spectroscopy”, Spectrochimica Acta B, 64, 141 (2009).

[8] J. Kwak, C. Lenth, C. Salb, E. Ko, K. Kim, K. Park, “Quantitative analysis of arsenic in mine tailing soils using double pulse-laser induced breakdown spectroscopy”, Spectrochimica Acta B, 64, 1105-1110 (2009).

[9] M. Brai, G. Gennaro, T. Schilliaci, L. Tranchina, “Double pulse laser induced breakdown spectroscopy applied to natural and artificial materials from cultural heritages A comparison with micro-X-ray fluorescence analysis”, Spectrochimica Acta B, 64, 1119-1127 (2009).

[10] J. Uebbing, J. Brust, W. Sdorra, F. Leis, K. Niemax, “Reheating of a Laser-Produced Plasma by a Second Pulse Laser”, Applied Spectroscopy, 45, 1419-1423 (1991).

[11] D. Stratis, K. Eland, M. Angel, “Dual-Pulse LIBS Using a Pre-ablation Spark for Enhanced Ablation and Emission”, Applied Spectroscopy, 54, 1270-1274 (2000).

[12] C. Gautier, P. Fichet, D. Menut, J. Lacour, D. L´Hermite, J. Dubessy, “Study of the double-pulse setup with an orthogonal bean geometry for laser-induced breakdown spectroscopy”, Spectrochimica Acta B 59, 975-986 (2004).

[13] C. Gautier, P. Fichet, D. Menut, J. Lacour, D. L´Hermite, J. Dubessy, “Quantification of the intensity enhancements for the double-pulse laser-induced breakdown spectroscopy in the orthogonal beam geometry”, Spectrochimica Acta B 60, 265-276 (2005).

[14] G. Cristoforetti, “Orthogonal Double-pulse versus Single-pulse laser ablation at different air pressures: A comparison of the mass removal mechanisms”, Spectrochimica Acta B, 64, 26-34 (2009).

[15] R. Saginnés, M. Sobral, E. Alvarez-Zauco, “The effect of simple temperature on the emission line intensification mechanisms in orthogonal double-pulse Laser Induced Breakdown Spectroscopy”, Spectrochimica Acta B, 68, 40-45 (2012).

[16] S. Choi, M. Oh, Y. Lee, S. Nam, D. Ko, J. Lee, “Dynamic effects of a pre-ablation spark in the orthogonal dual-pulse laser induced breakdown spectroscopy”, Spectrochimica Acta B, 64, 427-435 (2009).

[17] M.M. Suliyanti, A.N. Hidayah, M. Perdede, E. Jobiliong, S.N Abdulmadjid, N. Idris, M. Ramli, T. Lie, R. Hedwig, M.O. Tjia, K.H. Kurniawan, Z.S. Lie, H. Niki, K. Kagawa, “Double pulse spectrochemical analysis using orthogonal geometry with very low ablation energy and He ambient gas”, Spectrochimica Acta B, 69, 56 (2012).

[18] V. Sturm, L. Peter, R. Noll, “Steel Analysis with Laser-Induced Breakdown Spectrometry in Vacuum Ultraviolet”, Applied Spectroscopy, 54, 1275-1277 (2000).

[19] H. Blazer, M. Hoehme, V. Sturm, R. Noll, “Online coating thickness measurement and depth profiling of zinc coated sheet by laser-induced breakdown spectroscopy”, Spectrochimica Acta B, 60, 1172-1178 (2005).

[20] A. Lobe, J. Vrenegor, R. Fleige, V. Sturm, R. Noll, “Laser-induced ablation of a steel sample in different ambient gases by use of collinear multiple pulses”, Analytical and Bioanalytical Chemistry, 385, 326-332 (2006).

[21] V.S. Burakov, N.V. Tarasenko, M.I. Nedelko, V.A. Kononov, N.N. Vasilev, S.N. Isakov, “Analysis of lead sulfur in environmental samples by double pulse laser induced breakdown spectroscopy”, Spectrochimica Acta B 64, 141 (2009).

[22] G. Cristoforetti, M. Tiberi, A. Simonelli, P. Marsili, F. Giammanco, “Toward the optimization of double-pulse LIBS underwater: effects of experimental parameters on the reproducibility and dynamics of laser-induced cavitation bubble”, Appl. Opt. 51(7), 30-41 (2012).

[23] A. Ciucci, M. Corsi, V. Palleschi, S. Rastelli, A. Salvetti, E. tognoni, “New Procedure for Quantitative Elemental Analysis by Laser-Induced Plasma Spectroscopy”, Applied Spectroscopy, 53, 960-964 (1999).

[24] H.R. Griem, Plasma Spectroscopy, McGraw-Hill, New York, 1964.

[25] M. Joseph, N. Xu, V. Majidi, “Time-resolved emission characteristics and temperature profiles of laser-induced plasmas in helium”, Spectrochimica Acta B, 49, 89-103 (1994).

[26] J. A. Aguilera, J. Bengoechea, C. Aragón, “Spatial characterization of laser induced plasmas obtained in air and argon with different focusing distances” , Spectrochimica Acta B, 59, 461-465 (2004).

[27] S. Yalçin, D.R. Crosley, G. P. Smith, G. W. Faris, “Influence of ambient conditions on the laser air spark”, Applied Physic s B, 68, 121-130 (1999).

[28] J.A. Aguilera, C. Aragón, “Characterization of a laser-induced plasma by spatially resolved spectroscopy of neutral atom and ion emissions: Comparison of local and spatially integrated measurements”, Spectrochimica Acta B, 59, 1861-1876 (2004).

[29] J.A. Aguilera, C. Aragón, “Multi-element Saha-Boltzmann and Boltzmann plots in laser-induced plasmas”, Spectrochimica Acta B, 62, 378-385 (2007).

[30] V. Lazic, R. Barbini, F. Colao, R. Fantoni, A. Palucci, “Self-absorption model in quantitative laser induced breakdown spectroscopy measurements on soils and sediments”, Spectrochimica Acta B, 56, 807-820 (2008).

[31] C.A. D´angelo, D.M. Pace, G. Bertuccelli, “Laser induced breakdown spectroscopy on metallic alloys: solving inhomogeneous optically thin plasmas” , Spectrochimica Acta B, 63, 367-374 (2008)

[32] L. Sun, H. Yun, “Correction of self-absorption effect in calibration-free laser-induced breakdown spectroscopy by an internal reference method”, Talanta, 79, 388-395 (2009).

[33] E. Tognoni, G. Cristoforetti, S. Legnaioli, V. Palleschi, A. Salvetti, M. Mueller, U. Panne, G. Gornushkin, “A numerical study of expected accuracy and precision in Calibration-Free Laser-Induced Breakdown Spectroscopy in the assumption of ideal analytical plasma”, Spectrochimica Acta B, 62, 1287-1302 (2007).

[34] E. Tognoni, G. Cristoforetti, S. Legnaioli, V. Palleschi, “Calibration-Free Laser Induced Breakdown Spectroscopy: State of the art”, Spectrochimica Acta B, 65, 1-14 (2010).

[35] M-L- Shah, A.K. Pulhani, G.P. Gupta, G. M. Suri, “Quantitative elemental analysis of steel using calibration-free laser-induced breakdown spectroscopy”, Applied Optics, 51, 4612-4621 (2012).

[36] S. Pandhija, N.K. Rai, A.K. Rai, S.N. Thakur, “Contaminant concentration in environmental samples using LIBS and CF-LIBS”, Applied Physics B, 98, 231-241 (2010).

[37] A. De Giacomo, M. Dell´Aglio, O. De Pascale, S. Longo, M. Capitelli, “Laser induced breakdown spectroscopy on meteorites”, Spectrochimica Acta B, 62, 1606-1611 (2007).

[38] M. Corsi, G. Cristoforetti, V. Palleschi, A. Salvetti, E. Tognoni, “A fast and accurate method for the determination of precious alloys caratage by Laser Induced Plasma Spectroscopy”, The European Physical Journal D, 13, 373-377 (2001).

[39] S. Pandhija, A. K. Rai, “In situ multielemental monitoring in coral skeleton by CF-LIBS”, Applied Physics B, 94, 545-552 (2009).

[40] I. Borgia, L. Burgio, M. Corsi, R. Fantoni, V. Palleschi, A. Salveti, M. C. Squarcialupi, E. Tognoni, “Self-calibrated quantitative elemental analysis by laser-induced plasma spectroscopy: application to pigment analysis”, Journal of Cultue Heritae 1, 281-286 (2000).

2. Laser Induced Breakdown Spectroscopy

This chapter contains a general overview of the LIBS theory for the understanding of the work presented in this thesis. Fundamentals of LIBS technique, a novel quantitative self-calibrated method based on LIBS, and novel techniques focused on enhancing LIBS features are described in the next sections.

2.1. Fundamentals of LIBS

Atomic Emission Spectroscopy (AES) can be used to determine the identity, the structure and the environment of atoms by analyzing the radiation emitted by them. If we know the characteristic lines emitted by an atom, then their appearance in a spectrum establishes the presence of that element in the source. In conventional AES methods e.g. Inductive Coupled Plasma Mass Spectrometry (ICP-MS), X-Ray Fluorescence (XRF), etc., the specific procedures and instrumentation are determined by the characteristics of the sample and by the type of required analysis (i.e. qualitative or quantitative) but generally those methods demand expensive equipment and results typically involve complex sample preparation and time consuming steps.

In a relatively new AES technique called Laser Induced Breakdown Spectroscopy (LIBS), vaporization and excitation of the source is produced by light (e.g. a laser pulse). In LIBS, a laser pulse is focused on/in a sample in order to produce laser ablation. Laser ablation produces plasma from which qualitative and quantitative information of the sample can be obtained. LIBS has many advantages compared with conventional AES-based analytical methods. Advantages such as simplicity, real-time analysis, no sample preparation, etc., position LIBS as a unique method of elemental analysis to interrogate any material – in solid, liquid or gas phase – for in-situ and real time in many real-life situations. Figure 2.1 summarizes graphically the fundamental processes of LIBS that will be discussed in this section. That is: a) Laser – matter interaction, b) plasma formation, c) emitted light, and d) superficial damage of a solid sample.

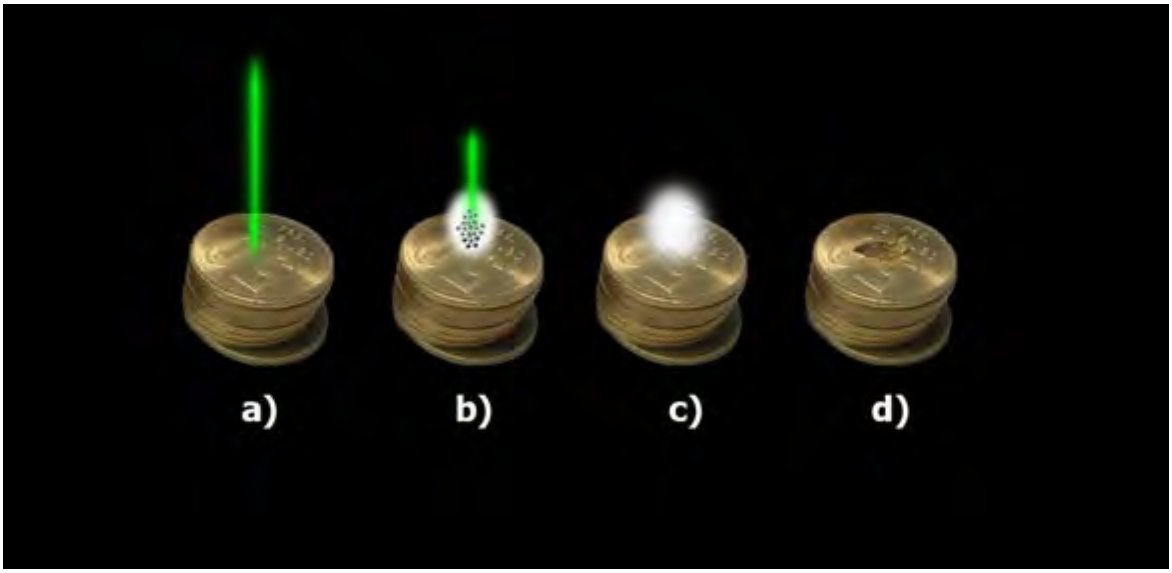

Figure 2.1. A schematic representation of the physical processes involved in LIBS: a) Laser – matter interaction, b) Plasma formation, c) Light emitted by the plasma, and d) crater formation.

a) Light-matter interaction

As mentioned before, in LIBS a laser pulse is focused on a surface sample to produce laser ablation. Laser ablation means using emitted laser energy to remove a portion of a sample by melting, fusion, sublimation, ionization and/or explosion [1]. Processes involved in laser ablation are complicated and depend on many laser pulse and material properties and involve many nonlinear effects. The following text describes the main parameters that influence laser-matter interaction.

A key parameter in laser ablation is the temporal width of the laser pulse. For example, for picosecond (ps) – femtosecond (fs) regimes, the laser energy is predominantly coupled into the material causing a fast transition from solid state to vapor phase prior to plasma formation. Coulomb explosion is the main bond breaking mechanism for those temporal regimes. In semiconductors and wide bandgap dielectrics, fs pulses produces electron-hole pairs by nonlinear processes such as multiphoton absorption, tunneling and avalanche ionization. For nanosecond (ns) laser pulses, thermal conductivity is the dominant mechanism that induces thermal vaporization (phase transitions occur from solid to liquid, liquid to vapor, vapor to plasma). The work presented in this thesis is based on the analysis of solid samples using ns-pulse width regime. For this reason, we are mainly interested in discussing processes and effects produced on ns temporal regime. Sub-nanosecond (ps or fs) pulse widths effects will be mentioned only for comparison purposes with the nanosecond regime if necessary.

Laser wavelength influences plasma formation, plasma development, and its properties. Shorter wavelengths, for instance, break down bonds easier than longer wavelengths and ionize atoms because of their higher photon energies. For example, a UV photon of 193 nm has a related energy of 6.4 eV. The bond energy of many elements are below the energy of a 193 nm photon and photoionization and non-thermal mechanisms may play a significant role in ablation and vaporization processes. Laser wavelengths also have a large influence in mass ablation rate, for shorter wavelengths are associated to higher mass ablation rates mainly because shorter wavelengths couple better into most of materials compared with longer wavelengths [1]. Nevertheless optimal wavelength coupling depends on the material properties, for example, IR wavelengths are highly reflected by metal targets, however, IR wavelengths couples better than UV wavelengths in aqueous solutions. On the other hand, longer wavelengths (IR) are associated with lower threshold fluences for laser-induced plasma as reported by Cabalín and Laserna [2]. For IR wavelengths, photon energies ionize atoms by inverse bremsstrahlung process; that is, photon energy of the pulse is transferred to continuously increase the kinetic energy of electrons in the generated vapor by sample breakdown.

Another key feature that strongly affects the laser – matter interaction is the phase of the sample. As discussed in Pasquini´s review [3], the way the plasma is initiated varies for different media. For solid targets the mechanisms of plasma initiation depends on the conductive nature of the sample. For metallic samples, ionization will start with absorption of laser photons by electrons on the conduction band. Those electrons will transfer its energy by collisions with the media (thermal conductivity). In semiconductor

and dielectric samples the creation of electron–hole pairs by multiphoton absorption is considered the main mechanism of vaporization. If the target is a gas, seed electrons will be generated by multiphoton absorption or cascade ionization. Tunnel effect can contribute at high irradiances (above 10^{12}W cm^{-2}). For liquid targets, the mechanism of breakdown is not well known. The liquid is treated as an amorphous solid but formation of initial seed electrons is described by cascade ionization and multiphoton absorption as well. Irradiance threshold needed for laser ablation depends on sample features, but typical values are in the range 10^8 – 10^{10} W/cm^2.

b) Laser-induced Plasmas

According to a conventional definition, ***Plasma*** *is a physical state of high electrical conductivity and mostly gaseous mechanical properties at high temperature* [4]. In other words, plasma can be seen as a highly ionized gas. But, where exactly a weakly ionized gas ends and where plasma starts may be easily misunderstood. Two fundamental characteristics of plasmas should be introduced for a more formal definition [5]. The Debye length λ_D should be much smaller than the plasma size.

$$\lambda_D = \left(\frac{\epsilon_0 T_e}{n_e e^2}\right)^{1/2} \qquad \text{Eq. (2.1)}$$

Where T_e and n_e represent electron temperature and electron density respectively (ϵ_0 is the permittivity in the vacuum and e stands for electron charge value). Physically, λ_D represents a separation distance between two opposite charges over which their field is

shielded out. The second fundamental characteristic of plasmas is the number of particles that should be inside a Debye sphere with volume given by $v = {}^{4}/_{3}\,\pi\lambda_D^3$. This number should be large enough to guarantee statistical Debye treatment (i.e. 1000 particles). Typical T and n_e values for laser induced plasmas fulfill Debye requirements. However, the acronym LIBS does not include the term "plasma" because LIBS is not always characterized by plasma formation. Sometimes, the Debye conditions are observed in LIBS experiments. Therefore, the use of the acronym LIPS (P stand for "plasma") is not recommended [6]. For simplicity, in LIBS, laser-induced plasmas (LIP) can be treated as a local assembly of atoms, ions, electrons and other particles in which charged species acts collectively remaining electrically neutral as assembly. The key parameters defining LIP are electron density and temperature and optical techniques already developed for diagnostics (Thomson scattering, plasma spectroscopy, interferometric techniques, etc.) of astrophysical plasmas can be successfully applied to characterize LIP. One of the most popular (and practical) techniques for electron density determination is the Stark broadening measurement. Stark broadening allows the determination of N_e of almost any chemical element. Stark broadening is usually appreciable for dense plasmas with $N_e \geq 10^{15} cm^{-3}$ emitting lines from only neutral and singled ionized species (for multiple ionized atoms Doppler effect tends to override Stark broadening). Therefore, the FWHM of spectral lines can be estimated for neutral atoms by:

$$\Delta\lambda_{1/2} = 2W\left(\frac{N_e}{10^{16}}\right) + 3.5A\left(\frac{N_e}{10^{16}}\right)^{1/4}\left[1 - \frac{3}{4}{N_D}^{1/3}\right]W\left(\frac{N_e}{10^{16}}\right) \qquad \text{Eq. (2.2)}$$

In this equation, the first term represents the electronic contribution and the second term represents a correction for ion contribution. Coefficients W, A, and N_D are slowly varying functions of the temperature T. Chapter 5 discusses the use of Stark broadening method for N_e estimation in a steel sample.

Strict thermodynamic equilibrium requires unbounded, spatially and temporally homogeneous plasma. In the laboratory, plasma spectroscopy deals with thermal equilibrium relations for level populations, particle velocity distributions and radiation fields less strict than in a blackbody radiator. For practical purposes in plasma spectroscopy Local Thermodynamic Equilibrium (LTE) is enough to describe the system through Boltzmann/Maxwell distributions. Among the various methods for temperature estimation, relative line intensity measurement is the most used technique in LIP. According to Boltzmann-Maxwell distributions, only two emission lines are necessary to obtain the temperature in the plasma, provided there is sufficient difference between their upper energy levels.

$$\frac{I_1}{I_2} = \frac{f_1 g_1 \lambda_2^3}{f_2 g_2 \lambda_1^3} exp\left[-\frac{E_1 - E_2}{kT}\right] \qquad \text{Eq. (2.3)}$$

Where E_1 and E_2 represents excitation energy levels from lines involved in the measurement, and $I, \lambda, g, \text{and } f$ represent intensity, wavelength statistical weight and oscillator strength of involved lines, respectively. However, Boltzmann plot technique uses several emission lines for specific specie achieving more accurate temperature estimation (More information about Boltzmann plots is presented in the next section). Saha-Boltzmann method may be used to increase the reliability on temperature calculation

using neutral and ionic lines improving the statistics; nevertheless lines with different ionization stages should appear in the spectrum and spectral information must be available for ionized lines (partition functions, transition probabilities, etc.). For detailed information about LIP characterization a topical review of Amoruso et al. can be consulted [7].

c) Laser induced plasma formation

Laser-induced plasma formation is a complicated event where heating, vaporization and plasma expansion occur simultaneously. Nevertheless, decoupling of the processes involved in plasma formation is carried out in order to simplify numerical models. As mentioned previously, when a high-power laser pulse hits a solid surface, a vapor over the surface is produced. The evaporated material will expand in a background gas or in vacuum. In the first case, vaporized material may interact with background gas (Helium, argon, air, etc.). For nanosecond laser pulses, the last part of the laser pulse may be absorbed by the expanded vapor forming plasma shielding. Plasma shielding influence how much material is ablated from the surface. In the plasma shielding process, the vapor absorbs laser energy and a higher ionization degree needed for plasma formation is achieved. The main mechanisms of laser absorption in laser-produced plasmas are inverse Bremsstrahlung and photoionization [8]. After the laser pulse ends, the plasma continues its expansion compressing the surrounding media and generating shockwaves. This interaction slows and limits the expansion of the plasma. The surrounding media will

influence the final plasma size, the speed of the expansion and the emission properties of the plasma.

d) Light emission of laser-induced plasmas

After plasma formation and continuum emission, ions and neutral atoms will emit discrete lines. Those spectral lines are characterized by its wavelength, shape and intensity. An electronic transition in any atom (neutral or ionized) from an upper energy level E_2 to a lower energy level E_1 determines the frequency (wavelength) of its emitted line. The frequency of the spectral line from the transition is given by:

$$h\nu_{21} = E_2 - E_1 \qquad \text{Eq. (2.4)}$$

Spectral line profiles and shifts are determined by broadening mechanisms. Doppler effect is a common broadening mechanism that produces Gaussian line profiles. Other common broadening mechanism is produced by the presence of intense electric fields in the plasma leading to symmetric Lorentz profiles. The presence of electric and magnetic fields by fast moving charges around emitting atoms inside the plasma modifies the atomic stationary states which results in shape broadening of emitted lines. This broadening mechanism is the so called Stark effect and it is responsible of shifting and splitting the energy levels of the emitting atoms. The Stark effect can be explained in terms of fast moving electrons around relatively slow ions and atoms in laser plasma environments. In

general, the Stark effect is the dominant broadening mechanism in LIBS plasmas and usually atoms emit light according to a Lorentzian profile having the form:

$$I(\nu) = I_0(\gamma/4\pi)^2/[(\nu - \nu_0)^2 + (\gamma/\pi)^2] \quad \text{Eq. (2.5)}$$

Where I_0 is the maximum intensity ν_0 and γ are the frequency at the line center and radiation damping respectively [1].

The intensity of a spectral line depends on the atomic population of the initial level as well as the transition probability to the final level, but also depends on the atomic concentration in the plasma. Spectral lines involving the ground state have larger transition probabilities and they are supposed to be more intense than lines that do not involve the atomic ground state.

Recombination between ions and free electrons is involved in the light emission process. Generally this process is characterized by a continuum emission due to the kinetic energy distribution of the electrons in the plasma. Free – free electronic collisions also correspond to a loss of kinetic energy and produce continuum radiation known as bremsstrahlung emission meaning “breaking radiation”. It is not easy to distinguish between both continuum emissions but in general recombination radiation is related to high frequencies and bremsstrahlung is related to lower frequencies. For nanosecond laser pulses, the continuum emission lasts several hundreds of nanoseconds.

e) Superficial damage

The laser-induced breakdown in a solid produces a crater in the sample surface. Crater size depends mainly on the amount of ablated mass. The amount of ablated mass is governed by many laser and material properties. Regarding wavelength, pulse duration, pulse energy, laser focused area, sample physical and chemical properties, an estimated crater size varies from some tens of μm to some hundreds of μm of diameter. Additionally, for nanosecond pulses, there is enough time for thermal wave propagation into the target. The thermal wave propagation may cause superficial damage by changing physical and chemical properties of the target beyond the produced crater.

2.2. Calibration Free LIBS technique

Until now, we have described LIBS as a powerful technique for in situ and real time analysis with advantages like simple or no sample preparation. These advantages position LIBS as a versatile technique for qualitative analysis, but the situation is different for quantitative analysis. In general, emission intensity of spectral lines from the analyte depends on the matrix where it is embedded. This matrix dependence leads to the necessity of calibration curves or matrix matched standards which in some practical situations are simply unavailable.

In 1999 a novel procedure, called Calibration Free Laser Induced Breakdown Spectroscopy (CF-LIBS), was proposed in order to overcome the mentioned matrix effect [9]. CF-LIBS procedure is based on the laser induced plasma physics allowing the possibility to perform quantitative analysis without calibration curves or matrix-matched samples. Instead of looking the matrix as an independent problem, CF-LIBS analyze matrix together with the analyte [8]. Here we describe briefly but concisely the procedure. For detailed information on CF-LIBS original publications can be consulted [9 – 11]. CF-LIBS procedure is based on considering both experimental and theoretical assumptions that simplify the analysis. Tognoni et al. summarized those assumptions and called them 0^{th} approximations [9]:

i) For stoichiometric analysis, the plasma composition is representative of the unperturbed target composition.

ii) The plasma is in local thermodynamic equilibrium (LTE) in the temporal and spatial observation window.

iii) The plasma can be modeled as a spatially homogeneous source.

iv) The spectral lines included in the calculation are optically thin.

v) Measured spectral range includes measurable lines from all elements present in the target.

For locally thin plasmas in LTE conditions, excited levels are populated according to Boltzmann distribution and ionization states obey Saha-Boltzmann equilibrium equation. For those specific conditions the integrated line intensity involving energy transitions E_k and E_i can be expressed as:

$$I_\lambda^{ki} = FC_s A_{ki} \frac{g_k e^{-(E_k/K_B T)}}{U_s(T)} \quad \text{Eq. (2.6)}$$

Where λ represents the wavelength of the transition, F is an experimental parameter that accounts for the optical collection efficiency and plasma density, C_s is the concentration of the emitting atom, A_{ki} is the transition probability, g_k is the k level degeneracy, K_B is the Boltzmann constant, T is the plasma temperature, and $U(T)$ is the partition function of the emitting species at plasma temperature.

Applying the following variable changes:

$$y = ln\left(I_\lambda^{ki}/g_k A_{ki}\right) \quad \text{Eq. (2.7)}$$

$$m = -1/K_B T \quad \text{Eq. (2.8)}$$

$$q_s = ln(C_s F/U_S(T)) \quad \text{Eq. (2.9)}$$

Equation (2.6) can be written as a linear equation in a two-dimensional space called the Boltzmann plane:

$$y = mE_k + q_s \quad \text{Eq. (2.10)}$$

Similar equations can be written for all species contained in the plasma. In LTE, all species have the same temperature value. Plasma temperature can be obtained by best linear fit of the points graphed in the Boltzmann plane according to equation 2.10.

The novelty of CF-LIBS is the use of the parameter q_s which is related with the concentration of the species C_S in the plasma. So, the concentration of all species can be calculated using the intersection value q_s of the linear regression in the Boltzmann plane:

$$C_S = \frac{U_S(T)}{F} e^{q_S} \qquad \text{Eq. (2.11)}$$

The F factor can be determined by normalizing the sum of all species concentration.

$$\sum_s C_s = \frac{1}{F} \sum_s U_s(T) e^{q_S} = 1 \qquad \text{Eq. (2.12)}$$

Spectroscopic parameters such as A_{ki}, g_k, E_k and U(T) can be retrieved from spectral databases [12 – 13].

2.3. Enhancing LIBS features

LIBS represents a powerful technique capable of characterizing the elemental chemical composition in a real-time, in-situ and non-contact way even for hazardous materials and hard-to-reach targets located at long distances from the LIBS set up. However, even all of those advantages, conventional LIBS has relatively poor sensitivity and reproducibility compared with conventional techniques. In this section we describe some techniques capable of enhancing LIBS sensitivity that have been developed in recent years.

Double pulse technique

Some elements are not easy to detect by LIBS such as halogens owing to their high excitation energy levels. For this reason LIBS sensitivity is limited in some applications such as geological and pharmaceutical ones. Increasing pulse energy generally increases the produced signal, but also increases sample damage and in some cases effects like self-absorption of some lines are more pronounced. One of the most attractive approaches to increasing LIBS sensitivity without losing LIBS advantages is the so called Double Pulse (DP) LIBS approach [1, 7, 14–15]. In DP-LIBS the addition of a second pulse increases the analytical performance of conventional LIBS through a better coupling between the laser pulse energy and the ablated matter [16]. Several set up configurations have been proposed for DP-LIBS (different geometric beam interaction with matter, combination of pulses with different wavelengths, delay times, energies, different collection geometries, etc.) and enhancement of the signal has been reported for all configurations. Two main geometries have been reported in the literature, collinear [17] and orthogonal [18–20] configurations (Figure 1.1). In collinear configuration, first and second pulses are propagated in the same path (collinear) and are focused orthogonally to the sample surface. In orthogonal configuration first and second laser pulses are propagated orthogonally from each other. When the first pulse hits the sample surface orthogonally and the second pulse (parallel to the sample surface) hits the plasma after certain delay time, the approach is called orthogonal reheating configuration. When the first pulse is propagated parallel to the surface sample, generating a spark and rarefying the near

atmosphere just above the sample, and a second pulse hits the sample surface in orthogonal direction, the approach is called orthogonal pre-ablation DP-LIBS. The mechanisms and physics causing the enhancement are not well understood yet and seem to be different depending on the set up configuration. For the orthogonal reheating set up, the enhancement is related with an increase in plasma temperature due to absorption and a better coupling of the second pulse energy with the plasma. For the orthogonal pre-ablative configuration, the enhancement is linked to the minimization of the atmospheric pressure created by the first pulse, where the plasma produced by the second pulse may be expanded easily. Reported results from many groups have been consistent with those mechanisms [14–20], however, further studies are necessary for a fully understanding of the processes involved in the enhancement for different configurations.

Resonance enhanced LIBS

Last decade Cheung's group demonstrated significant enhancement of LIBS sensitivity using a second resonant wavelength in double pulse configuration [21–22]. In this approach called resonance enhanced LIBS (RELIBS) authors showed that enhancement can be achieved minimizing continuum background by photo-resonant rekindling using resonant wavelengths as a second pulse. In DPLIBS configuration, typically a first laser pulse ablates the sample and a second pulse excites the species in the generated plasma after an inter pulse delay time. Basically, RELIBS differs from conventional LIBS and DP-LIBS in that plasmas are formed and heated by photoresonant excitation of the host

species in the plume, which means that chaotic explosion and intense continuum associated with thermal breakdown are avoided [7]. Additionally, by using an orthogonal configuration in conventional DP-LIBS or RELIBS approach, it is possible to minimize the superficial damage to a few nanograms (ng) or even less mass per pulse [23–25] making practically non-destructive analyses.

Plasma spatial confinement

Plasma spatial confinement has been reported recently as a cost-effective method for LIBS signal enhancement. Shock waves are produced when the laser induced plasma is generated in air. If shock waves may be reflected back (i.e. by a cavity) and reach the plasma, still in evolution, the reflected shock waves may compress the plasma plume. The compressed plasma leads to an increase on density particles, increasing collision rates between species. Higher collision rates will contribute to higher energy states in the atoms and consequently to an enhancement of the emission intensity. For spatial confinement, metal cavities with cylindrical shape, hemispherical shape and parallel walls have been proposed by some groups [26–28] reporting enhancement factors up to 12.

Spatial confinement of plasmas is a potential method for improving LIBS sensitivity and can be combined with other enhancing methods such as DP-LIBS approach [28] or magnetic confinement [29] without losing simplicity and cost effectiveness advantages. For example, Guo et al. reported an enhancement factor of 168 combining spatial confinement and DP-LIBS approaches [28]. A few papers have been published in the

literature and most of them rely on the experimental context but results showed that confinement is an appealing technique for enhancing signal without losing LIBS versatility.

2.4. References

[1] J. P. Singh, S. N. Thakur, “Laser-Induced Breakdown Spectroscopy”, Elsevier, 2007.

[2] L. M. Cabalín, J. J. Laserna, “”, Spectrochimica Acta B, 53 (1998), 723.

[3] C. Pasquini, J. Cortez, L. M. C. Silva, F. B. Gonzaga, “Laser induced Breakdown Spectroscopy”, Journal of the Brazilian Chemical Society, 18 (3), 463 – 512 (2007).

[4] Heinrich Hora, “Laser Plasma Physics: Forces and the nonlinear principle”, SPIE – The International Society for Optical Engineering, Bellingham, WA, 2000.

[5] R. J. Goldston, P. H. Rutherford, “Introduction to Plasma Physics”, Institute of Physics Publishing LTD, Philadelphia, PA, 1995.

[6] R. Noll, “Terms and notations for laser-induced breakdown spectroscopy”, Analytical and bioanalytical Chemistry, 385, 214-218 (2006).

[7] S. Amoruso, R. Bruzzese, N. Spinelli, R. Velotta, “Characterization of laser-ablation plasmas”, Journal of Physics B: Atomic and Molecular Optical Physics, 32, 131-172 (1999).

[8] A. W. Miziolek, V. Palleschi, I. Schechter, “Laser-Induced Breakdown Spectroscopy (LIBS): Fundamentals and Applications”, Cambridge University Press, New York, 2006.

[9] A. Ciucci, M. Corsi, V. Palleschi, S. Rastelli, A. Salvetti, E. Tognoni, “New Procedure for Quantitative Elemental Analysis by Laser-Induced Plasma Spectroscopy”, Applied Spectroscopy, 53 (8), 960 – 964 (1999).

[10] E. Tognoni, G. Cristoforetti, S. Legnaioli, V. Palleschi, “Review Calibration Free Laser-Induced Breakdown Spectroscopy: State of the art”, Spectrochimica Acta Part B 65, 1 – 14 (2010).

[11] E. Tognoni, G. Cristoforetti, S. Legnaioli, V. Palleschi, A. Salvetti, M. Mueller, U. Panne, I. Gornushkin, “A numerical study of expected accuracy and precision in Calibration-Free Laser-Induced Breakdown Spectroscopy in the assumption of ideal analytical plasma”, Spectrochimica Acta Part B, 62, 1287 – 1302 (2007).

[12] Kramida A., Ralchenko Yu, Reader J., and NIST ASD Team (2012). NIST Atomic Spectra Database (ver. 5.0), [Online]. Available: http:/physics.nist.gov/asd National Institute of Standards and Technology, Gaithersburg, MD.

[13] R. L. Kurucz, B. Bell, 1995 Atomic Line Data CD-ROM 23, Cambridge, Mass., Online available: http://www.cfa.harvard.edu/amp/ampdata/kurucz23/sekur.html, Smithsonian Astrophysical Observatory

[14] David A. Cremers and Leon J. Radziemski, “Handbook of Laser-Induced Breakdown Spectroscopy”, John Wiley & Sons Ltd., 2006.

[15] V.I. Babushok, F. C. DeLucia Jr., J. L. Gottfried, C. A. Munson, A. W. Miziolek, “Double pulse laser ablation and plasma: Laser induced breakdown spectroscopy signal enhancement”, Spectrochimica Acta Part B, 61, 999 – 1014 (2006).

[16] C. Gautier, P. Fichet, D. Menut, J. L. Lacour, D. L’Hermite, J. Dubessy, “Study of the double-pulse setup with orthogonal beam geometry for laser-induced breakdown spectroscopy”, Spectrochimica Acta Part B, 59, 975 – 986 (2004).

[17] C. Gautier, P. Fichet, D. Menut, J. Dubessy, “Applications of double-pulse laser induced breakdown spectroscopy (LIBS) in the collinear beam geometry to the elemental analysis of different materials”, Spectrochimica Acta Part B, 61, 210 – 219 (2006).

[18] J. Uebbing, J. Brust, W. Sdorra, F. Leis, K. Niemax, “Reheating of Laser-Produced Plasma by a Second Pulse Laser”, Applied Spectroscopy, 45 (9), 1419 – 1423 (1991).

[19] C. Gautier, P. Fichet, D. Menut, J. L. Lacour, D. L’Hermite, J. Dubessy, “Quantification of the intensity enhancements for the double-pulse laser-induced breakdown spectroscopy in the orthogonal beam geometry”, Spectrochimica Acta Part B, 59, 975 – 986 (2004).

[20] G. Cristoforetti, “Orthogonal Double-pulse versus Single-pulse laser ablation at different air pressures: A comparison of the mas removal mechanisms”, Spectrochimica Acta Part B, 64, 26 – 34 (2009).

[21] S. Y. Chan, N. H. Cheung, “Analysis of Solids by Laser Ablation and Resonance-Enhanced Laser-Induced Plasma Spectroscopy”, Analytical Chemistry, 72, 2087 – 2092 (2000).

[22] W. L. Yip, N. H. Cheung, “Analysis of aluminum alloys by resonance-enhanced laser-induced breakdown spectroscopy: How the beam profile of the ablation laser and the energy of the dye affect analytical performance” Spectrochimica Acta B, 64, 315-322 (2009.)

[23] S. L. Lui, N. H. Cheung, “Minimally Destructive Analysis of Aluminum Alloys by Resonance-Enhanced Laser-Induced Plasma Spectroscopy”, Analytical Chemistry, 77, 2617 – 2623 (2005).

[24] M. Suliyanti, A. Hidayah, M. Pardede, E. Jobiliong, S. Abdulmadjid, N. Idris, M. Ramli, T. Lie, R. Hedwig, M. Tijia, K. Kurniawan, Z. Lie, H. Niki, K. Kagawa, “Double pulse spectrochemical analysis using orthogonal geometry with very low ablation energy and He ambient gas”, Spectrochimica Acta B, 69, 56-60 (2012).

[25] N. H. Cheung, “Spectroscopy of Laser Plumes for Atto-Mole and ng/g Elemental Analysis” Applied Spectroscopy Reviews, 42, 235 – 250 (2007).

[26] X. K. Shen, X. N. He, H. Huang, Y. F. Lu, “Spatial Confinement Effects in Laser-Induced Breakdown Spectroscopy”, Conference Paper, Laser Applications to Chemical, Security, and Environmental Analysis (LACSEA), San Diego CA, 2010.

[27] L. B. Guo, C. M. Li, W. Hu, Y. S. Zhou, B. Y. Zhang, Z. X. Cai, X. Y. Zeng Y. F. Lu, “Plasma confinement by hemispherical cavity in laser-induced breakdown spectroscopy”, Applied Physics Letters, 98, 131501 1-3 (2011).

[28] L. B. Guo, B. Y. Zhang, X. N. He, C. M. Li, Y. S. Zhou, T. Wu, J. B. Park, X. Y. Zeng, Y. F. Lu, “Optimally enhanced optical emission in laser-induced breakdown spectroscopy by combining spatial confinement and dual-pulse irradiation”, Optics Express, 20 (2), 1436 – 1443 (2012).

[29] L. B. Guo, W. Hu, B. Y. Zhang, X. N. He, C. M. Li, Y. S. Zhou, Z. X. Cai, X. Y. Zeng, Y. F. Lu, “Enhancement of optical emission from laser-induced plasmas by combined spatial and magnetic confinement”, Optics Express, 20 (2), 1436 – 1443 (2012).

3. Instrumentation and experimental procedures of LIBS

A general overview of LIBS technique was presented in chapter 2. This chapter presents a brief description of implemented instrumentation in our experimental set up. After experimental set up description for both SP-LIBS and DP-LIBS, we report the sample preparation methodology, used in the analysis of pharmaceutical samples and the procedure followed for all LIBS signal measurements.

3.1. Instrumentation of LIBS

Figure 3.1 illustrates the main components of a conventional LIBS set up. Main components include a laser, a focusing lens, a detection system to spectrally resolve the collected light and a computer to process the signal and data storage. The specifications of each main component depend on LIBS applications. In this section we will give a general overview of the three major components and the specific apparatus used in our implemented experimental set up.

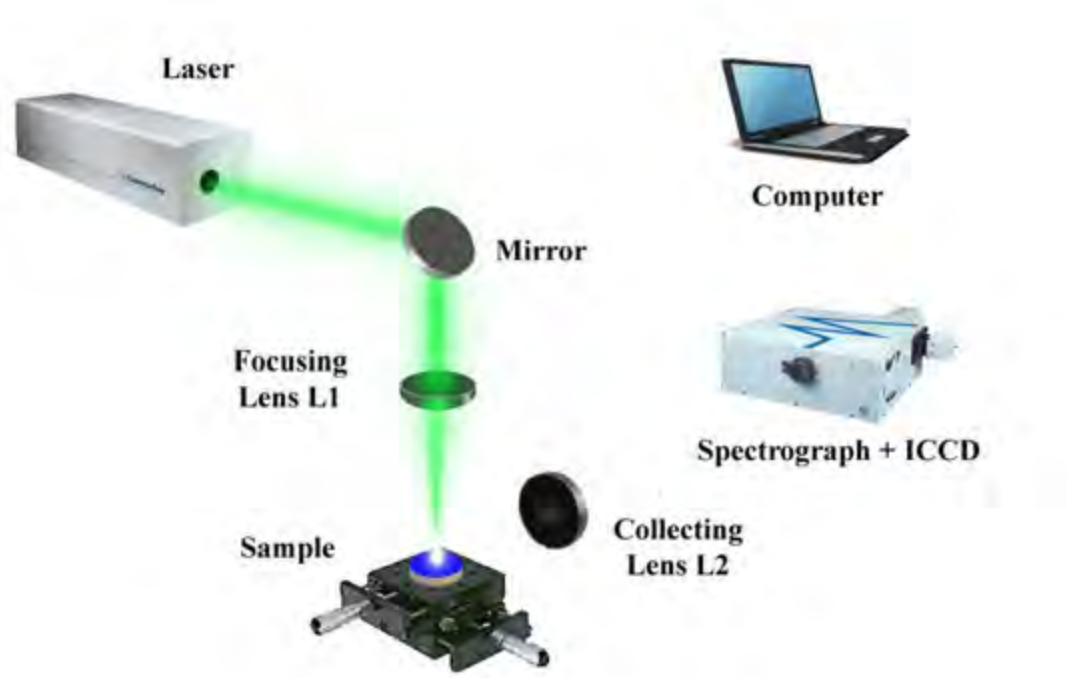

Figure 3.1. Typical LIBS experimental set up. In the illustration, laser pulses are focused over a sample mounted on an X-Y translational stage. Plasma light is collected by a bi-convex lens and focused into the slit of a spectrometer for spectra analysis.

For Raman experiments, a notch filter was placed between collecting lens L2 and the entrance slit of the spectrograph in order to filter laser radiation (532 nm). This set up was used in the analysis of excipients from pharmaceutical samples.

Laser system

The most common solid state laser source for LIBS instrumentation is the Q-switched Nd:YAG laser system. This flash lamp pumped laser has typical pulse widths in the range 6 – 15 ns and a fundamental wavelength at 1064 nm which is easily converted onto shorter wavelengths (532 nm, 355 nm and 266 nm) using nonlinear crystals via harmonic

generation processes. Nd:YAG lasers are commercially available with a relatively high output pulse energies (from mJ to J) , broad repetition operation rate (1 – 50 Hz) and in a broad range of sizes allowing both robust laboratory and portable LIBS systems. Other ns pulse laser systems, such as excimer lasers or CO_2 lasers, are also used by some groups around the world. Nowadays the use of femtosecond lasers is becoming more frequent in LIBS. For SP-LIBS experiments, a pulsed Nd:YAG laser (Quanta-Ray PRO-Series) operating at 532 nm with a 6 – 10 ns FWHM pulse duration at 10 Hz repetition rate was used for all the experiments. The used pulse energy depends on the experimental configuration, but typical values for conventional single pulse LIBS were in the range of 10 – 20 mJ for most experiments. For DP-LIBS experiments, we use two different pulses, an ablating pulse and a reheating pulse, produced by an Nd:YAG laser and an optical parametric oscillator (OPO), respectively, at 10 Hz repetition rate and 10 ns pulse duration. Pulses from the frequency doubled output of the Nd:YAG (532nm) were used as ablative pulses in both, SP-LIBS and DP-LIBS experiments. The reheating pulses tuned to 506 nm were optically delayed by 10 ns (with respect to the ablative pulses) by increasing their optical path length and the energy pulse was fixed at 7 mJ for all experiments. For Raman experiments, laser pulse energy was minimized in order to avoid laser ablation on the samples.

Sample holder

One important parameter that affects precision and accuracy in LIBS quantitative analysis is the known lens-to-sample distance LTSD. LTSD determines the irradiance on the

sample's surface and small variations affect considerably the ablated mass, the emission line intensities, and plasma features such as plasma temperature [1]. In order to avoid or minimize LTSD variations a custom-made sample holder was manufactured. Figure 3.2 shows a schematic representation of the sample holder. The main task for the sample holder was to keep constant the LTSD in the analysis of anti-diabetic tables by calibration curves technique. For this specific application, many tablets with different thicknesses were prepared as described in the next section. The sample should be thicker than the aluminum cover in order to press the EVA layer and assure LTSD constant. The sample holder was mounted on an X-Y stage allowing several shots at different places on the tablet surface. Other flat samples like steel or geological stones can be fixed in the same holder using a different (bigger hole in the) aluminum cover.

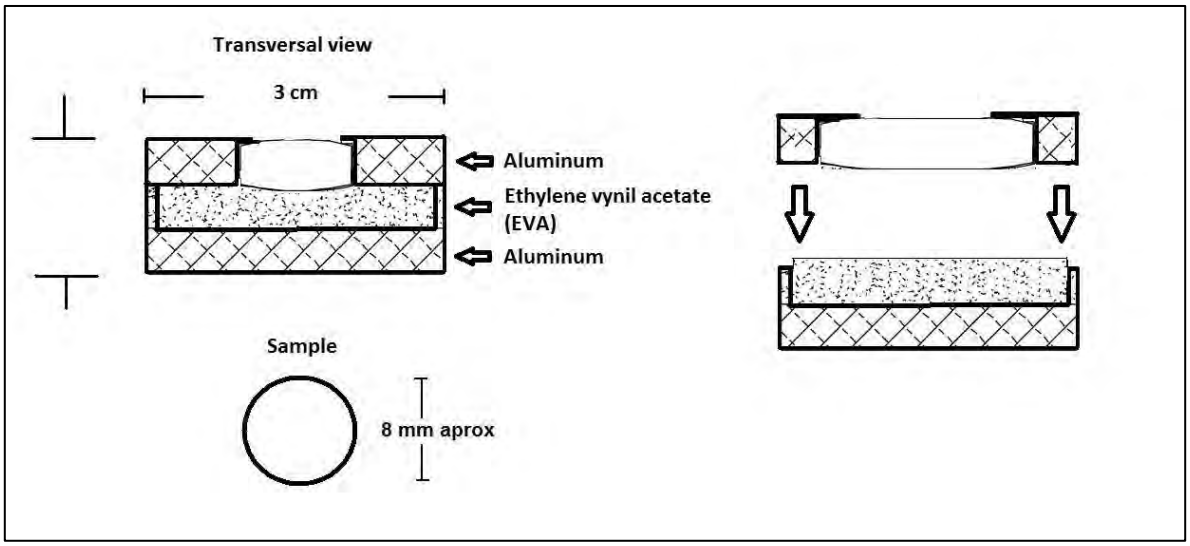

Figure 3.2. Schematic representation of a custom-made sample holder. Lens to sample distance (LTSD) may be constant for samples with different thicknesses.

Focusing and light collection system

In LIBS, laser pulses can be focused by lenses and mirrors. Typically a single lens is enough to focus a laser pulse in order to achieve laser ablation. But for some applications, mainly when LTSD needs to be adjustable, a more complex focusing system needs to be implemented. In our experiments, a single lens with a focal length of 150 mm was used to focus laser pulses. All focusing and collecting lenses used are made from BK-7 material with 25 mm diameter.

For light collection lenses, mirrors and fiber optic cables can be used. We used two different configurations for different experiments: lens system for SP-LIBS experiments and lens-fiber optics cable configuration for DP-LIBS experiments. A lens system consisting in two bi-convex lenses was first implemented in LIBS set up for plasma light collection. The system collects light efficiently and was used for the analysis of anti-diabetic tablets. As a drawback of this system, material ejection from the plasma production processes can damage the lenses because plasma is produced close to the lenses due to the short focal length of the system. In lens-fiber configuration, a single 100 mm focal length bi-convex lens couples light into a circular bundle end of 19 individual fibers. The lens was positioned at 2 focal length from both sample and fiber bundle end for an optimized light collection. The fiber bundle is configured as a circular array at one end and linear array at the other end. The linear array was coupled to the linear entrance slit of the spectrometer.

Spectrograph

The basics of LIBS stands on the time resolved detection of atomic spectra generated by the laser produced plasma. Important features of a good spectrometer for LIBS detection are: spectral resolution and wide band spectral range. Czerny-Turner spectrometers are widely used in order to disperse LIBS signal. Czerny-Turner spectrometers have a good spectral resolution but for many applications spectral range is limited to few nanometers (~40nm). Sequential measurements in different ranges of the spectrum allow the detection on a wider range but this procedure limits LIBS measurements to homogenous samples. For inhomogeneous samples, plasmas may be different from one area to another, producing shot to shot variations in the analysis. Spectrometers that perform simultaneous detection over a wide spectral range are Paschen–Runge and Echelle spectrometers. Echelle spectrometer has been used more frequently for LIBS measurements. The main advantages of Echelle system is its excellent resolution (comparable with best Czerny-Turner spectrometers) and the broad spectral range (200 – 780 nm). Those advantages make possible simultaneous multi-elemental analysis practically in the complete UV-VIS spectral rage avoiding spectral interferences and improving the LIBS figures of merit.

In our experiments, light was collected and focused into a 0.5 meter focal length Czerny-Turner spectrograph (Spectra Pro 500i Action Research Corp.) and spectrally dispersed by a 1200 grooves/mm grating and detected by an ICCD camera (Princeton Instruments, Inc.). Depending on the spectral range, light is dispersed with a spectral resolution of 0.04 (UV) – 0.3 nm (NIR).

Detector

Detection of light after its dispersion can be achieved using the simplest type of photodetectors such as photomultiplier tubes (PMT) or photodiodes (PD) or using complex array detectors such as photodiode arrays (PDA) or charge-coupled devices (CCD). PMTs or PDs are high speed detectors with the main advantage of having high sensitivity in the visible spectral region. As a drawback, for simultaneous detection of many lines, one PD should be used for each specific line. On the other hand, array detector devices collect light in a wide period of time (typically microseconds) but can detect simultaneously broad spectral ranges. Linear and bi-dimensional arrays of several sensors in one device such as photodiode arrays (PDA) and charge couple devices (CCD) have been intensively used in LIBS set ups. The higher number of sensors in the array, the higher the resolution acquired by the detector. Both PDA and CCD detectors may employ a sensitizer or intensifier for signal enhancement. Currently, Echelle spectrometers combined with intensified charge coupled devices (ICCD) represents the most powerful combination for LIBS analysis.

We used a detector (1024x256 pixel array) that covers a spectral window of 40 nm when the central wavelength is in the UV range, and approximately 35 nm when it is in the NIR range. For all experiments, laser pulse and detection system were synchronized in order to avoid bremsstrahlung and early plasma emission. Figure 3.1 at the beginning of this chapter shows the schematic experimental set up implemented.

3.2. Sample preparation

One of the advantages of LIBS is the minimal or non-sample preparation (over conventional techniques); nevertheless, for quantitative analysis this advantage is not always a fact. However, sample pre-treatment in LIBS is simple and generally does not require additional hazardous chemical compounds or solvents at all and consequently, the analysis remains environmentally friendly. This section describes a typical sample preparation step for powder samples such as pharmaceutical tablets. In brief, synthetic and commercial anti-diabetic tablets were grinded and mixed with a reference element (Br) and mechanically compressed in order to manufacture a solid sample that can be mounted in the previously described sample holder.

All experiments were performed with analytical reagent grade chemicals. Metformin hydrochloride ($C_4H_{11}N_5 \bullet HCl$) and Glyburide ($C_{23}H_{28}ClN_3O_5S$) were obtained from Sigma Aldrich, USA. Excipients were purchased from Química Meyer Mex. The internal standards, KBr and Benzophenone were obtained from PIKE Technologies, USA and Sigma-Aldrich, USA, respectively; K_2HPO_4 and H_3PO_4, were also obtained from PIKE Technologies, USA. High purity ethanol (99.5%) was used in sample preparation. HPLC grade methanol (Merck, USA) and ultrapure water were used for preparing mobile phase solutions.

Synthetic samples were prepared by grinding the analyte, excipient and internal standard altogether in an agate mortar. Samples were prepared starting with quantity A (mg) of

analytical standard and mixing with quantity B (mg) of excipient. The quantity A was selected according to the desired Cl concentration and the total sum of A and B was 400 mg for all synthetic samples. As a reference, 100 mg of internal standard (KBr) were added to improve quantitative measurements. So as to procure an optimal mixture, the grinding step in the agate mortar was performed in ethanolic suspension; this promotes smaller particle size and better homogenization. The mixing process was repeated twice until the sample was dried. After the mixing process, the sample was compacted under controlled pressure. The obtained samples were 8mm diameter circular tablets.

In addition, four commercial samples for each active agent were prepared as follows: ten commercial tablets from the same box were grinded and mixed in order to obtain an appropriate sampling process. Then again, 400 mg of grinded pharmaceutical product, and 100 mg of internal standard were homogenized in ethanolic suspension, as described in the previous paragraph. Three replicates were made for all different samples (both synthetic and commercial).

3.3. Procedures

This section describes the typical procedure to obtain LIBS signal for qualitative and quantitative analysis. Usual delay time, $t_{d,}$ and gate time, $t_{g,}$ were on the microsecond scale. Those times scales were selected to optimize signal to background ratio (SBR) for

each experiment. Figure 3.3 illustrates the temporal evolution of the signal in a typical LIBS experiment.

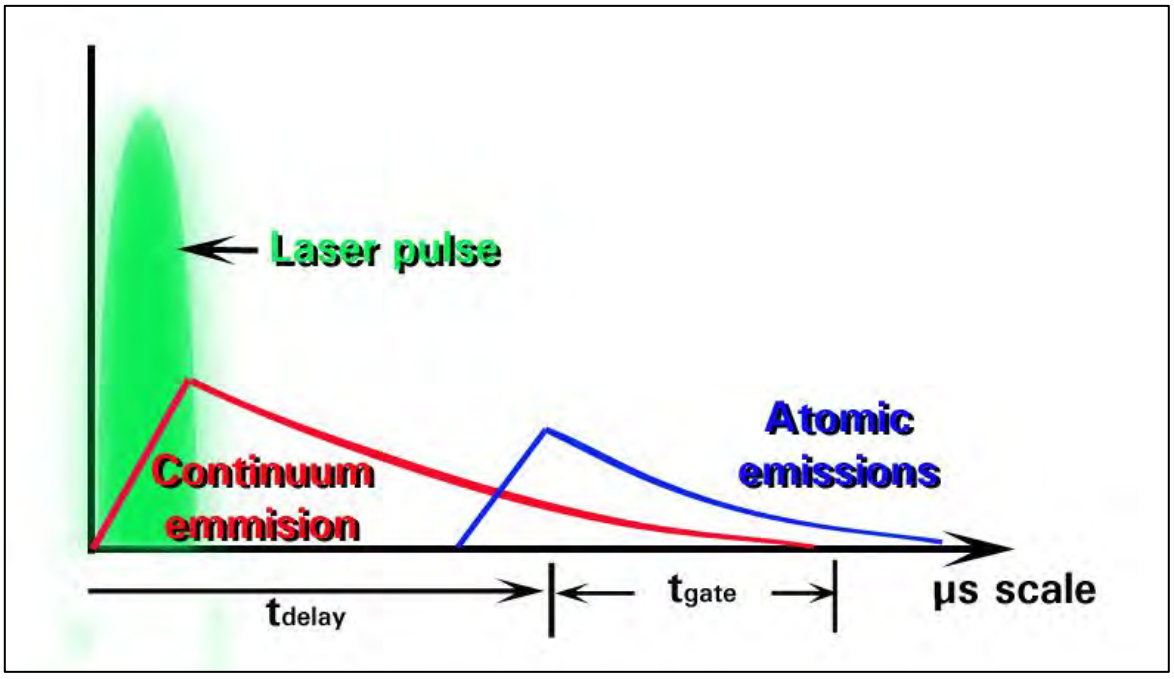

Figure 3.3. Temporal emission evolution of plasma is in the microsecond scale. Delay time and gated time for data acquisition depend on energy, sample properties and other parameters. Typical delay time values in our experiments are about 200 ns. Gate time values for signal acquisition are between 1 – 10 µs.

The possible non-uniformities of the laser energy and heterogeneities on the surface sample were minimized by averaging 10 spectra acquisitions from 50 different places on each tablet surface. For a given sample the average of 500 spectra took less than one minute, giving a single spectrum for each analyzed tablet. Repeatability was observed by analyzing each sample three times. Typical t_d values for the best SBR were on the ns scale (e.g. 300 ns) and t_g on the µs scale (e.g. 2 µs). The rest of background and continuum

emissions were subtracted from the integrated line intensity. Spectral correlation was performed using homemade software on the Matlab platform (MATLAB, The MathWorks Inc.) via the atomic spectral database from NIST [2]. Data processing and calculations were made in OriginPro software (OriginPro 6 1991–2007 OriginLab Corporation). Lorentzian fit was performed before the intensity ratio analysis.

3.4. References

[1] David A. Cremers and Leon J. Radziemski, "Handbook of Laser-Induced Breakdown Spectroscopy", John Wiley & Sons Ltd., 2006.

[2] Kramida A., Ralchenko Yu, Reader J., and NIST ASD Team (2012). NIST Atomic Spectra Database (ver. 5.0), [Online]. Available: http:/physics.nist.gov/asd National Institute of Standards and Technology, Gaithersburg, MD.

4. Results and discussion of quantitative analysis

The main goal of analytical methods is to provide with high precision and accuracy quantitative information for any sample. For quantitative information (concentration of constituents in a sample, absolute mass, surface concentration, etc.) an auxiliary technique known as calibration curve is usually employed. In calibration curves a linear relationship between element response and the mass or concentration of the analyte over a certain range is plotted. Most analytical techniques are based on calibration curves to obtain quantitative information.

This chapter presents two examples of quantitative analyses based on LIBS measurements; one of them tests the widely used technique of calibration curves and the other example tests the promising self-calibrated method known as Calibration Free (CF) – LIBS presented in chapter 2. LIBS performance characteristics, such as linearity and limit of detection (LOD), will be validated by calibration curves solving the specific problem of quantifying an active ingredient in pharmaceutical samples. After LIBS validation using a standard calibration method, Calibration Free LIBS technique will be tested for quantitative analysis in a stainless steel sample.

4.1. Quantitative analysis based on Calibration curves

The aim of this study was to develop a new rapid, accurate, economic and environmentally friendly method for industrial analysis of anti-diabetic active pharmaceutical ingredients (API) based on LIBS and supported by calibration curves and the addition of Internal Standards for improving the analytical performance. A brief description of the importance of anti-diabetic tablets as well as the nature of pharmaceutical samples is presented first. Then, quantitative results based in calibration curves are discussed. All experiments were performed at ambient conditions. Calibration curves were obtained by plotting the ratio of analyte signal to internal standard signal as a function of analyte concentration. For quantitative analysis eight different commercial anti-diabetic brands were tested with calibration curves. Furthermore, excipients such as calcium carbonate (CaCO3), lactose (C12H22O11H2O), talc (3MgO*4SiO2*H2O) and starch ($C_6H_{10}O_5$) were studied by LIBS and Raman spectroscopy to characterize them and to select an adequate excipient for synthetic sample preparation. Quantitative results were compared and validated with results from a standard method used as reference.

General overview

Control of the API content and a uniform distribution of lubricants and other components in commercial products are important to guarantee the quality of pharmaceuticals

worldwide. HPLC is by far the primary technique used to provide quantitative information of pharmaceutical samples. Nevertheless, the technique is time-consuming, expensive, and cannot be applied for on-line and real time monitoring production processes. In contrast, LIBS can detect the presence of elements in a sample in a more versatile way as stated in chapter 2. Besides, LIBS requires no additional chemical compounds or solvents at all, consequently, the analysis becomes environmentally friendly.

Pharmaceutical analysis presented in this section is performed on anti-diabetic samples. Diabetes represents one of the main chronic diseases around the world. Nowadays more than 340 million people worldwide have diabetes and World Health Organization (WHO) projects that diabetes deaths will increase by two thirds between 2008 and 2030 [1]. Besides the increase of diabetes, the production of both counterfeit and low quality drugs is increasing and this fact also affects human health and generates profit losses to pharmaceutical industries [2]. Type 2 diabetes is characterized by high glucose concentration in the blood, which is caused by both low pancreas secretion and reduced sensitivity of insulin. Currently, there is a wide variety of oral agents clinically available to help regulate glucose levels in blood such as sulfonylureas, meglitinides, biguanides, and thiazolidinediones [3, 4]. Sulfonylureas, such as glyburide or glybenclamide (Gly), glipizide, and glimepiride interact with sulfonylurea receptors on pancreatic β-cells to enhance insulin secretion and decrease blood-glucose levels. On the other hand, metformin (Met), the most common biguanide clinically available, decreases hepatic glucose production and increases the sensitivity of peripheral tissues to insulin [5]. At present, the blend of

Gly/Met is the oral drug combination of choice in clinical practice [6]. Quantitative analysis in this section is based on those most common anti-diabetic oral drugs, i.e. Met and Gly.

Results and discussion

An optical fingerprint of biguanides and sulfonylureas can be obtained by measuring the spectral emission of certain elements such as Cl. Halogen atoms, e.g. Cl, are characteristic in active ingredients but they are not contained in other components of the pharmaceutical sample (lubricant, coating, etc.). Figure 4.1 shows the molecular structures of Metformin and Glyburide. Met contains mostly C, N and H atoms, but every Met molecule contains also a single Cl atom. In the case of Gly, also a single Cl atom is present for each molecule. Thus, quantifying Cl atoms is possible to quantify Met and Gly in pharmaceutical tablets.

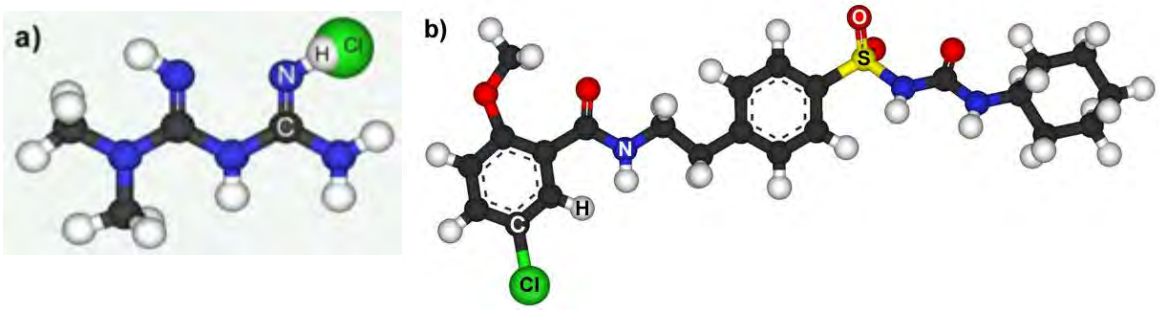

Figure 4.1. a) Metformin and b) Glyburide molecular structures. Halogen atoms, like Cl, are present in Active Pharmaceutical Ingredients (APIs).

For quantitative analysis, synthetic samples were prepared by varying its Cl concentration in order to perform calibration curves. The intensity of the Cl signal in the LIBS spectrum is linearly proportional to its content in the sample. To determine the Cl concentration, the integrated line intensity (peak area) from one Cl line of LIBS spectrum is plotted versus its concentration. If the concentration increases, the integrated line increases. The integrated line intensity can be improved by using the signal of an internal standard as specific reference, e.g., Br. After the addition of the internal standard, integrated line intensities from both elements (Cl and Br) will be affected equally by shot-to-shot pulse variation; this fact minimizes the error caused by possible energy variation during the experiment and any other variable instrumental response e.g. instrumental line broadening. In the following text ''Cl–Br ratio'' means the integrated line intensity ratio from analyte (Cl) peak and the internal standard (Br). The symbol (I) is used for first ionized species.

Synthetic samples may be divided in two sets depending on the target analyte used, that is: Met and Gly sets. For each set, an average calibration curve was obtained by using the Cl-Br ratio and the Cl concentration. The dynamic range of calibration curves were chosen to cover the Cl concentration from commercial samples.

Qualitative analysis

Frequently, matrix effects are the source of error on the quantitative determination of sample concentration in LIBS spectroscopy. Therefore the use of the same excipient for the synthetic samples as for the commercial formulations is of special importance. Typical

excipients used in the pharmaceutical industry such as calcium carbonate ($CaCO_3$), lactose ($C_{12}H_{22}O_{11}H_2O$), talc ($3MgO*4SiO_2*H_2O$) and starch ($C_6H_{10}O_5$) were characterized using LIBS and Raman spectroscopy.

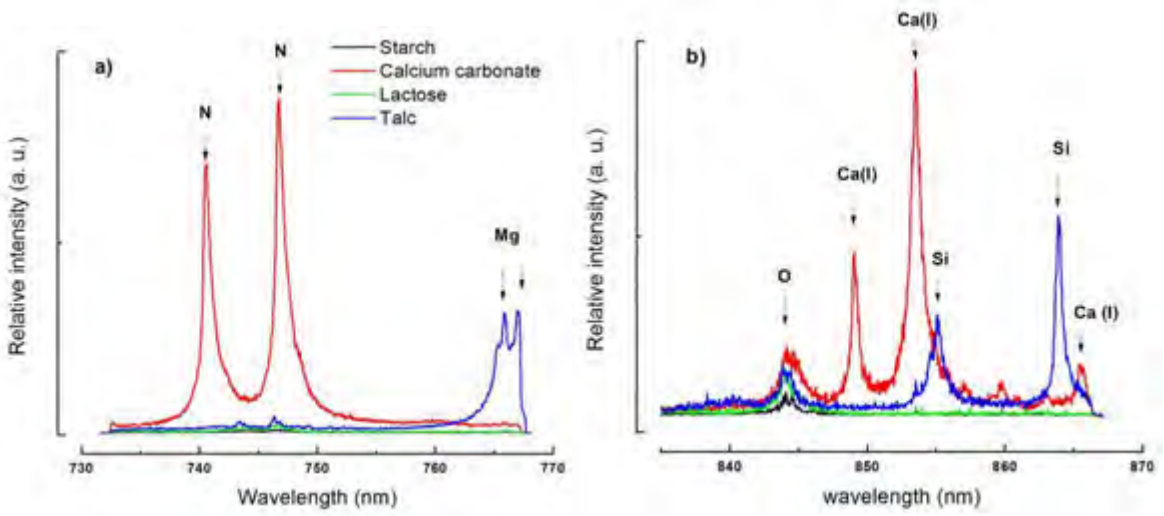

Figure 4.2. Typical excipients used in anti-diabetic tablets show spectral differences between each other over the visible-NIR region. As an example, it is shown two spectral windows at (a) 732-769nm and (b) 833-867nm. Spectral differences can be used as particular excipient optical "fingerprints". Lactose and starch present only weak N signals.

As can be seen in figure 4.2, LIBS spectra from two different wavelength ranges were evaluated from the above mentioned excipients. Particularly Mg and Ca(I) emissions (talc and calcium carbonate shown in figure 4.2 (a) and 4.2 (b), respectively) are present in those selected spectral windows. In the case of lactose and starch it is more difficult to identify its optical fingerprint in air due to their chemical composition (C, O, and H). Nevertheless, it is possible to identify excipients by Raman spectroscopy using the same

experimental set up as for LIBS. We performed Raman spectroscopy by adding a notch filter and changing some experimental parameters in order to avoid laser ablation (lens to sample distance, laser energy and time acquisition parameters t_d and t_g). In the case of Met, it is not possible to identify the excipient because all significant Raman emission bands correspond to the Metformin molecule due to its high concentration contents in all commercial samples (around 90%). For the Gly set, Raman spectroscopy identifies lactose as the excipient for all the commercial formulations as shown in figure 4.3. In this figure, the reference 1 represents a lactose reference spectrum from a Raman database, reference 2 represents the spectrum of analytic grade lactose and numbers 1-4 represents spectra for all four commercial samples. Therefore lactose was used as excipient for both Met and Gly sets of synthetic samples for LIBS experiments.

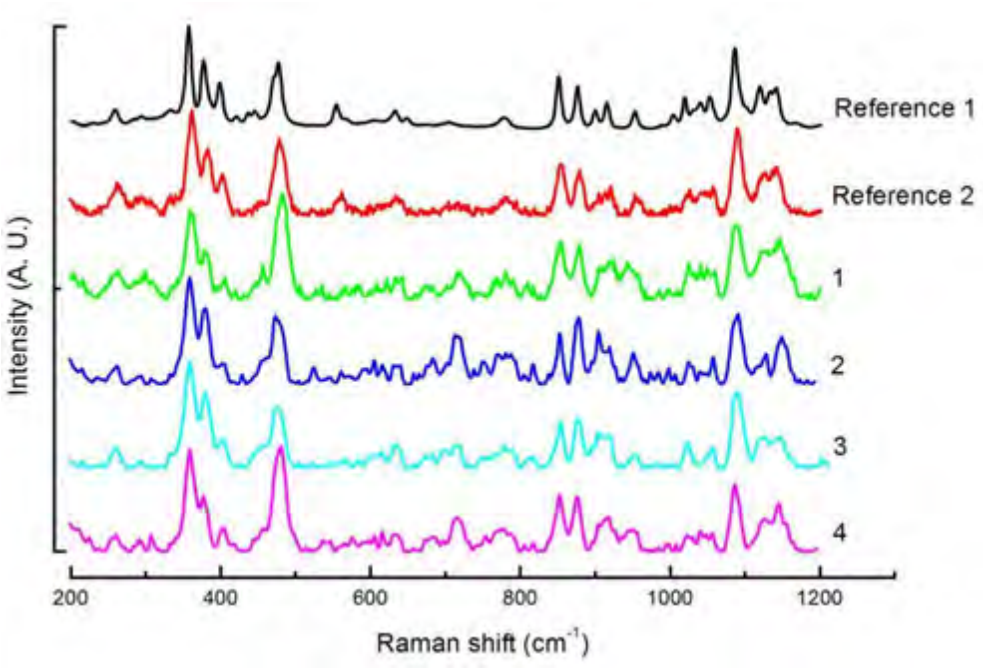

Figure 4.3. Raman spectra (200-1200cm-1) from two references of lactose and four commercial samples containing Gly as API and lactose as excipient.

Quantitative analysis

Internal standard

The fundamental principle of internal standard in chemical analysis is based on the addition of a component that has similar physicochemical properties than the analyte (depending on the pretreatment procedure). The internal standard should present chemical stability under experimental conditions; no spectral interactions between the internal standard and the analyte, nor with other sample components. It should be soluble in the assay medium and should not be a natural component of the sample. In this work, potassium bromide (KBr) was chosen as internal standard because Br and Cl have similar spectral and chemical characteristics, e.g. both elements have high and comparable first potential ionization values (13.01 and 11.84 eV for Cl and Br respectively) remaining mostly neutral if laser energy fluctuations occur throughout the experiment. Spectral databases show that the strongest single emission lines from Br and Cl (827.44 and 837.59 nm respectively) are sufficiently close to be detected simultaneously in the same spectral window for the Czerny-Turner spectrograph. Furthermore, there are no interference signals from K in the spectral window of interest [7]. In addition to the spectral characteristics, KBr is highly soluble in ethanol, so the homogenization in the sample preparation process was enhanced. Resolved individual signals from Br and Cl at 827.24 and 837.59 nm, respectively, were used for the Cl-Br ratio in the quantitative analysis. Figure 4.4 (a) shows the spectrum of the commercial sample of Met with 10% (weight

percent) of Cl concentration and the internal standard between 812 and 847 nm. The spectrum shows the emission of neutral and ionic species from Met such as N, N(I) and Cl and the emission of Br from the internal standard. It should be pointed out that the emission of N, N(I) and O from the API could not be discriminated from emissions of the same species present in atmospheric air. Nevertheless, air signals do not interfere with the Cl and Br lines of interest. On the other hand, Figure 4.4 (b) shows a LIBS spectrum of a commercial sample of Gly with a Cl concentration of 0.19% (weight percent). With the purpose of resolving the Cl emission at 837.59 nm, higher energy than that used for Met was employed. Thus, the emission of N, N(I) and Cl was enhanced compared with Met signal. Notice that the O signal is not spectrally resolved because of the broadening of the N(I) line at 845nm due to the use of higher pulse energy. Therefore, same spectral range but different energy and time parameters were used for the analysis of each active agent.

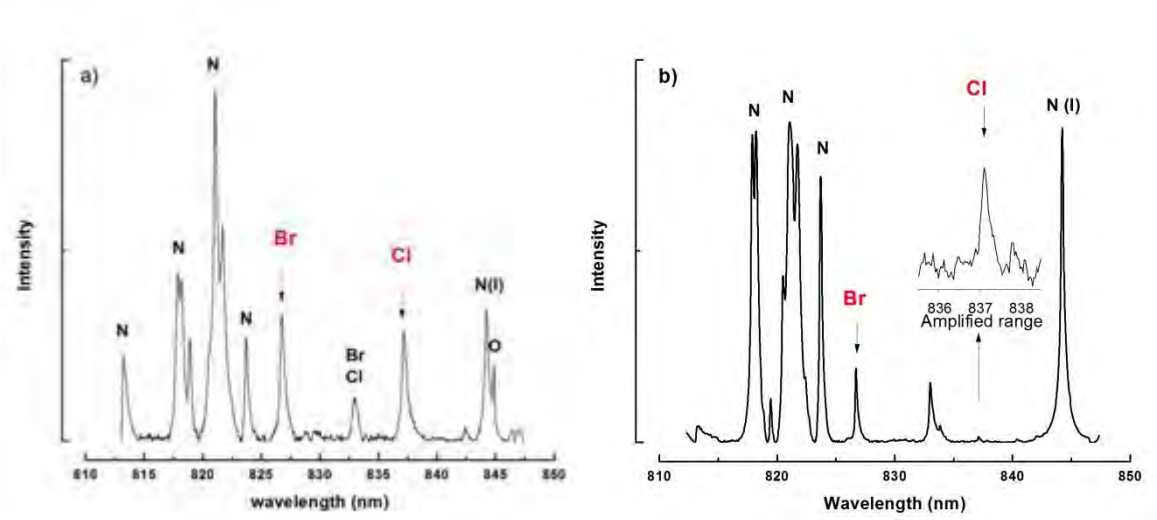

Figure 4.4. Emitted spectra from (a) metformin and (b) glyburide commercial samples mixed with an internal standard (KBr). The Cl and Br lines used for the analysis are arrow pointed on both graphs. In the case of glyburide spectra, an amplified zone illustrates the Cl emission at 837.24nm.

Calibration curves and analytical parameters

The calibration curve is a plot where the instrumental response (LIBS signal) changes over a certain range of analyte concentration. In our experiments, the calibration curves were obtained for different standard samples containing between 5.73 and 11.43% for Met and between 0.09 and 0.72% for Gly. For each standard sample, three replicates were made and analyzed in order to improve analytical precision. Statistical parameters and analytical characteristics for the determination of both Met and Gly are summarized in Table 4.1. The calibration curves were linear for tested Cl concentrations. A linearity ≥ 99.50% was obtained (Table 4.1). It is worth noting that a high linearity was achieved despite the fact that halogen elements, such as Cl, are spectrally difficult to detect due to their high excitation energies (>10 eV). For the highest and lowest Cl concentration, neither saturation nor linear deviations were observed. For this experiment, the optimal temporal acquisition parameters were 0.20 μs (t_d) and 1.00 μs (t_g.) producing the optimal signal to noise ratio (SNR). Limit of detection (LOD) achieved, under above mentioned conditions, are on the order of parts per million. This is a typical LOD value that can be reached in conventional LIBS experiments [8]. LOD can be estimated from calibration curves using the expression, $LOD = 3\,b\sigma_{Bkg}/m$, where m, σ_{Bkg}, and b, represent the slope, the background standard deviation and the *y*-axis intersection of the calibration curve [9]. LOD and limit of quantification ($LOQ = 3 \cdot LOD$) values are reported in table 4.1.

Table 4.1. Statistical parameters for LIBS determination of Met and Gly

	Met	**Gly**
Equation	$(Cl/Br)_r = 0.036(\%Cl) - 0.034$	$(Cl/Br)_r = 0.042(\%Cl) - 0.010$
r^2	0.9903	0.9993
Dynamic Range (%Cl)	5.73 – 11.43	0.099 – 0.723
Linearity (%)	99.50	99.59
Slope Standard Error	12.8×10^{-3}	-2.97×10^{-4}
Intercept Standard Error	1.46×10^{-3}	3.27×10^{-2}
LOD(% Cl)	3.50×10^{-2}	1.10×10^{-2}
LOQ(% Cl)	11.2×10^{-2}	3.65×10^{-2}

Despite the high energies necessary for excitation of Cl atoms, the Gly samples have relatively low Cl concentration. It is shown by other authors that the sensitivity in the case of halogen elements and signal to noise ratio can be both enhanced by producing the induced breakdown in a noble gas atmosphere [10–12]. St-Onge et al reported an improved factor of 7.3 on signal detection when they analyzed the emitted Cl line at 837.59 nm using a helium flow over pharmaceutical samples [13]. Nevertheless, in our work, an easy and practical method is proposed, where all experiments were performed under standard conditions with satisfactory determination of both analytes. Besides, the Cl concentration in pharmaceutical samples was sufficiently high to be detected by the proposed method according to the lowest concentration detected for this element under atmospheric conditions (around ~0.035% using the same line at 837.59 nm) [12, 14]. In order to quantify the lowest content of Cl in Gly samples (~0.1 %), the pulse energy and the optimal temporal acquisition parameters were between 16 and 20 mJ per pulse and the t_d was 0.25 μs, in order to minimize the background signal and t_g was expanded to

2.00 µs in order to collect the analyte signal for a longer period of time. With the parameters mentioned above, the achieved linearity for Gly was 99.59%.

Application to pharmaceutical formulations

After testing the linearity of calibration curves, LIBS Method has been applied to the determination of the active ingredients, Met and Gly, by using their Cl content. Figure 4.5(a) shows the Met calibration curve obtained from synthetic samples (previous section) and four different commercial samples, containing 500 mg of Met (according to the manufacturer), labeled from 1 to 4. Statistical parameters from calibration curves are summarized in Table 4.1. In this work, typical ranges of Cl concentration (weight percent) from commercial samples lie between 6-11% and 0.1-0.2% for Met and Gly, respectively.

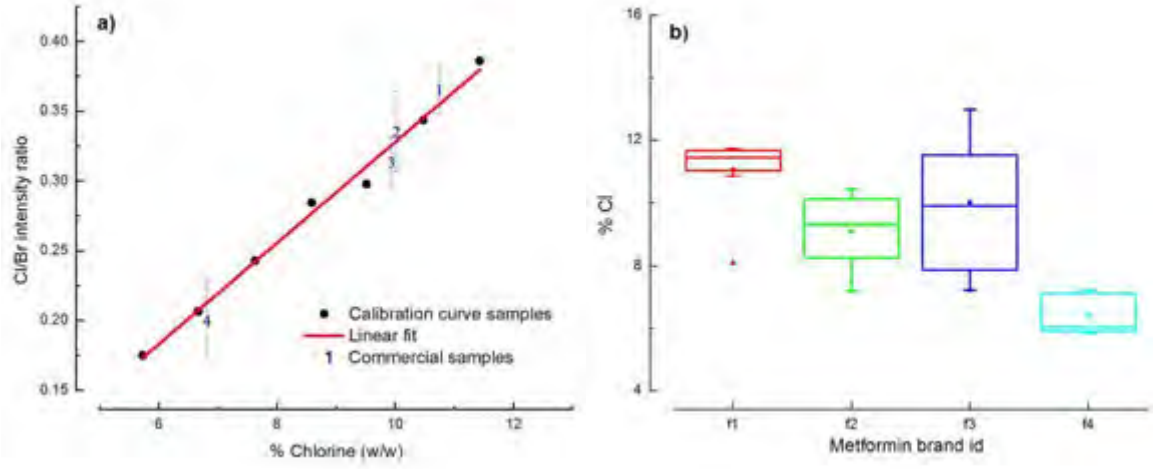

Figure 4.5 (a) Metformin-containing commercial samples (1-4) are well predicted according to calibration curve analysis. Seven synthetic samples at different Cl concentrations were fitted achieving linearity higher

than 99%. (b)According to statistical analysis two pharmaceutical brands (2 and 3) presents wider spread distributions. The outlier (in brand 1) is present in the analysis.

As can be seen in figure 4.5(a), commercial samples are well fitted to the calibration curve taking into account the API concentration labeled on the commercial boxes. According to the above results, matrix effects are negligible or not evident because Met represents around 90% of the total weight in commercial tablets. Vertical error bars represent the standard deviation of the three used replicates. One outlier was observed according to a box and whisker analysis as shown in Figure 4.5(b) (small triangle). This outlier from sample 1 was not considered in the analysis of the Cl content. In the same figure it can be noticed that the Cl concentration shows a Gaussian (normal) distribution in brands 1, 2 and 3. Furthermore, brands 2 and 3 present considerable spread of data according to its box size. Nevertheless, the simple grinding process proposed in this method gives satisfactory predictions for Met in commercial samples as it is shown in Table 4.2.

Table 4.2. Recoveries obtained with the proposed LIBS method in the analysis from Met and Gly pharmaceutical formulations

Samples	Met			Gly		
	Labeled weight (mg/Tablet)	Found weight (mg/Tablet)	% R (RSD)	Labeled weight (mg/Tablet)	Found weight (mg/Tablet)	% R (RSD)
1	500.00	524.39	104.88 (6.29)	5.00	4.47	89.78 (4.62)
2	500.00	462.88	92.58 (7.02)	5.00	5.33	106.53 (9.77)
3	500.00	513.46	102.69 (9.24)	5.00	5.39	107.77 (8.77)
4	500.00	471.11	94.22 (6.37)	5.00	4.79	95.91 (6.97)

For the case of samples containing Gly as the active agent, typical values of Cl concentration are about 0.18% of the total mass, which corresponds to 5 mg of API over 160 mg of the total tablet mass. Figure 4.6(a) shows four commercial samples labeled from 1 to 4 and the respective calibration curve. For the sake of clarity only the 4 points closer to the commercial samples are shown in the calibration curve covering a Cl weight percent between 0.09 and 0.72%. In the case of the Gly LIBS results, no matrix effect is expected because both synthetic and commercial samples contain lactose as excipient. The four Gly brands show normal distribution and no outliers are present, as can be seen in figure 4.6(b).

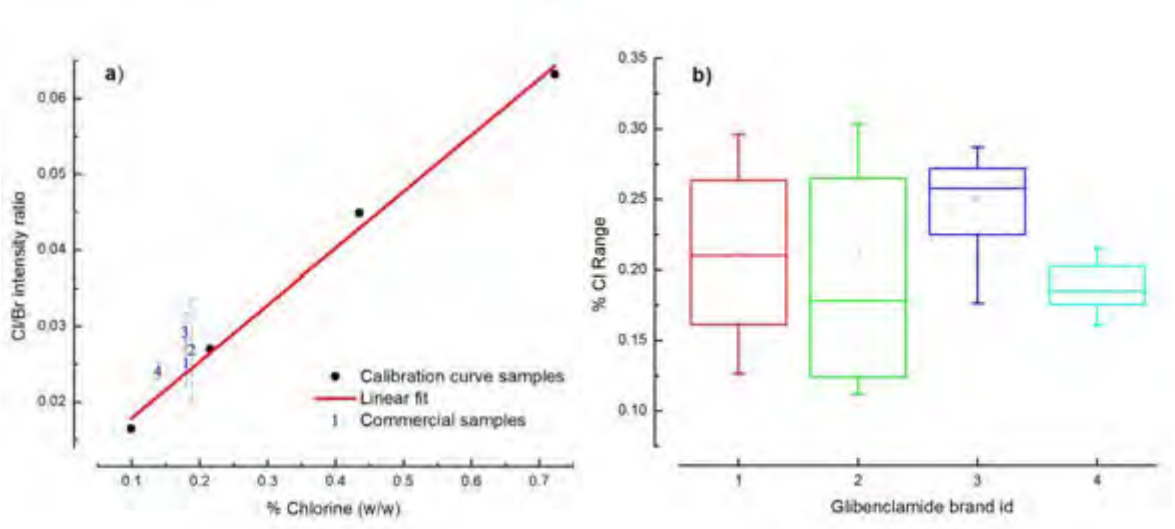

Fig. 4.6 (a) Glyburide-containing commercial samples (1–4) are well predicted according to their respective calibration curve analysis. For the sake of clarity, only a fraction of the curve containing commercial samples is shown (0.1–0.7%). Achieved linearity is higher than 99%. (b) According to statistical analysis the two pharmaceutical brands (1 and 2) present wider spread distributions.

Boxes of brands 1 and 4 are smaller because those brands present smaller standard deviations than brands 2 and 3 (Table 5.2). Results based on LIBS and the simple preparation steps suggest the use of this method for a rapid on-line/in-situ monitoring of APIs due to their elemental composition in the pharmaceutical industry with an acceptable level of accuracy.

Results obtained in this work show that the proposed LIBS method is able to quantify pharmaceutical ingredients in solid dosages by monitoring specific elements such as Cl. Results can be obtained in just a few minutes with simple sample preparation using small amounts of pharmaceutical dosage (grams). Therefore, the proposed methodology can be implemented to monitor the pharmaceutical production process in situ in real time and qualitative and quantitative analysis could be used for inspection and recognition of authenticity.

4.2. Quantitative analysis based on Calibration Free-LIBS

In the previous section, quantitative analysis has been performed using calibration curves. Synthetic samples with similar or identical chemical composition than tested samples are

needed for the calibration curves in order to overcome matrix dependence. Moreover, additional sample preparation was needed because of the addition of an internal standard. Furthermore, for some specific analytical problems, synthetic samples cannot be produced even if sample composition is well known. For those reasons, calibration curves cannot be applied as a universal technique in quantitative analysis.

Calibration Free (CF) LIBS approach was developed to overcome matrix-matched sample dependence taking into account the matrix together with the analyte as part of the analytical problem [15]. Still a better and more systematic approach needs to be developed to promote CF-LIBS universality. Nevertheless, CF-LIBS has been applied in a broad number of situations achieving, in most cases, good results and acceptable accuracy. CF-LIBS has shown promise in industrial applications due its non-contact multi-elemental and real time analysis mainly for metallic samples. This section presents the quantitative analysis of an industrial steel sample by CF-LIBS. Steel samples represent an interesting problem due to its chemical composition and complex emission spectrum to evaluate and test our CF-LIBS implementation in a real and challenging application.

For CF-LIBS analysis relevant spectral information, such as ionization energy values for each element, upper and lower level energies or transitions probabilities for each line, was taken from the NIST atomic spectra database [7]. In our case, it was not possible to measure all the elements present in the steel sample due to instrumental limitations; i.e., the strongest C line emits close to 250 nm but the sensitivity of our detector is limited to the wavelength range 280-900 nm. Other C lines and S lines are overlapped with stronger Fe lines in the Vis-NIR range. Nevertheless, the undetected elements are traces in the

analyzed steel matrix and the relative error can be considered as negligible in the quantitative analysis. For quantitative analysis, we used a spectral range from 400 to 440 nm excluding lines involving the ground state. Spectra were processed by AtomicSpectra (described in Appendix A).

Results and discussion

This section deals with detection and quantification of chemical components in a stainless steel sample by LIBS and CF-LIBS techniques. The experimental set up and methods for data acquisition Light collection system are discussed in detail in chapter 3. For CF-LIBS analysis, plasma parameters are determined by spectral line broadening. To minimize instrumental effects on line broadening, we use the minimum entrance slit width of the spectrometer (10 μm). Experimental parameters were chosen to maximize signal to continuum ratio. Spectra used in the analyses were generated by accumulating the signal of 30 laser shots.

Spectral analysis

Because the choice of suitable lines is a crucial step for optimum quantitative analysis in CF-LIBS we take special attention on selecting a spectral window for the analysis. Fortunately, steel samples emit signal practically in all UV-Vis region. Nevertheless care should be taken with resonant lines of any element to minimize errors by self-absorption

if it is present in the plasma. Besides, because the density and concentration of species in the plasma may vary from laser pulse to pulse, line emissions from all possible elements should be detected in the same spectral window in order to achieve good quantitative results. Lines with spectral interferences from other elements must be avoided. All those steps should improve the precision in the plasma temperature calculation by the Boltzmann plot method, and consequently, the quantitative results.

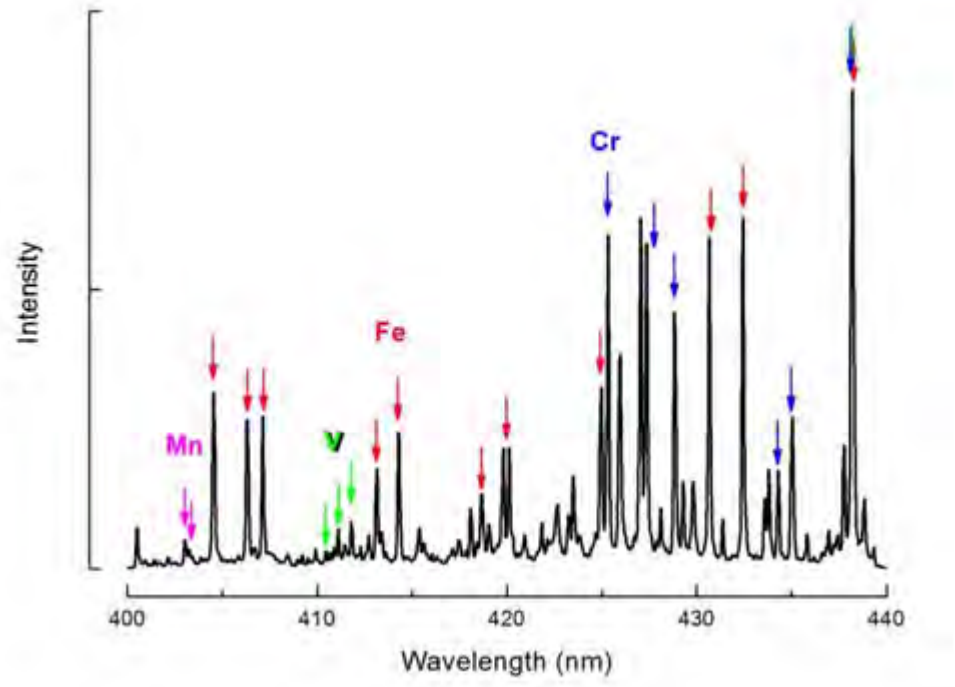

Figure 4.7. Spectral "fingerprint" of a steel sample taken by LIBS technique. Spectral emission of Fe, Cr, Mn and V elements are present in the range 400 – 440 nm.

Figure 4.7 shows 121 emission lines of a steel sample in the range 400 – 440 nm from Fe, Cr, Ni and Mn species. From the total 121 lines, only 43 lines can be used for quantitative

analysis. The most frequent problem on this range is the spectral superposition between lines from different elements.

Optically thin plasma

The estimation of electron density and temperature using spectral information demands optically thin plasmas as light sources to avoid self-absorption effects. Most of the literature assumes plasmas as optically thin sources and exclude lines involving ground state (resonant lines) in order to avoid under or overestimations in plasma parameters due to self-absorption in resonant lines causes a distortion in the line profile resulting in a broadened line. Nevertheless some authors have reported theoretical and experimental methods for measurement and correction of self-absorption in laser induced plasmas [13].

To measure self-absorption effects, intensity ratio of two emission lines from the same species having the same upper energy level can be used. In the absence of self—absorption the intensity ratio should be similar to the ratio of their corresponding transition probabilities [14].

Table 4.3. Comparison between the intensity ratio of two non-resonant lines and the ratio of their corresponding transition probabilities.

Wavelength	Upper Energy level	Transition probability	Intensity ratio	Transition probability ratio
400.52 nm	37521.161 cm^{-1}	$2.04x10^{7}$	**3.79**	**3.74**
407.17 nm	37521.161 cm^{-1}	$7.64x10^{7}$		

Table 4.3 presents intensity ratio and transition probability ratio between two Fe lines in order to evaluate the existence of self-absorption in our experiments. The consistency between both ratios supports the assumption of optically thin laser induced plasma when analyzing the steel sample under experimental conditions presented in this section. This result is expected due to optical thickness is associated with very high dense plasmas but, in general, not for laser-induced plasmas. Therefore, self-absorption effects may be neglected in the following analysis.

Local Thermodynamic Equilibrium

Strict thermodynamic equilibrium requires unbounded, spatially and temporally homogeneous plasma. In the laboratory, plasma spectroscopy deals with thermal equilibrium relations for level populations, particle velocity distributions and radiation fields less strict than in a blackbody radiator. For practical purposes in plasma spectroscopy Local Thermodynamic Equilibrium (LTE) is enough to describe the system through Boltzmann/Maxwell distributions. The validity of LTE is critical to guarantee CF-LIBS accuracy in quantitative results. To ensure LTE in time-dependent and inhomogeneous plasmas with thermal spatial gradients, further conditions need to be placed on the electron density [15]. The most popular criterion used in the literature to assess the validity of LTE is the McWhirter criterion [15–16]. McWhirter criterion defines the minimum electron number density needed for LTE in laboratory plasmas.

$$n_e > 1.6x10^{12}T^{1/2}(\Delta E_{nm})^3 \qquad \text{Eq. (4.1)}$$

In the last expression, temperature, T, and energy, E, are expressed in K and eV respectively. According to McWhirter criterion, minimal n_e values for laser induced plasmas stands near $1x10^{16}$ cm^{-3}.

Since spectral line broadening and wavelength shifts are mainly governed by collisions of charged species, electron density may be calculated by the FWHM of a Stark-broadened line given by the relation:

$$\Delta\lambda_{1/2} = 2W\left(\frac{n_e}{10^{16}}\right)\text{Å} \qquad \text{Eq. (4.2)}$$

Where $\Delta\lambda_{1/2}$ represents the FWHM of the spectral line and W is the electron-impact parameter (ionic contribution has been neglected). Konjevic et al. reported experimental data on Stark widths and shifts for spectral lines and electron-impact parameters W for non-hydrogenic atoms in a critical review [17]. The review reported main parameters for 7 Fe lines. One of those lines correspond to the Fe spectral emission centered in 426.047nm with a factor $W$of 0.11 Å. Measuring the FWHM of the experimental emission of this line and using the reported parameter was calculated by equation 4.2. The calculated n_e by Stark broadening is $\sim 10^{17} cm^{-3}$; a value higher than McWhirter´s criterion supporting the assumption of LTE.

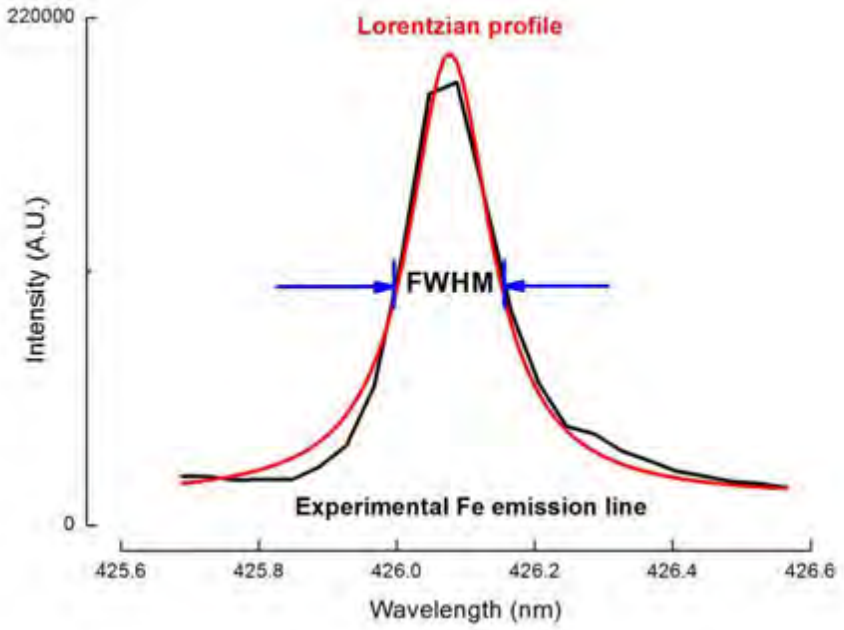

Figure 4.8. FWHM of 426.04nm Fe spectral emission used to calculate the electron density n_e from a steel sample plasma. Experimental data (black line) fits fairly well with a Lorentzian curve supporting the hypothesis of broadening by Stark effect.

Other mechanisms such as Doppler effect, resonance by absorption, and instrumental mechanisms may broaden spectral lines. Nevertheless, all those mechanisms are safely neglected in the present analyses. Instrumental broadening is minimized by setting the entrance slit of the spectrograph to its minimal aperture. Harilal et al. [18] reported a linewidth FWHM of 0.02nm caused by the Doppler broadening in laser induced Sn plasmas. This broadening represents half of the instrumental resolution and may be neglected. Besides Stark-broadened lines exhibits Lorentzian profiles and typical lines in our experiments fit fairly well with a Lorentzian profile (r^2> 0.983) as shown in Figure 4.6.

Correlation coefficient from Lorentzian profile was higher than correlation coefficient from Gaussian profile (profile associated with Doppler broadening) according to this spectral line. Experimental data was fitted also with a Voigt profile and slightly improvement in correlation coefficient was obtained (r^2> 0.986), nevertheless FWHM does not present a significant change.

Plasma temperature

According to Boltzmann-Maxwell distributions, only two emission lines are necessary to obtain the temperature in the plasma, provided there is sufficient difference between their upper energy levels. However, Boltzmann plot technique uses several emission lines for a specific species achieving more accurate temperature estimation. Saha-Boltzmann method may be used to increase the reliability on temperature calculation using neutral and ionic lines improving the statistics; nevertheless lines with different ionization stages should appear in the spectrum and spectral information must be available for ionized lines (partition functions, transition probabilities, etc.). In the present chapter, the temperature was deduced from the Boltzmann plot method. For a plasma in LTE conditions, a plot proportional to the line intensity vs. its energy of the upper level should fit to a straight line where the slope is related with temperature (see chapter 2) according to:

$$m = -\frac{1}{kT}$$

The temperature was estimated using 21 Fe lines for which all necessary information is well known and available [7]. The correlation coefficient of the linear fit is better than 0.91 (fitting obtained from black numbers in Figure 4.9). A good linear fit not only validates the plasma temperature estimation with good accuracy, but also serves to support the assumption of Maxwellian electron distribution needed for LTE conditions.

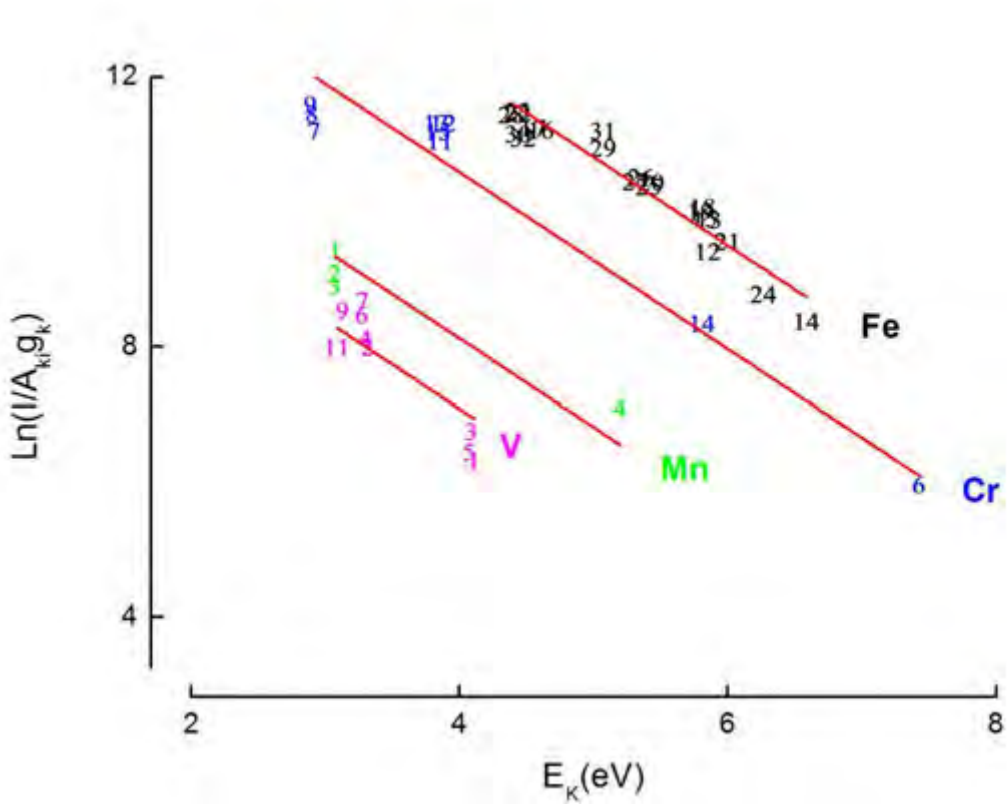

Figure 4.9. A family of lines in Boltzmann plot for Fe (21 spectral lines), Cr (8), Mn (4), and V (9) species from a steel sample. The slope is the same for all Boltzmann family lines and was calculated by fitting Fe data points. This calculated slope from Fe line was fixed for other element lines.

When fitting all species shown in Figure 4.7, all fitted curves exhibited similar slopes but different intercepts with the axes. The fact that all family Boltzmann lines present similar slopes support the assumption of LTE in the laser induced plasma. Nevertheless, the slope computed with Fe information was taken as the representative value and this value was fixed for all other species in the fitting step in order to determine only one temperature value for quantitative analysis (Figure 4.9).

Quantitative results

After evaluating optical thinness and LTE conditions, it is found that CF-LIBS method can be used for quantitative results based on the steel laser induced plasma. The concentration of the species can be calculated using the expression (chapter 2):

$$C_S = \frac{U_S(T)}{F} e^{q_s} \qquad \text{Eq. (4.3)}$$

Where C_S represents the concentration of each specie, $U_s(T)$ is the partition function evaluated at certain plasma temperature, q_s is the intercept of the fitted line in the Boltzmann plot for each specie and F represents an experimental factor that can be removed by normalization:

$$\sum_S C_S = 1 \qquad \text{Eq. (4.4)}$$

We also used microprobe analysis [19] as a reference method to determine the elemental concentration in the steel sample. CF-LIBS and reference results are plotted in Figure 4.10. It should be noticed that the reference method identified 6 elements (Fe, Cr, V, Mn, C and

S), two more than LIBS approach; however, sample information is needed in the reference method for precise and accurate results.

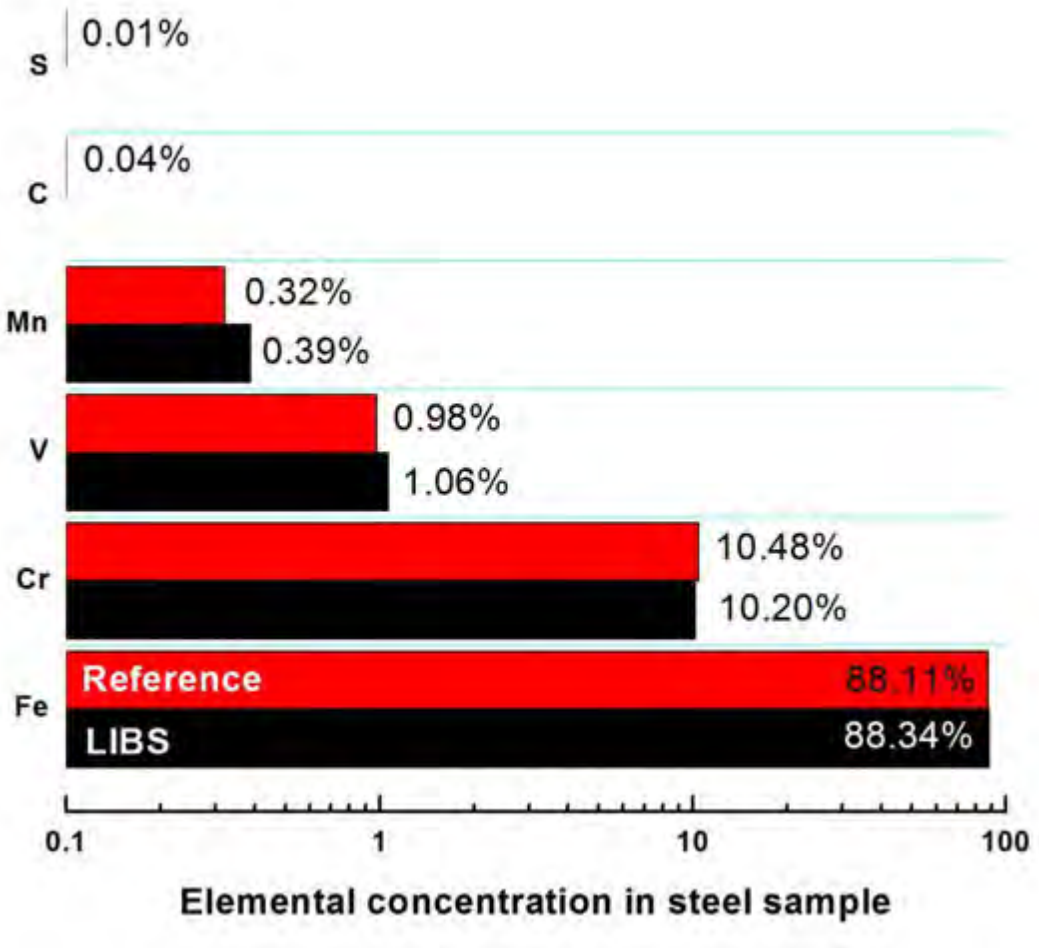

Figure 4.10. Element concentration of Fe, Cr, V, and Mn in a steel sample calculated with CF-LIBS (black bars) and Microprobe (red bars) method. Bars are plotted in a logarithmic scale.

Table 4.1 shows relative uncertainties values between CF-LIBS and microprobe results. Shah et. al. reported similar uncertainties in major elements (Fe and Cr) when compared CF-LIBS with certified values of a steel sample [22]. In the case of trace elements Shah and co-workers obtain better uncertainties than we do. One possible explanation for the

uncertainty value of M element is the few lines used in the wt. concentration for trace elements in the Boltzmann plot (4 lines for Mn). In the case of V element, the 9 spectral emissions used in the linear fit have practically two different upper energy level values ($\sim 3eV$ and $\sim 4eV$). It should be noted that Shah et.al. used an Echelle-type spectrograph in order to analyze a wide wavelength range between 250 to 550 nm. This is a great instrument in order to select optimal emission lines in a wide spectral range.

Table 4.4. Comparison of elemental contents of steel sample determined CF-LIBS and microprobe analysis.

	Concentration (wt. %)		
Element	CF-LIBS	Reference method	Relative uncertainty (%)
Fe	88.34	88.11	0.26
Cr	10.20	10.48	2.67
V	1.06	0.98	7.55
Mn	0.39	0.32	17.9
C	-	0.04	-
S	-	0.01	-

The conclusion is that CF-LIBS can be used for monitoring in real time quantitative information of the major constituents in a sample (as Fe and Cr in our example) with relatively good uncertainties ($< 5\%$). The relative uncertainties are comparable with those reported in the literature on steel samples and metallic alloys [22-24]. For a complete quantitative analysis (including good results for trace elements) the development of a better and more systematic approach is needed. CF-LIBS may be very useful as a real-time, in-situ approach for preliminary analysis without the need of calibration curves or reference standards.

4.3. References

[1] Data supplied by the World Health Organization (WHO). Media center. Diabetes. Fact sheet No. 312, online: http://www.who.int/mediacentre/factsheets/fs312/en/index.html, 2012.

[2] A. Patrignani, M. Musumeci, F. Bosco, M. Pane, "Counterfeiting: a global spread, a global threat". Trends Organ Crim., 12(1), 59-77 (2009).

[3] S. E. Inzzuchi, "Oral antihyperglycemic theraphy for type 2 diabetes: scientific review", JAMA, 287(3), 360-372 (2002).

[4] A. J. Krentz, CJ Beiley, "Oral antidiabetic agents: current role in type 2 diabetes mellitus", Drugs, 65(3), 385-411 (2005).

[5] A. Nourparvar, A. Bulotta, U. Di Mario, R. Perfetti, "Novel strategies for the pharmacological management of type 2 diabetes", Trends Pharmacol Sci., 25(2), 86-91 (2004).

[6] G. E. Dailey, "Glybenclamide/metformin tablets: A new therapeutic option for the management of type 2 diabetes", Expert Opinion on Pharmacotherapy, 4(8), 1417-1430 (2003).

[7] Ralchenko, Yu., Kramida, A.E., Reader, J., and NIST ASD Team (2010). NIST Atomic Spectra Database (ver.4.0.1), [Online]. National Institute of Standards and Technology, Gaithersburg, MD. Available: http://physics.nist.gov/asd [2010, May 9].

[8] A. Miziolek, V. Palleschi, I. Schechter, “Laser-Induced Breakdown Spectroscopy (LIBS) Fundamentals and Applications” Cambridge University press, UK, 166-167 (2006).

[9] R. Noll, “Laser-Induced Breakdown Spectroscopy Fundamentals and Applications”, Springer-Verlag, 212-215 (2012).

[10] J. Anzano, B. Bonilla, B. Montul-Ibor, J. Casas-Gonzalez, “Rapid characterization of analgesic tablets by laser-induced breakdown spectroscopy (LIBS)”, Med. Chem. Res., 18(8), 656-664 (2009).

[11] D. A. Cremers, L. J. Radziemski, “Detection of chlorine and fluorine in air by laser-induced breakdown spectroscopy”, Anal. Chem., 55(8), 1252-1256 (1983).

[12] M. Tran, Q. Sun, B. W. Smith, J. D. Winefordner, “Determination of F, Cl, and Br in solid organic compounds by laser-induced plasma spectroscopy”, Appl. Spectrosc., 55(6), 739-744 (2001).

[13] L. St-Onge, E. Kwong, M. Sabsabi, E.B. Vadas, “Quantitative analysis of pharmaceutical products by laser-induced breakdown spectroscopy”, Spectrochimica Acta Part B., 57(7), 1131-1140 (2002).

[14] L. Dudragne, Ph. Adam, J. Amourox, “Time-Resolved Laser-Induced Breakdown Spectroscopy: Application for Qualitative and Quantitative Detection of Flourine, Chlorine, Sulfur and Carbon in Air”, Appl. Spectrosc., 52(10), 1321-27 (1998).

[15] E. Tognoni, G. Cristoforetti, S. Legnaioli, V. Palleschi, “Calibration-Free Laser-Induced Breakdown Spectroscopy: State of the art”, Spectrochimica Acta B, 65, 1-14 (2010).

[16] S. Pandhija, N.K. Rai, S.N. Thakur, “Contaminant concentration in environmental samples using LIBS and CF-LIBS”, Applied Physics B, 98, 231-241 (2010).

[17] Hans N. Griem, *Principles of Plasma Spectroscopy*, Cambridge University Press, 1997.

[18] G. Cristoforetti, A. De Giacomo, M. Dell´Aglio, S. Legnaioli, E. Tognoni, V. Palleschi, N. Omenetto, “Local Thermodynamic Equilibrium in Laser-Induced Breakdown Spectroscopy: Beyond the McWhirter criterion”, Spectrochimica Acta B, 65, 86-95 (2010).

[19] N. Konjevic, A. Lesage, J. R. Fuhr, W. L. Wiese, “Experimental Stark Widths and Shifts for Spectral Lines of Neutral and Ionized Atoms (a Critical Review of Selected Data for the Period 1989 Through 2000)”, Journal of Physical and Chemical Reference Data, 31, 819-827 (2002).

[20] S. Haliral, B O´Shay, M. Tillack, “Spectroscopic characterization of laser-induced plasma”, Journal of Applied Physics 98, 13306-1–7 (2005).

[21] D.G.W. Smith, Short Course in Microbeam Techniques (Minearological Association of Canada, 1976).

[22] M. L. Shah, A. K. Pulhani, G. P. Gupta, B. M. Suri, “Quantitative elemental analysis of steel using calibration-free laser-induced breakdown spectroscopy ”, Applied Optics 51, 4612- 4621 (2012).

[23] E. Tognoni, G. Cristoforetti, S. Legnaioli, V. Palleschi, A. Salvetti, M. Mueller, U. Panne, I. Gornushkin, “A numerical study of expected accuracy and precision in Calibration-Free Laser-Induced Breakdown spectroscopy in the assumption of ideal analytical plasma”, Spectrochimica Acta B 62, 1287-1302 (2007).

5. Effects of DP-LIBS in CF-LIBS approach

In previous chapters laser-induced breakdown spectroscopy (LIBS) was stated as a versatile and practical technique for elemental analysis for a wide number of materials and applications [1-3]. Within conventional methodology single pulse LIBS can achieve excellent qualitative information for unknown samples in a practical way and relatively good quantitative results using auxiliary techniques such as calibration curves or self-calibrated methods. However, when sample damage is an important issue, conventional LIBS analysis is considered destructive. Sample damage depends on physical and chemical properties of the sample as well as laser pulse features such as wavelength and pulse energy. Typical craters produced with the laser induced breakdown have diameters of hundreds of micrometers. Besides the sample damage, also the intensity of the LIBS signal depends critically on the laser pulse energy. Increasing the laser pulse energy will increase the ablated material and consequently will increase the intensity of the emission lines. By using the orthogonal double pulse (DP) LIBS scheme [4-6], it is possible to increase the signal intensity without increasing the amount of ablated material. An important number of papers have discussed the use of DP-LIBS configurations and their authors have reported the use of pulses with relative high energies in the range of tens to hundreds of mJ [7-13].

For quantitative analysis, the use of DP-LIBS generally depends on standards and calibration curves [7, 14]. DP-LIBS enhances signal intensities for all elements present in a sample, but whether it is possible to use DP-LIBS together with a self-calibrated method for quantitative analysis has not yet been proved. In this chapter, we demonstrate that CF-LIBS [15] can be successfully used to analyze plasmas generated by DP-LIBS by means of low ablative energies (~0.25mJ). The use of low ablative energies diminishes the sample damage becoming increasingly important for critical applications, such as the analysis of art works, archeological artifacts, jewelry, etc. CF-LIBS (theory has been discussed in chapter 2 and experimental details in chapter 4) is a multi-element quantitative analysis approach based on the measurement of plasma parameters and line intensities produced by traditional LIBS experiments. CF-LIBS has been carried out in several experimental conditions. In most cases, spectra have been acquired at atmospheric conditions using single nanosecond laser pulses as the generation and excitation source of the plasma. In general, laser pulse energies vary from 1mJ to more than 100 mJ [16].

Results and discussion

Signal enhancement

Compared with SP-LIBS, as shown in figure 5.1, neutral and ionic species of the steel sample were considerably enhanced by DP-LIBS. For both SP and DP-LIBS cases (figure 5.1), the ablative energy was the same (0.25 mJ). For this particular ablative energy, SP-LIBS produced a signal only for the strongest lines of Fe and Cr. However, in the DP

configuration, a better signal is produced when the second pulse hits the vapor produced by the first pulse. For the sake of clarity, SP signal is multiplied by a factor of 10 in figure 5.1.

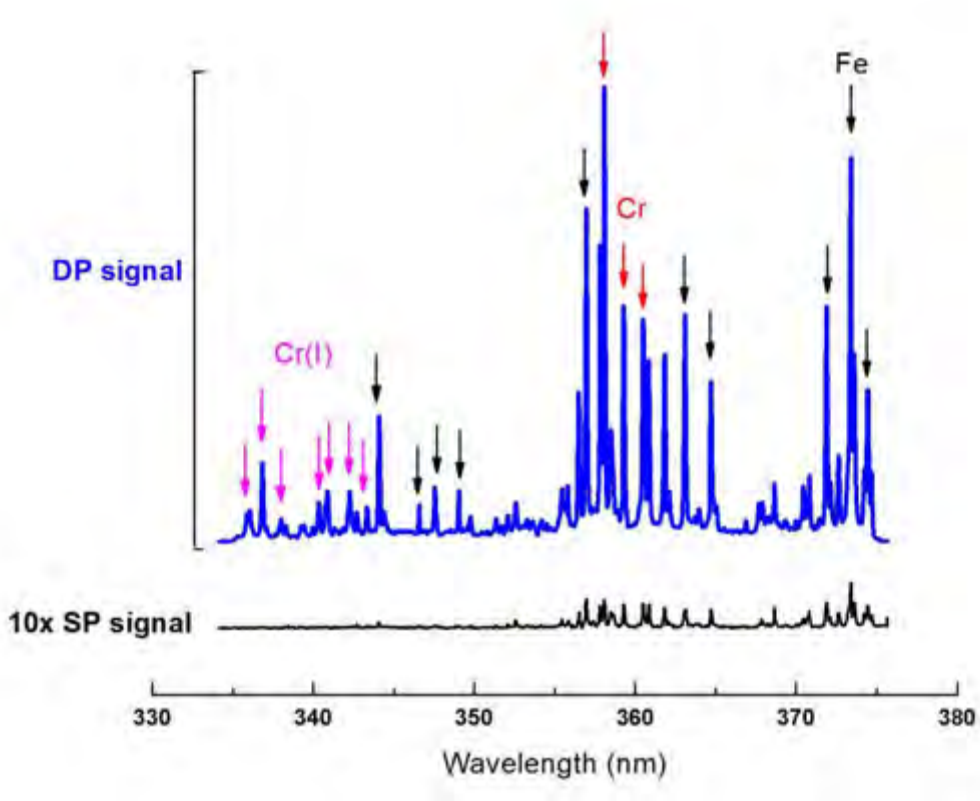

Figure 5.1. LIBS emission spectra of a stainless steel sample under SP and DP plasma generation. Lines of Fe, Cr, and Cr(I) are clearly enhanced by DP configuration.

We define the enhancement factor as the ratio between the maximum intensity value for a single peak produced by DP-LIBS and the maximum intensity value for the same peak produced by SP-LIBS using the same ablative energy. Figure 5.2 shows the dependence of the signal enhancement of Fe, Cr, and Cr(I) with respect to the ablative energy. Each

symbol in the graph (square, circle or triangle) represents the average enhancement factor of 17, 3, and 7 emission lines for Fe, Cr, and Cr(I) respectively.

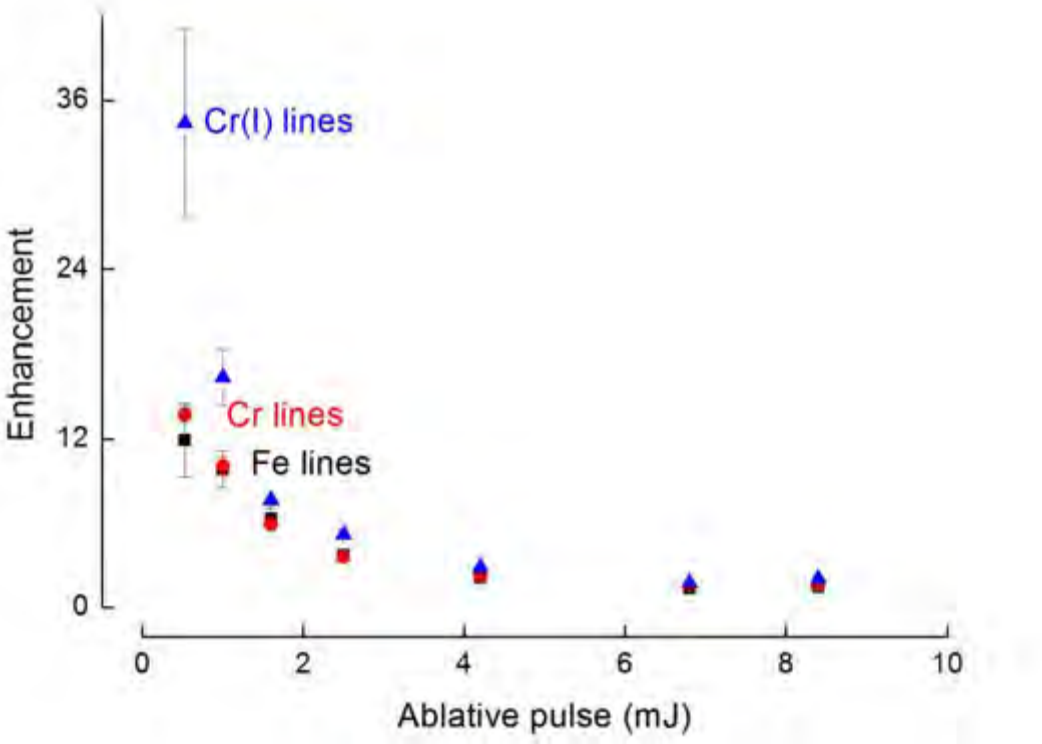

Figure 5.2. Enhancement of Fe, Cr, and Cr(I) lines at different ablative pulse energies. Symbols represent the average of 17, 3, and 7 lines for Fe, Cr, and Cr(I) species respectively. Maximum enhancement for all lines can be achieved at low ablative energies.

The enhancement at the lowest ablative energy (0.25 mJ) is not presented in the graph since it cannot be calculated because at this particular energy, SP-LIBS does not produce adequate signal (only the strongest Fe and Cr lines). The highest enhancement showed in figure 5.2 is for an ablative energy of 0.50 mJ. Gautier et al. reported that lines with relatively high excitation energy levels exhibit higher enhancement compared with lines of lower excitation energy levels [11]. In our experiments we could not corroborate the

correlation reported by Gautier because the range of the excitation energy levels of the lines we used (~3 – 13eV) was narrower than Gautier's range (~3 – 22eV). Nevertheless, we found that all neutral lines exhibit similar enhancement values (12) for Fe and Cr, but Cr(I) ionic lines, with relatively high excitation energy levels, exhibited three times more enhancement than neutral lines (34). This result is consistent with Gautier's correlation. The enhancement for the three species decreased when the ablative energy is increased. When the first and second pulses have similar energies (~7 mJ), the enhancement factor is about two. This result suggests that, for the reheating scheme, interpulse delay is related directly to the ablative pulse energy. That is, for higher energies, higher interpulse delay times should be used. This relationship can be observed in other works related to orthogonal reheating scheme [4, 11, 12]. In our experiments the maximum enhancement factor is achieved with ablative energies in the range of hundreds of micro joules for an inter-pulse delay time of 10ns.

Quantitative analysis

The algorithm we implemented in the CF-LIBS approach is briefly described in chapter 2 and it has been described in detail elsewhere [15, 16]. Relevant spectral information was taken from the NIST atomic spectra database [17].

To test the feasibility of DP-LIBS in combination with CF-LIBS, we compared SP and DP spectra with similar intensities and their effects on plasma temperature (T) and electron number density (n_e). In our experimental conditions, similar line intensities can be reached

when the ablative energy in SP-LIBS is twice the ablative energy in DP-LIBS (Figure 6.3); i.e., 0.50mJ for SP-LIBS and 0.25mJ for DP-LIBS.

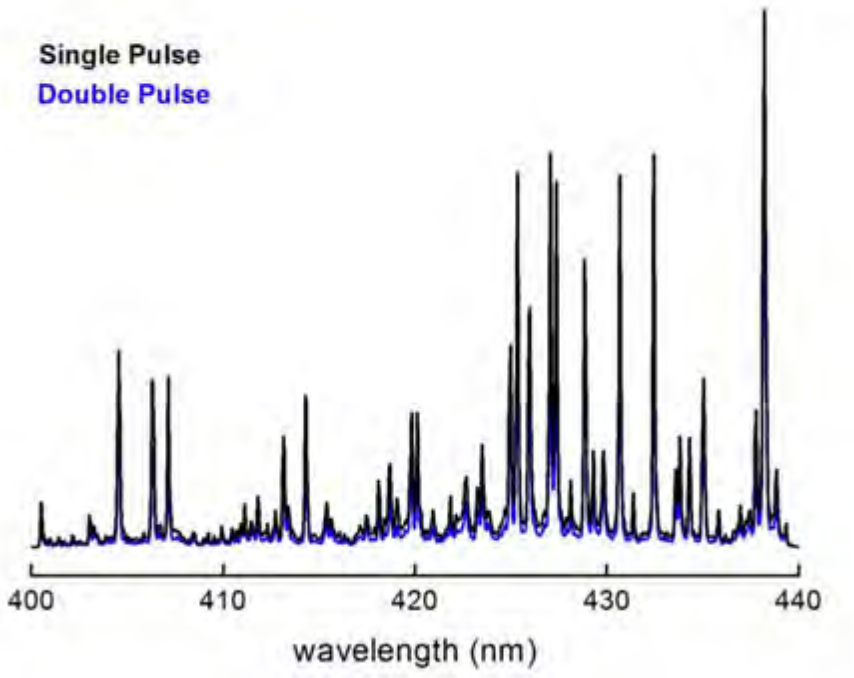

Figure 5.3. SP and DP spectra with similar line intensities. This condition can be achieved when energy of the ablative pulse in SP (0.50mJ) is twice the energy of the ablative pulse in DP (0.25mJ) configuration.

To confirm CF-LIBS results, we evaluated CF-LIBS at three different energies (for both SP and DP configurations) with practically the same quantitative results but different plasma parameters (T and n_e).

Table 5.1. Plasma parameters from SP-LIBS and DP-LIBS

Experiment	Plasma temperature (K)	Electron density (cm^{-3})
SP-LIBS	8500 ± 640	$7.4x10^{16}$
DP-LIBS	8850 ± 630	$6.9x10^{16}$

We calculated the plasma parameters from Fe lines because its high content in the steel alloy. Besides, Fe atoms emit many lines. Table 5.1 shows T and n_e for SP- LIBS (0.50 mJ) and DP-LIBS (0.25 mJ) experiments. Plasma temperature is practically the same for SP and DP according to the Boltzmann plot analysis. Gautier et al. [11, 18] found similar results with different materials and different experimental parameters (energy pulses and inter-pulse delay time). The increase in total energy (first pulse plus second pulse) increases the intensity of the lines but not the plasma temperature and the distribution of excited states over different excitation energy levels does not change. The n_e is slightly higher for the plasma formed by SP-LIBS than by DP-LIBS. Nevertheless the McWhirter criterion [19] was fulfilled and Local Thermodynamic equilibrium (LTE) was assumed in both cases. The n_e value is calculated from the Stark broadening of the Fe I line at 426.05 nm using a Lorentzian line shape fit of the experimental data, as reported in a previous work [20]. Figure 5.4 shows the Lorentzian line shape (red line) obtained by fitting experimental emission (black) line at 406.05nm of both a) SP-LIBS and b) DP-LIBS.

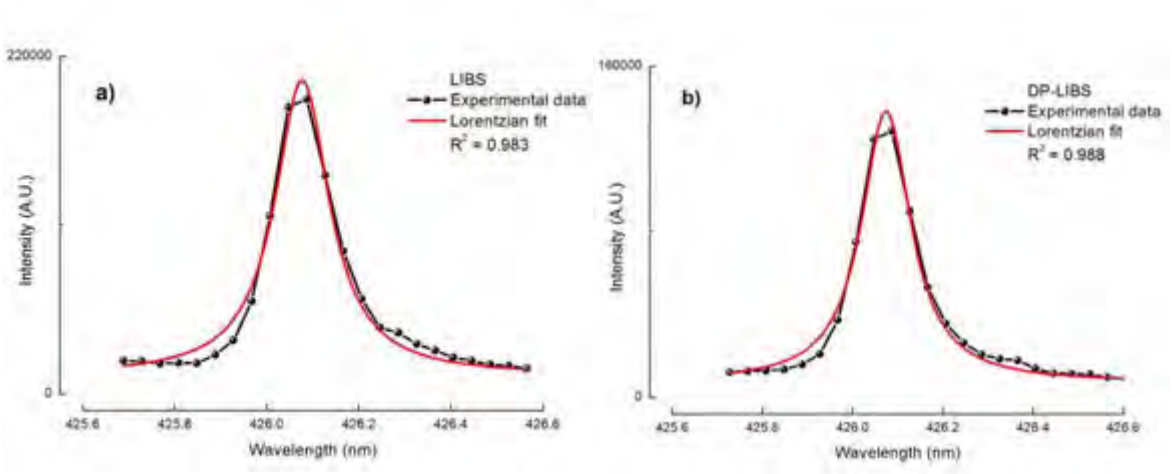

Figure 5.4. (a) SP-LIBS and (b) DP-LIBS Lorentzian fitted curves from experimental Fe emission line at 426.05nm.

Fitted peaks, from both experimental data, have a correlation higher than 0.98 with the Lorentzian profiles. Based on the calculated T and n_e, the quantitative analysis is practically the same for both cases, i.e. SP-LIBS at 0.5mJ and DP-LIBS (0.25 mJ + 7 mJ). The results in our comparison, summarized in Table 5.2, show a similar prediction on the elemental concentration. The relative error of SP and DP experiments lies between 0.25% (Fe) and 10% (Mn).

Table 5.2 Concentration elements in a steel sample obtained by Microprobe analysis, Calibration-Free LIBS based on SP-LIBS and Calibration-Free LIBS based on DP-LIBS

Element	Concentration based on micro-probe analysis (%)	Concentration based on CF-LIBS (%)	
		SP analysis	DP analysis
Fe	88.11	88.34	88.12
Cr	10.48	10.20	10.50
Mn	0.32	0.38	0.34
V	0.98	1.06	1.03
C	0.04	-	-
S	0.01	-	-

Table 5.2 also shows the concentration calculated with microprobe analysis as a reference method [21]. A comparison between SP and DP results shown in Table 6.2 can be seen graphically in Figure 5.5.

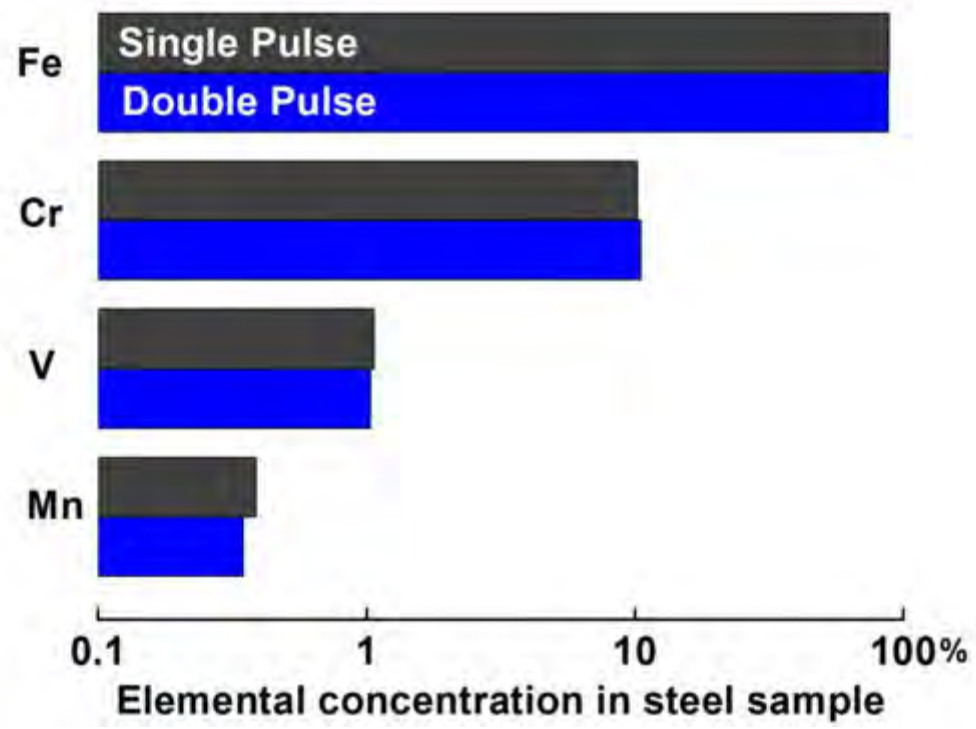

Figure 5.5. Elemental concentration of Fe, Cr, V, and Mn in a steel sample calculated with SP-LIBS (black bars) and DP-LIBS (blue bars) and CF-LIBS approach. Bars are plotted in a logarithmic scale.

Sample damage

To quantify the sample damage, superficial and volumetric damage is presented first. Then, calculations of removed mass will be reported. A comparison between craters formed by SP LIBS (5mJ) and DPLIBS (2.5mJ) will be discussed. Those craters are produced in the analysis of SP-LIBS and DP-LIBS in combination with CF-LIBS presented in this chapter.

Figure 5.6 shows a typical crater produced by laser induced breakdown. For this particular crater 30 laser pulses of 5mJ each were accumulated. As can be seen in the Figure 5.6, crater size is similar to a circular shape with approximately 100µm of diameter. Above in the Figure, a crater profile was inserted in order to show the laser damage depth (black profile). Besides crater formation, thermal effects produce damage around the crater. Considering thermal effects as part of the superficial sample destruction, the sample damage extends over a circular region of approximately 600 µm of diameter.

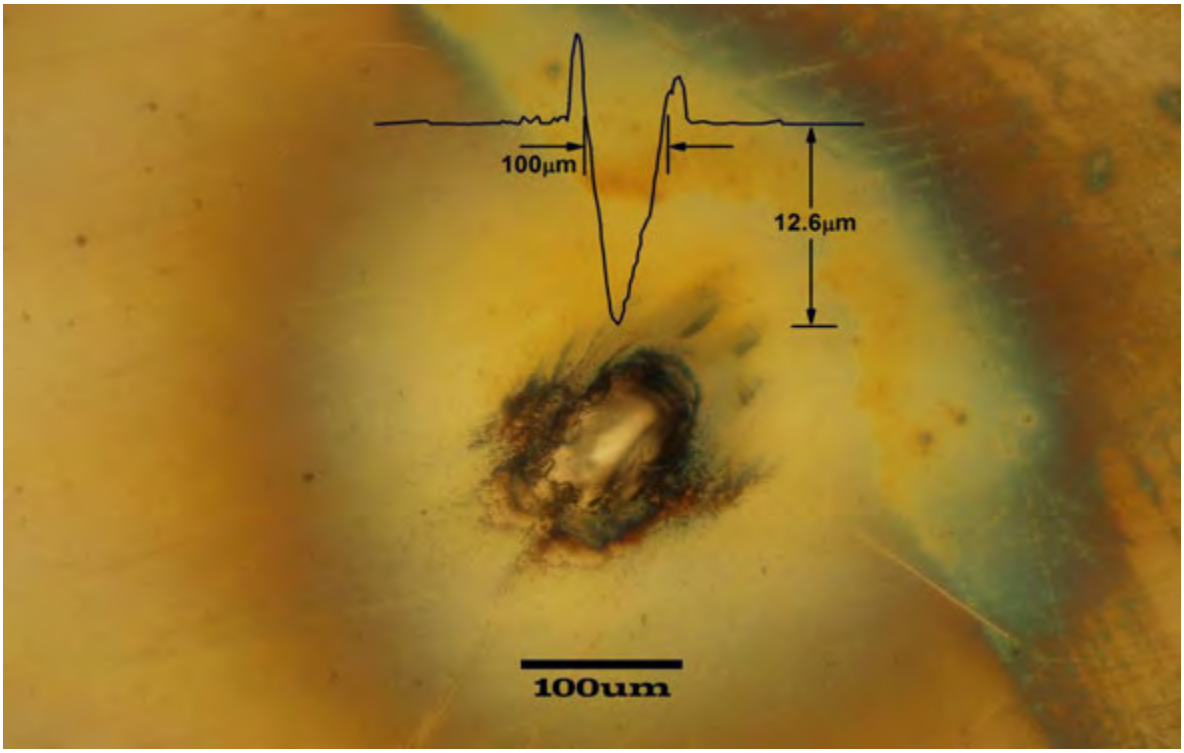

Figure 5.6. Reflection microscopic image of a crater produced by 30 accumulated laser shots with single energy of 5mJ in conventional LIBS set up. Above in the figure a crater profile is shown for reference size.

Assuming a volumetric damage with symmetrical conical shape with radius of 50µm and high of 12.6 µm, steel removed mass is about 250 ng.

In the case of DP-LIBS experiment, ablative pulses of 2.5mJ produced similar crater shape than crater discussed above but with smaller dimensions. As in SP-LIBS experiment, figure 5.7 shows a crater produced by 30 laser pulse accumulations. Compared with crater shown in figure 5.6, DP-LIBS ablative pulses produced smaller superficial and volumetric sample damage. Figure 5.7 shows a superficial crater with approximately circular shape with less than 50 µm of diameter.

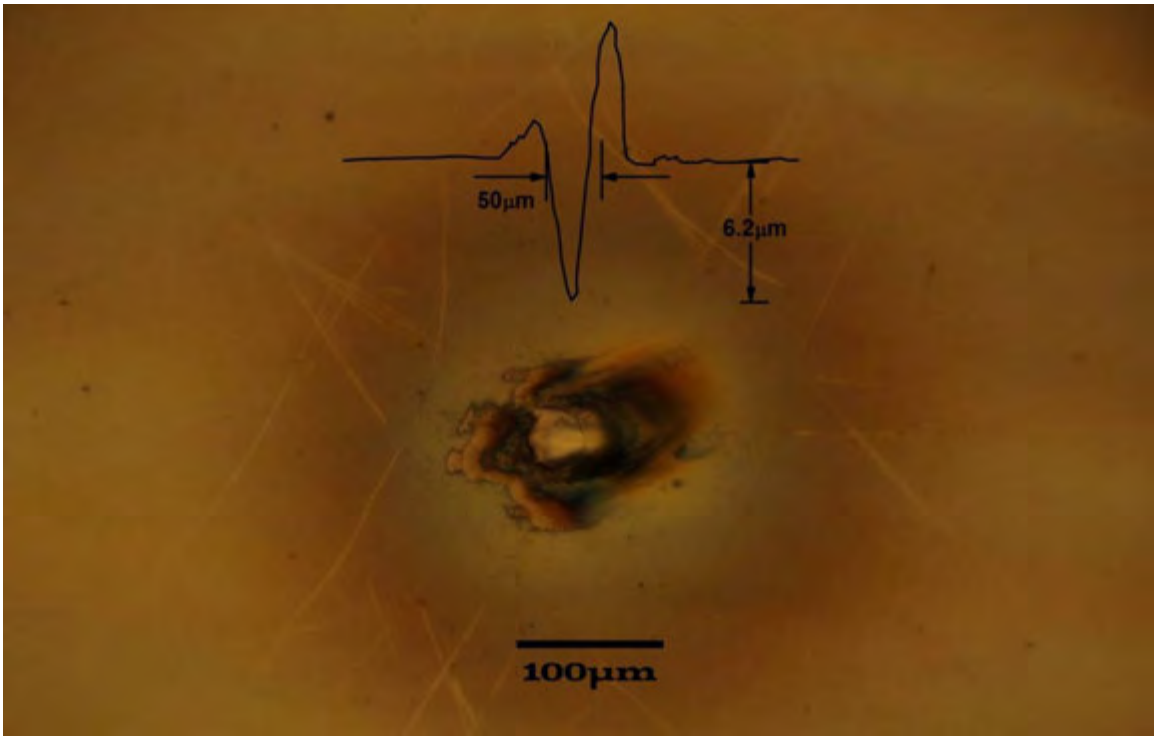

Figure 5.7. Reflection microscopic image of a crater produced by 30 accumulated laser shots with single ablative energy of 2.5mJ in orthogonal DP-LIBS configuration. Above in the figure a crater profile is shown for reference size.

The crater profile (black plot above in the figure) shows a penetration depth of 6.2 µm in the stainless steel sample. Considering the thermal effects, superficial damage can be extended at a circular zone with approximately 300 µm of diameter. Using the same assumptions as in the case of SPLIBS but with parameters from the crater produced by DPLIBS ($r = 25\mu m, h = 6.2\mu m$), steel removed mass is about 20 ng. Comparing both analyzed cases, sample damage can be diminished a factor of 13 using DP-LIBS instead of conventional SP in the CF-LIBS approach.

In summary, we have demonstrated that both techniques, CF-LIBS together with DP-LIBS, can be used for quantitative analysis. DP-LIBS, combined with CF-LIBS, can achieve same results than traditional CF-LIBS (with single pulse) but sample damage can be diminished by a factor of 13. The use of low ablative energies becomes increasingly important for critical applications such as art works analyses, archeological artifacts characterization, jewelry, etc. Additionally, the use of low ablative energies together with CF-LIBS opens up the possibility to perform rapid quantitative micro-analysis without standards or matrix-matched samples using LIBS-based lower power portable systems.

References

[1] R. Gaudiuso, M Dell'Aglio, O. De Pascale, G. Sensei, A. De Giacomo, "Laser Induced Breakdown Spectroscopy for Elemental Analysis in Environmental, Cultural Heritage and Space Applications: A Review of Methods and Results", Sensors 10, 7434 (2010).

[2] F. Doucet, G. Lithgow, R. Kosierb, P. Bouchard, M. Sabsabi, "Determination of isotope ratios using Laser-Induced Breakdown Spectroscopy in ambient air at atmospheric pressure for nuclear forensics", J. Anal. At. Spectrom. 26, 536 (2011).

[3] U. Contreras, M.A. Meneses-Nava, N. Ornelas-Soto, O. Barbosa-Garcia, P.L. López-de-Alba, J.L. Maldonado, G. Ramos-Ortiz, F.J. Acevedo-Aguilar, L-Lopez-Martinez, "Fast and Environmentally Friendly Quantitative Analysis of Active Agents in Anti-Diabetic Tablets by an Alternative LIBS and a Validated RP-HPLC Method", Appl. Spectrosc., 66(11), 1294 (2012).

[4] J. Uebbing, J. Brust, W. Sdorra, F. Leis, K. Niemax, "Reheating of a Laser-Produced Plasma by a Second Pulse Laser", Appl. Spectrosc., 45, 1419 (1991).

[5] J.P. Singh, S.N. Thakur, Laser-Induced Breakdown Spectroscopy (Elsevier 2007).

[6] A.W. Miziolek, V. Palleschi, I. Schechter, Laser-Induced Breakdown Spectroscopy (LIBS). Fundamentals and applications (Cambridge University Press, 2006) pp. 517-520.

[7] V.I. Babushok, F.C. DeLucia Jr, J.L. Gottfried, C.A. Munson. A.W. Miziolek, "Double pulse laser ablation and plasma: Laser induced breakdown spectroscopy signal enhancement", Spectrochimica Acta B 61, 999 (2006).

[8] M.M. Suliyanti, A.N. Hidayah, M. Perdede, E. Jobiliong, S.N Abdulmadjid, N. Idris, M. Ramli, T. Lie, R. Hedwig, M.O. Tjia, K.H. Kurniawan, Z.S. Lie, H. Niki, K. Kagawa, “Double pulse spectrochemical analysis using orthogonal geometry with very low ablation energy and He ambient gas”, Spectrochimica Acta B 69, 56 (2012).

[9] S.C. Choi, M.K. Oh, Y. Lee, S. Nam, D.K. Ko, J. Lee, “Dynamic effects of a pre-ablation spark in the orthogonal dual-pulse laser induced breakdown spectroscopy”, Spectrochimica Acta B 64, 427 (2009).

[10] G. Cristoforetti, “Orthogonal Double-pulse versus Single-pulse laser ablation at different air pressures: A comparison of the mass removal mechanisms”, Spectrochimica Acta Part B 64, 26 (2009).

[11] C. Gautier, P. Fichet, D. Menut, J.L. Lacour, D. L´Hermite, J. Dubessy, “Quantification of the intensity enhancements for the double-pulse laser-induced breakdown spectroscopy in the orthogonal beam geometry”, Spectrochimica Acta B 60, 265 (2005).

[12] C. Gautier, P. Fichet, D. Menut, J.L. Lacour, D. L´Hermite, J. Dubessy, “Study of the double-pulse setup with an orthogonal beam geometry for laser-induced breakdown spectroscopy”, Spectrochimica Acta B 59, 975 (2004).

[13] R. Sanginés, H. Sobral, E. Alvarez-Zauco, “The effect of sample temperature on the emission line intensification mechanisms in the orthogonal double-pulse Laser Induced Breakdown Spectroscopy”, Spectrochimica Acta B 68, 40 (2012).

[14] V.S. Burakov, N.V. Tarasenko, M.I. Nedelko, V.A. Kononov, N.N. Vasilev, S.N. Isakov, “Analysis of lead sulfur in environmental samples by double pulse laser induced breakdown spectroscopy”, Spectrochimica Acta B 64, 141 (2009).

[15] A. Ciucci, M. Corsi, V. Palleschi, S. Rastelli, A. Salvetti, E. Tognoni, “New Procedure for Quantitative Elemental Analysis by Laser-Induced Plasma Spectroscopy”, Appl. Spectrosc. 53, 960 (1999).

[16] E. Tognoni, G. Cristoforetti, S. Legnaioli, V. Palleschi, “Calibration-Free Laser-Induced Breakdown Spectroscopy: State of the art”, Spectrochimica Acta B 65, 1 (2010).

[17] Y. Ralchenko, A.E. Kramida, J. Reader, NIST ASD Team (2011), NIST Atomic Spectra Database (ver.4.1.0), [Online]. Available: http://physics.nist.gov/asd [2012]

[18] C. Gautier, P. Fichet, D. Menut, J. Dubessy, “Applications of the double-pulse laser-induced breakdown spectroscopy (LIBS) in the collinear beam geometry to the elemental analysis of different materials”, Spectrochimica Acta B 61, 210 (2006).

[19] R.W.P. McWhirter, R.H. Huddlestone, S.L. Leonard, Plasma Diagnostic Techniques (Academic Press New York, 1965) pp. 201-264.

[20] S. Pandhija, N.K. Rai, A.K. Rai, S.N. Thakur, “Contaminant concentration in environmental samples using LIBS and CF-LIBS”, Appl. Phys. B 98, 231 (2010).

[21] D.G.W. Smith, Short Course in Microbeam Techniques (Minearological Association of Canada, 1976).

6. General conclusions

For successful LIBS implementation, it has been proved that time-resolved and spectral-resolved optical emissions of pharmaceutical samples can be used to characterize their atomic composition and quantify an analyte in a faster and more practical way than conventional methods. Additionally, the use of Internal Standards has improved the analytical performance of the developed method by keeping relatively easy sample preparation step of the samples. Moreover CF-LIBS, a self-calibrated method, has been successfully implemented and it has been proved in the quantitative analysis of industrial steel samples. According to our results, CF-LIBS can be used for monitoring in real time quantitative information of the major constituents in metallic samples with relatively good uncertainties ($< 5\%$). The relative uncertainties are comparable with those reported in the literature on steel samples and metallic alloys. Our findings corroborate the potential use of CF-LIBS as a real-time, in-situ approach for preliminary analysis without the need of calibration curves or reference standards as stated in LIBS literature.

As our results demonstrate for the first time, orthogonal DP-LIBS at low ablative energies can be used in CF-LIBS approach for quantitative analysis. This finding means that, under our experimental conditions or similar, required energy for ablation can be diminished by a factor of two due to the analyte signal enhancement achieved by the second pulse. The reduction on the ablative energy allows a reduction in removed mass by a factor of 13. This finding becomes increasingly important for critical applications, such as the analysis

of art works, archeological artifacts, jewelry, etc. We hope our findings may contribute to the development and maturation of LIBS in a mid-term period of time. One remaining question is how other parameters of DP-LIBS configuration (inter-pulse delay time, wavelength, etc.) affect in the CF-LIBS results. A complete analysis may play an important role in the optimization of the enhancement factor and minimal sample damage. Besides, effects of other DP-LIBS configuration in CF-LIBS may be analyzed.

Universality of LIBS is expected due to further technological improvements are projected in the upcoming years; i.e., technological innovations will allow better spectral resolutions by better spectrometers; improvement in sampling efficiency by better and faster detectors is expected in upcoming years; spectral information will be available in the VUV range; compact and more stable lasers may reduce costs and increase the set ups flexibility achieving more precise analysis; and so on. Further methodological improvements from laboratories around the world are also expected to accelerate the maturation of LIBS as a universal technique. The imminent maturation of LIBS position the technique as a unique approach for many real-life problems In many fields (mining, environmental, on-line quality control in production processes, on-site in-situ applications, etc.).

7. Appendix

Appendix A: Software implementation

Friendly and easy-to-use “AtomicSpectra” software was developed in matlab platform for data processing and CF-LIBS analysis. Appendix A describes the main implemented steps for chemical identification of an unknown sample and its quantitative analysis. Those steps include pre-processing data, peak identification, and CF-LIBS algorithm. Besides those main steps, the implemented software can achieve minor but important tasks such as synthetic spectra plotting of all elements and ions (first and second order of ionization), spectra interpolation (spline and cubic methods), and so on. Those minor tasks are not discussed.

Data processing

Background correction in spectroscopy is a common first step in spectra analysis and several methods have been widely reported in the literature [1-2]. Over the last years numerous algorithms have been developed and successfully applied to solve specific problems. However, it has been a challenge to develop algorithms that does not require the prior knowledge of the background behavior. The problem of background signal is particularly important in LIBS. LIBS spectra have poor reproducibility because of intrinsic

violent laser-matter interaction which promotes high fluctuations in the signal. Besides, small laser energy fluctuations can cause significant changes in the plasma, affecting background and signal emission adding difficultness to background prediction.

LIBS background may be minimized by resolving temporally the spectra for long time delays as discussed in chapter 3. When plasma initiates, a continuum emission dominates the signal. This continuum decays and spectral lines appear becoming narrower as the time progresses. After certain time, the continuum emission decreases almost to the baseline. This is the best delay time that can be used for data acquisition. Nevertheless this approach sometimes is not convenient because important information such as ionized emission lines may be lost and even at an optimal time delay, small background and baseline signals must be subtracted. Atomicspectra implemented a background subtraction step based on a polynomial algorithm. The basic idea is to generate individual windows that calculate background subtraction in a specific section of the spectrum. The smaller the selected window, background subtraction line is closer to the spectrum at every wavelength.

User may decide the parameter value for the best background correction. Figure 7.1 shows a spectrum using two different parameters. In this figure, blue lines represent the experimental spectrum, red lines are the experimental spectrum with subtracted background and green lines represent the subtracted background. When peak identification is the main task both parameters satisfied it because in the spectra with subtracted background there is no change on the wavelength. However, when the main task involve other peak parameters such as FWHM or integral area of a certain peak the

parameter becomes very important. For this reason it is important to choose an adequate background subtraction parameter.

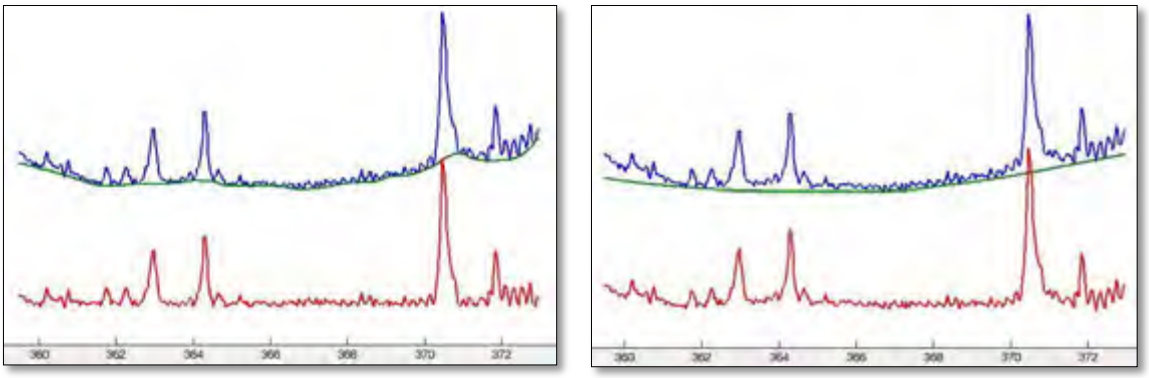

Figure 7.1. Background and baseline subtraction using two different parameters with the same subtraction method.

Synthetic spectra

As discussed in previous chapter, spectral information is taken from the NIST atomic spectra database [3]. In the NIST database, wavelength and relative intensities are available for most of the lines of all elements and ions. With this information is possible to generate a synthetic spectrum of any species at any spectral region by fitting each line to a Lorentzian profile (because of broadening produced by collisions as discussed in chapter 2). Figure 7.2 illustrates Fe synthetic spectra generated by Lorentzian profiles based on NIST information (wavelength and line intensities) in the range 370 nm – 380 nm. Lorentzian parameters were optimized to obtain best Lorentzian fitting with experimental spectra as will be pointed in chapter 5.

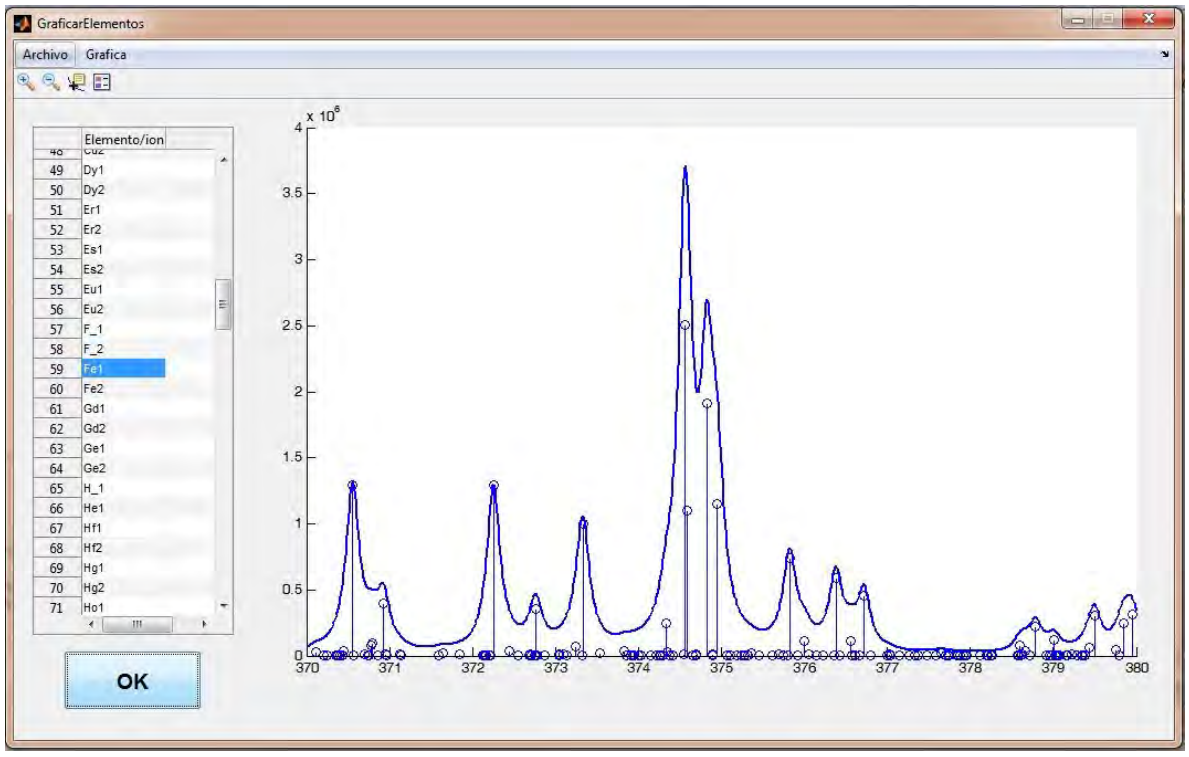

Figure 7.2. Fe synthetic spectra generated by Lorentzian profiles and NIST information (wavelength and line intensities).

Peak identification

In general, a sample´s spectrum is represented in a plot by the intensity versus the wavelength (or another parameter related with energy transitions, i.e. frequency). A typical LIBS spectrum contains the characteristic spectral lines from all the elements present in the sample. In principle, the spectrum represents a scaled spectral superposition of all individual elements. When lines of the spectrum are identified, then chemical composition can be estimated.

But identification of a given element is not just the simple choice of the nearest wavelength when compared with a certified database. Many parameters and phenomena are involved in real experiments such as wavelength displacements, superposition of near lines from different elements, change of relative intensities of lines from the same element, concentration of the specific element in the sample, matrix effects, and so on. Any or all of those phenomena may affect the correct identification of the chemical composition for a given sample.

Wavelength calibration

The first step in peak identification is the correct measurement of wavelength. Although good signal-to-noise ratio and high dispersion are essential for this purpose, accurate wavelength calibration of the spectrometer is fundamental. The correct association of a pixel with its correspondent wavelength must exist for a wide spectral range. Typically, setting the central pixel by mechanical means and calibrating the rest of the detector by reference spectra is enough for some spectroscopic techniques. In general, this method can be implemented for broadband spectrometers to calibrate the overall spectral region (250nm – 900 nm) minimizing pixel-to-wavelength discrepancy, like in Echelle-type spectrometers. Nevertheless, this method presents obvious limitations for other spectrometers. Using a typical Czerny-Turner spectrometer and a 1024 pixel array detector, at least three reference lines should appear for each spectral window with an adequate separation from each other. This requirement is not fulfilled in real situations

for all spectral windows. Even for the best reference spectral lamps, there are some spectral regions where there are not strong elemental lines. For LIBS applications specific spectral window with accurate pixel-wavelength association is needed in order to achieve exact peak identification in multi-elemental analysis overall pixel array. Asimellis et.al. [4] proposed a high accurate technique to calibrate wavelength based on the grating dispersion function in the visible and near-infrared spectral region (NIR). For a typical Czerny – Turner spectrometer, the central wavelength is set by rotating the grating to the central pixel of the array. The angular dispersion is typically considered as wavelength independent and in linear relationship with groove frequency; however, the intrinsic problem for those spectrometers is that angular dispersion varies strongly at longer wavelengths and large groove densities. Asimellis calibration considers the angular dispersion and the inverse angular dispersion of a grating as dependent of the wavelength. That is:

$$r(nm/pixel) = 10^9 P cos[arcsin(\lambda G/2cosx) + x]/GF \qquad \text{Eq. (3.1)}$$

In last expression, r and P represent the dispersion function and Pixel size in the array respectively. Symbols G, 2x, and F stand for groove density, deviation angle and spectrometer focal length parameters, respectively. In a brief description, the wavelength n for any pixel separated from the central pixel $(n - 512)$ is calculated by:

$$\lambda(n) = \lambda^{512} + r^{512}(n - 512) \qquad \text{Eq. (3.2)}$$

And the dispersion calculation applies a linear approximation calculated over a series of small wavelength windows. Given a central wavelength, linear regression coefficients are

calculated based on a curve fitting formulas of the dispersion function of a specific spectrometer.

$$r = \alpha\lambda + \beta \qquad \text{Eq. (3.3)}$$

For detailed information original publication can be consulted in the literature [4]. We successfully implemented and tested this wavelength calibration technique using our own instrumental parameters. Table 7.1 summarizes instrumental values used in our calculations. This technique is useful in the visible and near infrared region (600 nm – 900 nm) where dispersion is more pronounced. In the range UV-Vis (280 nm – 600nm) Asimellis method is not effective and wavelength can be corrected by simply displacing a constant shift to all wavelengths. We will refer to this calibration as shifted calibration in this chapter.

Table 7.1. Instrumental values from the Czerny Turner Spectrometer.

Name	Symbol	Units	Value
Grating groove frequency	G	Lines/mm	1200
Spectrometer focal length	F	mm	497.4
Array pixel size	P	μm	25
Spectrometer half – deviation angle	X		16.37°

We use the absolute difference between a calibrated wavelength and a reference wavelength as the discrepancy, that is, $discrepancy = \left|\lambda_{calibrated} - \lambda_{reference}\right|$. Reference lines information is taken from NIST atomic spectra database [3]. For the analysis of the spectral window centered at 460 nm we used lines of Cr and Cr I from a

stainless steel sample. In the case of the spectral window centered at 830 nm we used lines from an anti–diabetic tablet, containing mainly N, as reference.

Table 7.2. Discrepancies between calibrated and reference lines over two different spectral regions.

UV – Vis Range				Vis – NIR Range			
Reference wavelength	Element	Discrepancy shifted calibration	Discrepancy Asimellis calibration	Reference wavelength	Element	Discrepancy shifted calibration	Discrepancy Asimellis calibration
449.686	Cr	0.039	0.057	818.487	N	0.229	0.009
452.647	Cr	0.019	0.032	818.802	N	0.058	0.020
454.596	Cr	0.015	0.024	820.036	N	0.044	0.023
455.866	Cr I	0.053	0.059	821.072	N	0.041	0.010
460.075	Cr	0.000	0.000	821.634	N	0.049	0.004
464.617	Cr	0.001	0.009	822.314	N	0.037	0.010
469.846	Cr	0.034	0.049	824.239	N	0.029	0.026
470.727	Cr	0.066	0.050	827.244	Br	0.004	0.000
471.843	Cr	0.028	0.046	833.47	Br	0.104	0.057
475.611	Cr	0.071	0.093	844.636	O	0.120	0.011

Table 7.2 shows the discrepancy between lines for calibration methods (shifted and Asimellis calibration) and reference lines for two spectral windows, i.e. UV – Vis (440 nm – 480 nm) and Vis – NIR (810 nm – 850 nm). In UV – Vis range values of shifted calibration discrepancies are lower than Asimellis's calibration. In the case of Vis – NIR region Asimellis discrepancy is lower than shifted one for all analyzed lines. Information in Table 2 can be summarized in figure 7.3.

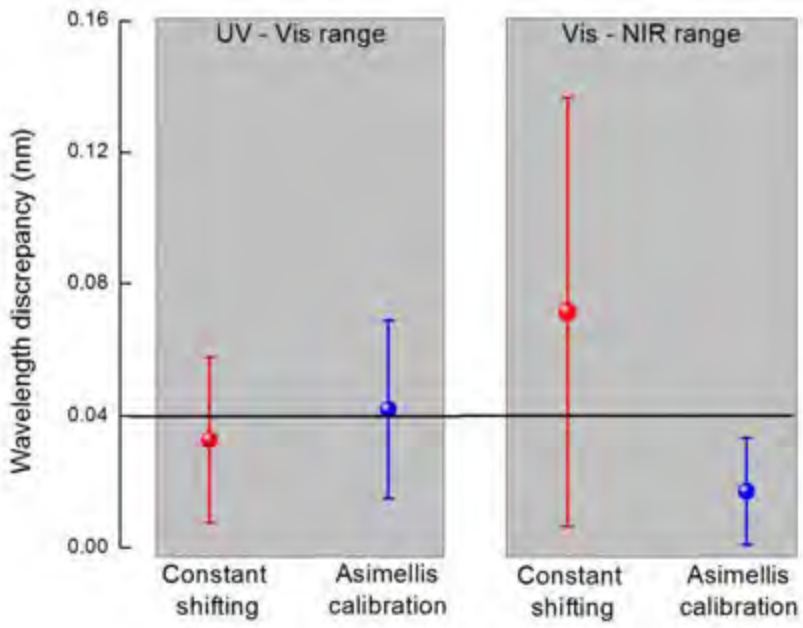

Figure 7.3. Average discrepancy values and standard deviations for shifted and Asimellis calibrations in the UV – Vis and Vis – NIR regions.

Both calibration methods work satisfactorily in the UV – Vis spectral range and average discrepancy values stay close to the instrumental resolution (~0.04 nm) for both methods. In figure 7.3 average discrepancy values and their standard deviation are plotted as circles and error bars respectively for both methods in UV – Vis (left side in the plot) and Vis – NIR (right side in the plot) spectral regions. As stated in equation (1), dispersion is more pronounced for long wavelengths and shifted calibration fails (>600 nm) but Asimellis calibration works satisfactorily and discrepancy values stay lower than the instrumental resolution for all analyzed lines. Asimellis has better accuracy in the NIR range; however, this method can be used for all UV/Vis/NIR spectral windows. If more accurate calibration is needed in the UV – Vis range (280 nm – 600 nm) shifted calibration should be used.

Correlation

Comparing the LIBS experimental spectrum with a reference spectra database is the next step after wavelength calibration for chemical composition identification. Different techniques have been proposed for line spectral identification [5-9]. Correlation coefficient has been the most popular technique and it has been applied successfully to quantify the spectral similarity between experimental and reference spectra by many groups [5-7]. We implemented correlation coefficient technique in AtomicSpectra software.

As an example, figure 7.4 shows an experimental spectrum (blue spectrum) taken from a stainless steel sample and the spectrum generated by the superposition of Fe, Cr, and Cr I synthetic lines. Table at the right side in figure 7.4 shows the individual correlation coefficients for Cr2, Fe1, Cr1, Ni1, and Mn1 (1 stands for neutral species and 2 stands for single ionized species in the software nomenclature). Species are listed in decreasing order according to their correlation coefficient value. AtomicSpectra can calculate correlation coefficient from individual and superposition of user-selected species.

It should be noted that interferences decrease the value of the correlation coefficient affecting spectral identification. Interferences can be produced by the presence of spectral lines of other elements or inherent noise and background emission. For this reason, the correlation coefficient not always indicates the correct element identification

in complex spectra. Visual inspection and spectroscopist's expertise should be incorporated after the correlation in the identification process.

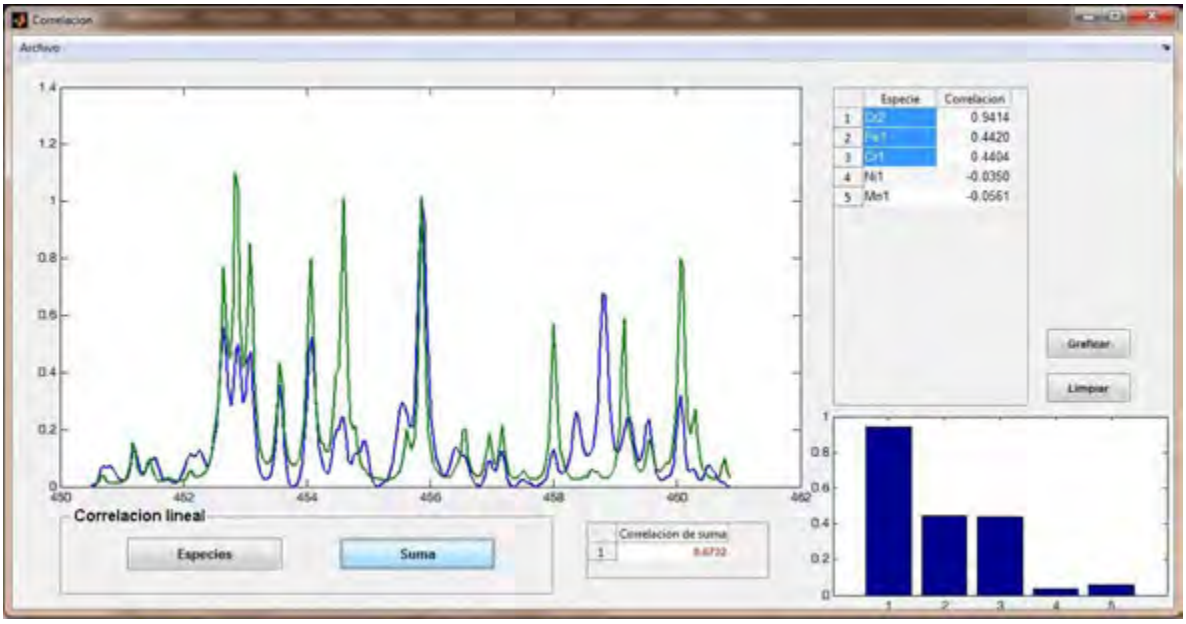

Figure 7.4. Graphical User Interface generated by Matlab platform for correlation coefficient calculation between experimental and synthetic spectra. In this example, correlation between stainless steel experimental spectrum (blue) and synthetic spectra (green) from Fe, Cr and Cr ionized is shown.

CF-LIBS algorithm

Calibration Free (CF) LIBS approach has been described briefly in chapter 2. In this section it is described the Graphical User Interface implemented in AtomicSpectra for CF-LIBS analysis. Because of robustness, the implemented CF-LIBS algorithm for quantitative

analysis is based in the integral of the line over a Lorentzian profile (area) instead of spectral intensity value.

Basically, the algorithm links NIST atomic spectra database information with integrated areas for each experimental peak in the analysis. Integrated area is calculated over a fitted Lorentzian profile for each experimental peak after processing signal (background subtraction and wavelength calibration mainly). The problem of optimizing areas is solved by least squares method. The sum of all fitted peaks should be as similar as the experimental spectrum. This problem falls into the non-linear least squares category where the number of peaks is fixed for a certain spectral range and intensities represent independent variables. The problem of optimizing areas is very important, because in CF-LIBS, the quantitative analysis is very sensitive to the integral area.

Figure 7.5 illustrates an example of optimizing the sum of 33 calculated individual areas (black Lorentzian profiles). The superposition of 33 Lorentzian profiles generates a spectrum (green spectrum in the Figure) fitted to the experimental spectrum (blue spectrum) by least square algorithm. After the best area fitting, the algorithm stores the information and user links it to the corresponding element parameters in order to quantify the chemical composition using CF-LIBS approach.

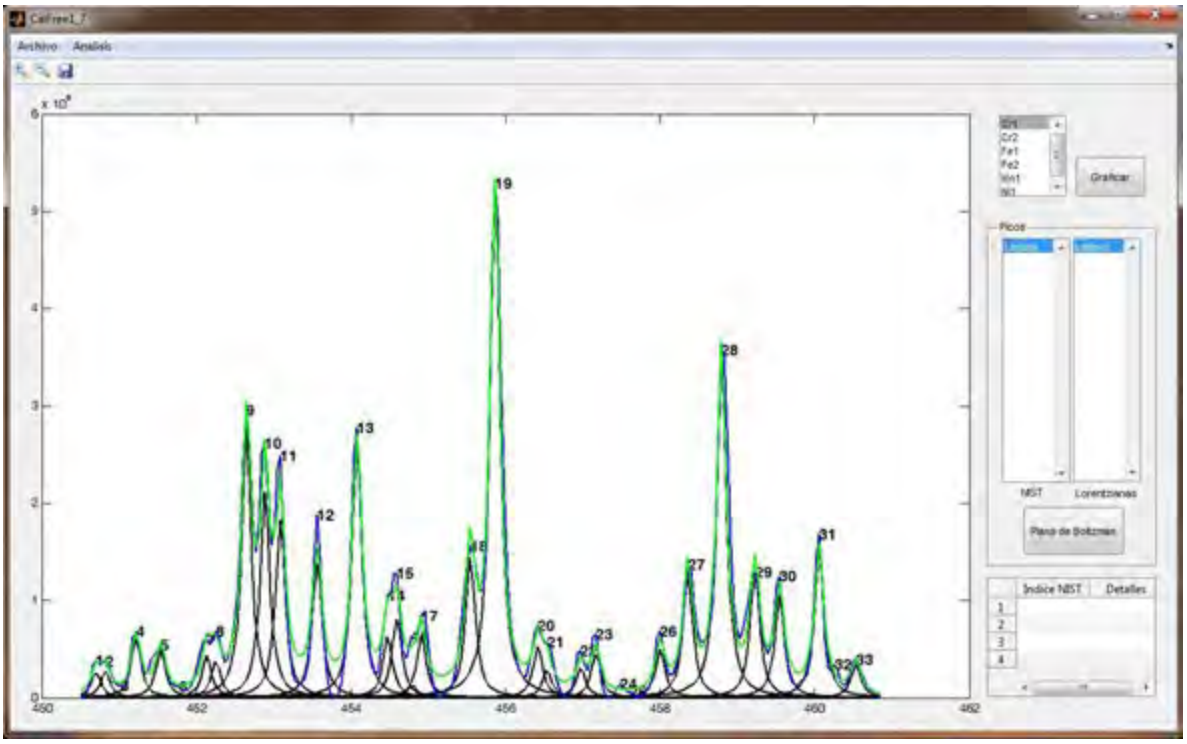

Figure 7.5. Spectra from: 33 individual Lorentzian profiles (black lines), superposition of 33 Lorentzian profiles (green line), and experimental (blue line). 33 Lorentzian profiles are optimized to best fit the superposition profiles with experimental spectrum.

References

[1] B. Beier, and A. Berger, “Method for automated background subtraction from Raman spectra containing known contaminants”, Analyst, 134 (6), 2009, 1198-1202.

[2] I. B. Gornushkin, P. E. Eagan, A. B. Novikov, B. W. Smith, and J. D. Winefordner, “Automatic Correction of Continuum Background in Laser-Induced Breakdown and Raman Spectrometry”, Applied Spectroscopy, 57 (2), 2003, 197-207.

[3] Kramida A., Ralchenko Yu, Reader J., and NIST ASD Team (2012). NIST Atomic Spectra Database (ver. 5.0), [Online]. Available: http:/physics.nist.gov/asd National Institute of Standards and Technology, Gaithersburg, MD.

[4] G. Asimellis, A. Giannoudakos, and M. Kompitsas, “Accurate wavelength calibration in the near-infrared for multielement analysis without the need for reference spectra”, Applied optics 45 (35) 2006, 8855-8862.

[5] I. B. Gornushkin, U. Panne, J. D. Winefordner, “Linear correlation for identification of materials by laser induced breakdown spectroscopy: Improvement via spectral filtering and masking”, Spectrochimica Acta B, 64, 2009, 1040-1047.

[6] I. B. Gornushkin, M. Mueller, U. Panne, and J. D. Winefordner, “Insights into Linear and Ranck Correlation for Material Identification in Laser-Induced Breakdown spectroscopy and Other Spectral Techniques” Applied Spectroscopy, 62 (5), 2008, 542-553.

[7] P. R. Griffiths and Limin Shao, “Self-Weighted Correlation Coefficients and Their Application to Measure Spectral Similarity”, Applied Spectroscopy, 63(8), 2009, 916-919.

[8] A. Gulliver, and J. Stadel, “Automated spectral line identification”, Publications od the Astronomical Society of the Pacific, 102, 1990, 587-591.

[9] M. Saritha, V. P. N. Nampoori, “Identification of spectral lines of elements using artificial neural networks”, Microchemical Journal, 91, 2009, 170-175.

Appendix B: Published indexed articles

November 15, 2012 / Vol. 37, No. 22 / OPTICS LETTERS 4591

Double-pulse and calibration-free laser-induced breakdown spectroscopy at low-ablative energies

V. Contreras,[1,2] M. A. Meneses-Nava,[1,3] O. Barbosa-García,[1] J. L. Maldonado,[1] and G. Ramos-Ortiz[1]

[1]*Centro de Investigaciones en Óptica A. C., Loma del Bosque 115, León, Gto. 37150, Mexico*

[2]*e-mail: ulises@cio.mx*

[3]*e-mail: tono@cio.mx*

Received August 7, 2012; revised September 27, 2012; accepted September 28, 2012; posted October 1, 2012 (Doc. ID 173951); published November 6, 2012

The use of double-pulse laser-induced breakdown spectroscopy (DP-LIBS) in quantitative analysis generally depends on standards and calibration curves. To our knowledge, in this Letter, we report the first quantitative analysis based on DP-LIBS at low ablative energies with a self-calibrated method. We compare the effects of plasmas on the calibration-free LIBS technique, generated by DP-LIBS, and the traditional single-pulse (SP) LIBS on a steel sample. Our analyses reveal that when SP-LIBS and DP-LIBS reach comparable emission line intensities, plasma parameters and quantitative analysis are practically the same for both experiments. Additionally, we report the behavior of the emission enhancement of some elements (Fe and Cr) at low ablative pulse energies (0.2–8 mJ) using the orthogonal reheating DP-LIBS configuration. © 2012 Optical Society of America

OCIS codes: 300.6365, 140.3440, 160.3900.

In recent years laser-induced breakdown spectroscopy (LIBS) has become a versatile and practical technique for elemental analyses for a wide number of materials and applications [1–3]. When sample damage is an important issue, however, LIBS is considered to be a destructive technique. It is well known that the intensity of the LIBS signal depends critically on the laser pulse energy. Increasing the laser pulse energy will not only increase the intensity of the emission lines but also will increase the ablated material. By using the orthogonal double-pulse (DP) LIBS scheme [4–6], it is possible to increase the signal intensity without increasing the amount of ablated material. An important number of papers have discussed the use of DP-LIBS configurations, and their authors have reported the use of pulses with relative high energies in the range of tens to hundreds of microjoules [7–13].

For quantitative analysis, the use of DP-LIBS generally depends on standards and calibration curves [7,14]. DP-LIBS enhances signal intensities for all elements present in a sample, but whether it is possible to use DP-LIBS together with a self-calibrated method for quantitative analysis has not yet been proved. In this Letter, we demonstrate that calibration-free LIBS (CF-LIBS) [15] can be used successfully to analyze plasmas generated by DP-LIBS by means of low ablative energies. The use of low ablative energies becomes increasingly important when critical applications, such as the analysis of art works, archeological artifacts, jewelry, and so on are considered. CF-LIBS is a multielemental quantitative analysis approach based on the measurement of plasma parameters and line intensities produced by traditional LIBS experiments. CF-LIBS has been carried out in several experimental conditions. In most cases, spectra have been acquired at atmospheric conditions using single-nanosecond laser pulses as the generation and excitation source of the plasma. In general, laser pulse energies vary from 1 mJ to more than 100 mJ [16]. We show that a quantitative analysis is possible by CF-LIBS based on plasmas produced by a DP-LIBS configuration at low ablative energies (~0.25 mJ). For DP-LIBS experiments, we use two different pulses, an ablating pulse and a reheating pulse, produced by an Nd:YAG laser and an optical parametric oscillator (OPO), respectively, at a 10 Hz repetition rate and a 10 ns pulse duration. Ablative pulses produced by the frequency-doubled (532 nm) output of the Nd:YAG were also used as single pulses in traditional single-pulse LIBS experiments. These pulses were focused perpendicularly onto the sample surface by a convex lens with a 150 mm focal length. Reheating pulses, produced by the OPO system were tuned to 506 nm and were focused parallel to the sample onto the vapor or plasma produced by the ablative pulses using a convex lens with a 100 mm focal length. The reheating pulses were optically delayed by 10 ns (with respect to the ablative pulses) by increasing their optical path length, and the energy pulse was fixed at 7 mJ for all experiments. Light was collected by a 150 mm focal length lens and focused on the end of a bundle of 19 optical fibers in a hexagonal array. The fiber optics bundle was coupled to the entrance slit of a Czerny–Turner spectrograph (0.5 m focal length) equipped with 1200 l/mm grating and connected to an intensified charge coupled device (ICCD) detector. To minimize instrumental effects on the spectra, we use the minimum entrance slit width of the spectrometer (10 μm) to reduce line broadening. Experimental parameters were chosen to maximize signal to continuum ratio. Spectra used in the analyses were generated by accumulating the signal of 30 (single or paired) laser shots.

For CF-LIBS analysis, relevant spectral information—such as ionization energy values for each element, upper and lower level energies, or transitions probabilities for each line—was taken from the National Institute of Standards and Technology atomic spectra database [17]. In our case, it was not possible to measure all the elements present in the steel sample because of instrumental limitations; that is, the strongest C I line emits close to

0146-9592/12/224591-03$15.00/0

INVESTIGACIÓN Revista Mexicana de Física 58 (2012) 184–190 ABRIL 2012

Identificación de aceros por espectroscopia de rompimiento inducido por láser (LIBS) y análisis de componentes principales

U. Contreras[a], M.A. Meneses-Nava[a], D. Torres-Armenta[a], J. Robles-Camacho[b] y O. Barbosa-García[a]
[a]*Grupo de Propiedades Ópticas de la Materia, Centro de Investigaciones en Óptica A.C., Loma del Bosque 115, 37150 León, México.*
[b]*Laboratorio de Arqueometría del Occidente, Instituto Nacional de Antropología e Historia, Centro INAH Michoacán, Madero Oriente 799, Morelia, 58000, México.*

Recibido el 18 de enero de 2012; aceptado el 27 de marzo de 2012

En la actualidad existe una producción de más de 100 000 aceros diferentes de acuerdo a su composición química y propiedades mecánicas; sin embargo, una vez en el mercado, no existe técnica alguna capaz de identificar y clasificar cualquier acero según su clase o grado. En este trabajo se describe un método capaz de identificar y clasificar aceros a través de la determinación de su composición química. El método propuesto se basa en un análisis de espectroscopia atómica procedente de la técnica LIBS así como del análisis multivariado de los espectros de emisión. Para aceros pertenecientes a diferentes clases se detectaron diferencias espectrales considerables debidas a su composición elemental, lo que hace posible su identificación de una manera rápida. En el caso de dos aceros analizados de una misma clase, pero de distinto grado, la información espectral no es suficiente para una discriminación satisfactoria a simple vista ya que las diferencias en composición son relativamente bajas ($< 0.5\,\%$); sin embargo, con el análisis de componentes principales (PCA) se logró la discriminación de las 4 muestras de acero (de acuerdo a su clase y grado).

Descriptores: Espectroscopia de rompimiento inducido por láser; LIBS; PCA; aceros; métodos multivariados.

Nowadays there exist more than 100 000 different types of steels according to their chemical and physical properties. Nevertheless there is not a unique method capable to identify or classify any sample of steel according to its class or grade. In this work it is described a method capable to identify and classify steels due to the chemical composition determination. The proposed method is based in the analysis of atomic spectra by Laser Induced Breakdown Spectroscopy (LIBS) and Principal Component Analysis (PCA). For steels from different classes it is possible to discriminate them due to their chemical composition. For steels from the same class but different grade, the information on the spectra is not sufficient for a satisfactory discrimination because of the relatively low difference in composition ($< 0.5\,\%$); however, discrimination of all analyzed samples is possible using PCA.

Keywords: Laser induced breakdown spectroscopy; LIBS; PCA; Steels; multivariate analysis.

PACS: 93.30+w; 40.62.Fi; 52.38.Mf; 02.50.Sk

1. Introducción

Desde las primeras evidencias antropológicas de manipulación de meteoritos sideríticos (Fe/Ni) hace más de 6000 años y el inicio de la "Era de Hierro" entre 1500 y 1000 a.C., con la concebida evolución metalúrgica, el acero se ha convertido en una de las aleaciones más importantes en la vida del ser humano debido a la amplia gama de propiedades físicas que se obtienen al combinar ciertos elementos a baja concentración con el hierro [1]. Hoy en día existen más de 100 000 estándares de aceros agrupados en más de 200 clases de acuerdo a su composición química, en donde cada clase contiene a su vez aceros a diferentes grados (en donde varía la concentración de algunos de sus elementos químicos) [2]. Se han desarrollado técnicas de identificación como la prueba magnética, la cual puede diferenciar aceros sin respuesta magnética (aceros de clase 300 por ejemplo) de aquellos que presentan propiedades magnéticas. Sin embargo, esta prueba no es capaz de diferenciar, por ejemplo, entre un acero 303 y un acero 304 (ninguno presenta respuesta magnética) que pertenecen a una misma clase y distinto grado. También existen técnicas que utilizan reactivos químicos capaces de discriminar entre aceros inoxidables y aceros oxidables. Otras pruebas existentes permiten la identificación de algún elemento específico como molibdeno (Mo) o Azufre (S), discriminando aceros que contienen estos elementos específicos de aquellos que no los contienen [3]. A pesar de la amplia gama de pruebas para la identificación de aceros, no existe una técnica establecida para la identificación y clasificación de cualquier tipo de acero de manera rápida y confiable.

La espectroscopia de rompimiento inducido por laser (LIBS por su acrónimo en inglés) es una técnica capaz de analizar la composición atómica de cualquier material sin importar el estado de agregación en que se encuentre. En el caso de materiales sólidos, cuando un pulso láser de alta potencia golpea una superficie, la energía del láser se transforma en calor y la temperatura del material sólido se incrementa produciendo una rápida fusión y/o evaporación del material. Debido a que el vapor producido está formado por átomos, iones y electrones y puede alcanzar temperaturas muy altas (del orden de 1×10^4 K) se produce un plasma. En el caso de pulsos de algunos nanosegundos (o de mayor duración), parte del pulso láser es absorbido por el plasma aumentando su ionización y temperatura. Después de este proceso conocido como ablación láser, prosigue una emisión continua (bremsstrahlung) producida principalmente por el choque entre electrones libres, una emisión por recombinación de electrones

Fast and Environmentally Friendly Quantitative Analysis of Active Agents in Anti-Diabetic Tablets by an Alternative Laser-Induced Breakdown Spectroscopy (LIBS) Method and Comparison to a Validated Reversed-Phase High-Performance Liquid Chromatography (RP-HPLC) Method

Victor Ulises Contreras,[a,*] Marco A. Meneses-Nava,[a] Nancy Ornelas-Soto,[a] Oracio Barbosa-García,[a] Pedro L. López-de-Alba,[b] José L. Maldonado,[a] Gabriel Ramos-Ortiz,[a] Francisco J. Acevedo-Aguilar,[b] Leticia López-Martínez[b]

[a] *Centro de Investigaciones en Óptica, A.P. 1-948, 37150 León, Gto., México*
[b] *Departamento de Química, Universidad de Guanajuato, Cerro de la Venada s/n, C.P. 36040Gto., México*

Laser-induced breakdown spectroscopy (LIBS) is evaluated as a potential analytic technique for rapid screening and quality control of anti-diabetic tablets. This paper proposes a simple LIBS-based method for the quantitative analysis of two active pharmaceutical ingredients (APIs): metformin (Met) and glybenclamide (Gly). In order to quantify both APIs, chlorine (Cl) concentration was estimated by employing the Cl/Br optical emission ratio, where Br was introduced as internal standard. Calibration curves were prepared, achieving linearity higher than 99%. On the other hand, for comparison to the proposed method, an isocratic reversed-phase high-performance liquid chromatography (RP-HPLC) method was also developed for quantitative determination of the same analytes by ultraviolet (UV) detection. The chromatographic separation was achieved on a Phenomenex Hypersil C18, 250 mm × 4.6 mm, 5 µm column. The mobile phase was K_2HPO_4/H_3PO_4–CH_3OH and flow rate was 1.0 mL min^{-1}. The method is linear over a range of 10–60 µg mL^{-1} for Gly and 5–30 µg mL^{-1} for Met and the correlation coefficients were ≥0.99. Recoveries were found to be in the range of 95–101%. Furthermore, four different commercial brands of each active agent were evaluated by both proposed LIBS and chromatographic methods and results were compared with each other. The comparison was satisfactorily validated by analysis of variance (ANOVA).

Index Headings: **Pharmaceuticals; API; Metformin; Glybenclamide; Laser-induced breakdown spectroscopy; LIBS; Spectroscopy.**

INTRODUCTION

Diabetes is a chronic disease that not only affects people's health but also imposes a large economic burden on individuals, families, national healthcare systems, and economies worldwide. Type 2 diabetes is characterized by high glucose concentration in the blood, which is caused by both low pancreas secretion and reduced sensitivity to insulin. Currently, there is a wide variety of oral agents clinically available to help regulate glucose levels in blood such as sulfonylureas, meglitinides, biguanides, and thiazolidinediones.[1,2] Sulfonylureas, such as glybenclamide (Gly), interact with sulfonylurea receptors on pancreatic β-cells to enhance insulin secretion and decrease blood-glucose levels. On the other hand, metformin (Met), the most common biguanide clinically available, decreases hepatic glucose production and increases the sensitivity of peripheral tissues to insulin.[3] At present, the blend of Gly/Met is the oral drug combination of choice in clinical practice.[4] Nowadays more than 220 million people worldwide have diabetes and the World Health Organization (WHO) projects that diabetes deaths will double between 2005 and 2030.[5] Besides the increase of diabetes, the production of both counterfeit and low-quality drugs is increasing and this fact also affects human health and results in loss of profit to pharmaceutical industries.[6] Control of the active agent content in commercial products is important to guarantee the quality of pharmaceuticals worldwide.

Laser-induced breakdown spectroscopy (LIBS) represents a powerful atomic analytical technique because of its intrinsic characteristics such as simple pretreatment or none at all, speed, and availability of multi-elemental analysis. LIBS requires no additional chemical compounds or solvents at all, and consequently, the analysis is environmentally friendly. At present, LIBS-based analysis of food, agricultural, geological, environmental, and biomedical solid samples for macro and micro elemental determination has emerged as an important analytical field because of its viability.[7–13] LIBS is a technique based on the analysis of the optical emission of a plasma plume containing individual neutral and ionic species from elements present in a sample. In general, a pulsed laser vaporizes and excites the surface of the sample in order to produce time-dependent emission lines. Emission line intensities indicate the relative population of each species, allowing a qualitative and quantitative analysis of solid, liquid, and gaseous samples. In the pharmaceutical field, some works have shown the effectiveness of applying the LIBS technique mostly for qualitative determination of some active ingredients in solid and liquid formulations.[14–16] Quantitative analysis of pharmaceutical products has been reported using noble gas environments to produce plasma that enhances the sensitivity to halogen elements present in active pharmaceutical ingredients (APIs).[17] Lubricants, coating characterization, thickness, and uniformity of the pharmaceutical tablets have also been analyzed using LIBS.[18–20]

On the other hand, chromatography is the most frequently used technique for pharmaceutical analysis, and for anti-diabetic drugs, several high-performance liquid chromatography (HPLC) methods have been reported for Met and a bit less for Gly analysis but all of them are restricted for their

Received 14 May 2012; accepted 9 July 2012.
* Author to whom correspondence should be sent. E-mail: ulises@cio.mx.
DOI: 10.1366/12-06724

0003-7028/12/6611-1294$2.00/0

PERSONAL INFORMATION

Victor Ulises Lev Contreras Loera

Loma del Bosque 115 Lomas del Campestre, León, Gto., México
+52 4774414200 +52 4771201830
ulev22@gmail.com
ulises@cio.mx

Sex Male | Date of birth 22/01/1983 | Nationality Mexican

EDUCATION AND TRAINING

March 2013
PhD in Natural Sciences (Optics)
Centro de Investigaciones en Óptica A. C. (CIO), León México

December 2008
Master degree in Natural Sciences (Optics)
Centro de Investigaciones en Óptica A. C. (CIO), León México

October 2006
Bachelor in Physics
Universidad Autónoma de Zacatecas, Zacatecas, México

SCIENTIFIC PRODUCTS

International Publications

V. Contreras, M.A. Meneses-Nava, O. Barbosa-García, J.L. Maldonado, G. Ramos-Ortiz, “Double Pulse and Calibration Free Laser-Induced Breakdown Spectroscopy at Low Ablative Energies”, Optics Letters 37 (2012) 4591-93.

Victor Ulises Contreras, Marco A. Meneses-Nava, Nancy Ornelas-Soto, Oracio Barbosa-García, Pedro L. Lopez-de-Alba, Gabriel Ramos-Ortiz, Jose L. Maldonado, Francisco J. Acevedo-Aguilar, Leticia Frausto, “Fast and Environmentally Friendly Quantitative Analysis of Active Agents in Anti-Diabetic Tablets by an Alterantive LIBS and a Validated RP-HPLC Method”, Applied Spectroscopy, 66(11), 2012, 1294-1301.

U. Contreras, NE Ornelas-Soto, MA Meneses-Nava, O. Barbosa-Garcia, PL L-de-Alba, L L-Martinez, “Quantitative analysis of metformin in anti-diabetic tablets by laser-induced breakdown spectroscopy”, Proceedings SPIE 8011 (2011) 80112Q DOI: 10.1117/12.902173.

Ulises Contreras, O. Barbosa-García, J.L. Pichardo-Molina, G. Ramos-Ortiz, J.L. Maldonado, M.A. Meneses-Nava, N.E. Ornelas-Soto, P.L. López-de-Alba, “Screening method for identification of adulterate and fake tequilas by using UV-VIS spectroscopy and chemometrics”, Food Research International 43 (2010) 2356-23-62.

N. Ornelas-Soto, O. Barbosa-Garcia, M. Meneses-Nava, G. Ramos-Ortiz, J. Pichardo-Molina, J.L. Maldonado, **U. Contreras**, L. Lopez-Martinez, P. Lopez-De-Alba, F. Lopez-Barajas. “Spectroscopic analysis of pharmaceutical formulations through the use of chemometric tools” Proceedings Paper Vol. 7499, (2009).

Ivan Moreno, **Ulises Contreras**, “Color distribution from multicolor LED arrays” Optics Express Vol. 15. No. 6 (2006).

I. Moreno, **U. Contreras**, R. I. Tzonchev, “Cluster configurations of red, green, and blue

LEDs for white light illumination", SPIE vol. 5739, Pag. 162-168 (2005).

National Publications

U. Contreras, M. A. Meneses-Nava, D. Torres-Armenta, J. Robles-Camacho, O. Barbosa-Garcia, "Identificación de aceros por espectroscopia de rompimiento inducido por láser (LIBS) y análisis de componentes principales", Revista Mexicana de Física 58 (2012) 184-190.

Ulises Contreras-Loera, O. Barbosa-García, G. Ramos-Ortiz, J.L. Pichardo Molina, M.A. Meneses-Nava, J.L. Maldonado, "Identificación y discriminación de Tequilas reposados in situ para la protección de marca", Revista Electrónica Nova Scientia, Num. 2 Vol. 1, Mayo-Octubre 2009.

Invited Talks and Conferences

"Laser induced breakdown spectroscopy: basics and applications", Seminario de los Departamentos de Ingeniería Física e Ingenierías Química, Electrónica y Biomédica. División de Ciencias e Ingenierías Campus León. Universidad de Guanajuato (October 24th 2012).

"Spectroscopic Techniques: A few of applied optics" 25 Aniversario de la Unidad Académica de Física. Universidad Autónoma de Zacatecas (May 31st 2012).

"Laser-Induced Breakdown Spectroscopy (LIBS): Basics and quantification methods". Ciclo de seminarios UAF Agosto-Diciembre 2011. Universidad Autónoma de Zacatecas (October 27th 2011).

"Atomic fingerprints", Centro de Estudios Tecnológicos, industrial y de servicios No. 21, Semana Nacional de Ciencia y Tecnología, León, Gto. (September 2011).

"Laser Induced Breakdown Spectroscopy (LIBS)", Centro de Nanociencias y Nanotecnología-UNAM, Ensenada, B.C., Mex. (March 2011)

"Screening method for identification of adulterate and fake tequilas by using UV-VIS spectroscopy and chemometrics". Ciclo de Seminarios UAF Enero-Junio 2009. Universidad Autónoma de Zacatecas (May 28th 2009).

Congresses

U. Contreras, M. Meneses-Nava, J. Robles, G. Ramos-Ortiz, J. Maldonado, O. Barbosa-García, "Effects Of Single and Double Pulse Orthogonal Configuration In Calibration Free – LIBS Technique At Low Ablative Energies" 7th International Conference on Laser Induced Breakdown Spectroscopy (LIBS 2012), Luxor, Egypt (29th September – 4th October 2012)

U. Contreras, N. Ornelas-Soto, Marco A. Meneses-Nava, Oracio Barbosa-Garcia, Pedro L. Lopez –de-Alba, Leticia Lopez-Martinez. "Quantitative analysis of metformin tablets by Laser-Induced Breakdown Spectroscopy" 22nd General Congress of International Commission for Optics (ICO-22), Puebla, Mex. (Agosto 2011).

U. Contreras, N. Ornelas-Soto, Marco A. Meneses-Nava, Oracio Barbosa-Garcia, Pedro L. Lopez –de-Alba, Leticia Lopez-Martinez, "Quantitative analysis of active agents in anti-diabetic tablets by Laser-Induced Breakdown Spectroscopy", North American Symposium on LIBS (NASLIBS), Clearwater Beach, Florida, EUA (Jul. 2011).

Ulises Contreras, Nancy Ornelas-Soto, Marco A. Meneses-Nava, Oracio Barbosa-Garcia, Pedro L. Lopez –de-Alba, Leticia Lopez-Martinez. "Rapid screening for quality control and adulteration in anti-diabetic drugs: Quantitative and Qualitative analysis by LIBS". OSA Optics and Photonics Congress: Imaging and Applied Optics 2010. Tucson, Az. USA. (7-9 June 2010).

U. Contreras, O. Barbosa-Gacía, G. Ramos-Ortiz, J. L. Pichardo-Molina, J.L. Maldonado, M. A. Meneses-Nava, Nancy Ornelas, P. L. Lopes-de.Alba. "Screening method for identification of white and rested tequila brands using spectroscopy and chemometrics" LXII Congreso Nacional de Física, Sociedad Mexicana de Física, Acapulco, Gro. (Oct. 2009).

V.U.L. Contreras-Loera, A. Vazquez-Duran, M. A. Meneses-Nava, O. Barbosa-Garcia, G.

Ramos-Ortiz, J. L. Maldonado-Rivera, M. Torres-Cisneros. “Substrate preparation with AG Nanoparticles to detect SERS signals from Rhodamine B”. LXI Congreso Nacional de Física, Sociedad Mexicana de Física, Zacatecas, Zac. (Oct 2008).

I. Moreno, **U. Contreras**, L. M. Molinar, “Design of convex LED arrays for uniform far-field irradiance”, XLVIII Congreso Nacional de Física, Sociedad Mexicana de Física, Guadalajara, Jal. (Oct 2005).

I. Moreno, **U. Contreras**, R. Tzontchev, “Cluster configurations of red, green, and blue LEDs for white light illumination”. The International Symposium Photonics West 2005. San José, California USA (22-27 Ene 2005).

Memberships

Optical Society of America (OSA) www.osa.org

Society of Photo-Optical Instrumentation Engineers (SPIE) www.spie.org

Society for applied spectroscopy (SAS) www.s-a-s.org

PERSONAL SKILLS

Mother tongue(s): Spanish

Other language(s)

	UNDERSTANDING		SPEAKING		WRITING
	Listening	Reading	Spoken interaction	Spoken production	
English	B2	C1	C1	C1	C1
	TOEFL ITP. Score: 587				

Levels: A1/2: Basic user - B1/2: Independent user - C1/2 Proficient user
Common European Framework of Reference for Languages

Communication skills: I have been developed scientific communication skills through my experience in international congresses and national invited talks and conferences during my PhD training.

Organisational / managerial skills: I have developed organisational and leadership skills through my experience as vice-president (2009) and president (2010) of the SPIE-CIO student chapter. Currently responsible for outreach activities for a team of 30-40 people.

Computer skills: Good command of:
- Microsoft Office™ tools.
- MATLAB
- OriginLab
- Unscrambler

Other skills: I have been involved in courses and workshops related with Business for scientists.

Personal interests: I enjoy photography and practicing sports, particularly soccer.